Abstract

Generators of Mammalian Vestibular Surface Responses to Head Motion

by

Gary Christopher Gaines, II

Director: Timothy A. Jones, Ph.D.

DEPARTMENT OF COMMUNICATION SCIENCES AND DISORDERS

The linear vestibular sensory evoked potential (VsEP) is thought to be the compound electrical response of peripheral macular neurons and central neural relays, and as such used to directly assess macular function. The VsEP is used in animal research to study, among other things, the genetic basis of deafness and balance disorders. Although the neural generators of the linear VsEP have been described in the bird, the precise central neural generators have not been documented for the mouse model. Because the mouse is such a valuable model in vestibular research, it is important to clearly identify the peripheral and central generators of VsEPs in mice. In order to complete such studies, various preface studies were completed to insure the accuracy of measurement with the generator studies. These studies included evaluation of VsEP response morphology with change in brain temperature; evaluation of drug on the VsEP response (i.e., Ketorolac); and the evaluation of stimulus duration on the VsEP response. During generator studies, VsEPs before and after strategic surgical manipulations of vestibular pathways were recorded. This included isolation of the eighth nerve from central relays and destruction of

central candidate neural generators. The extent of lesions was characterized histologically and changes in response components were documented. Response components critically dependent on particular peripheral and central structures were identified. These studies have increased the understanding of the neural generators of the VsEP, and in turn, enhanced the ability to assess peripheral and central vestibular function and detect vestibular disease.

Generators of Mammalian Vestibular Surface Responses to Head Motion

A Dissertation

Presented To

The Faculty of the Department of Communication Sciences and Disorders

East Carolina University

In Partial Fulfillment

of the Requirements for the Degree

Doctor of Philosophy

by

Gary Christopher Gaines, II

November, 2012

GENERATORS OF MAMMALIAN VESTIBULAR SURFACE RESPONSES TO HEAD MOTION

by

Gary Christopher Gaines, II

DIRECTOR OF DISSERTATION: _____

Timothy A. Jones, Ph.D.

COMMITTEE MEMBER: _____

Sherri M. Jones, Ph.D.

COMMITTEE MEMBER: _____

Andrew Stuart, Ph.D.

COMMITTEE MEMBER: _____

Kevin O'Brien, Ph.D.

CHAIR OF THE DEPARTMENT OF COMMUNICATION SCIENCES AND DISORDERS:

_____

Gregg D. Givens, Ph.D.

DEAN OF GRADUATE SCHOOL:

_____

Paul J. Gemperline, Ph.D.

ACKNOWLEDGEMENTS

I would like to thank my loving wife Allyson for supporting me through my doctoral education. Without you, this would not have been possible. I would like to thank my family and friends for their continued support and encouragement. You have been there through thick and thin. This would not have been possible without the support of my dissertation committee, Sherri M. Jones, Ph.D., Andrew Stuart, Ph.D. and Kevin O'Brien, Ph.D. Your time, comment, and suggestions throughout this process were very much appreciated. Last, but most certainly not least, I would like to thank Timothy A. Jones, Ph.D. I would like to recognize your commitment to excellence and wonderful guidance throughout this process. Because of you, I have discovered a keen interest in the search for new knowledge and now I have the tools to pursue it. Thank you for all of your time, understanding, countless rounds of edits, support, and encouragement. Your mentorship will certainly not be forgotten. This work was supported by NIH NIDCD 3 R01 DC006443-04S1 (Sherri M. Jones, Ph.D., University of Nebraska – Lincoln), the National Organization for Hearing Research Foundation, the American Academy of Audiology Foundation, and the Department of Communication Sciences and Disorders at East Carolina University, Greenville, NC.

Table of Contents

LIST OF TABLES

LIST OF FIGURES

surgical manipulation. Note that a greater amount “late component” residual activity is present in the 2.0 ms tracing. When utilizing the 1.0 ms stimulus duration, it was possible to remove/reduce this activity and concentrate on the principle VsEP response components.104

LIST OF SYMBOLS AND ABBREVIATIONS

ABR(s)	Auditory brainstem response(s)
bpm	Beats per minute
C	Celsius
CL	Plasma clearance rate
Cmax	Maximum plasma concentration
COX	Cyclooxygenase
C(t)	Plasma concentration
da/dt	Derivative of acceleration over time
dB peSPL	Decibels peak equivalent sound pressure level
D(t)	Cumulative dose
EAM	External auditory meatus
EDTA	Ethylenediaminetetraacetic Acid
EEG	Electroencephalogram
EKG	Electrocardiographic
EMG	Electromyography
f	Frequency
g/ms	Gravity-force per millisecond
LD50	Dose giving 50% mortality rate (lethal-dose 50%)
MLF	Medial longitudinal fasciculus
µV	Microliter
µV	Microvolt

ms	Millisecond
NSAID	Non-steroidal anti-inflammatory drug
PFA	Paraformaldehyde
pH	Potential hydrogen
RM MANOVA	Repeated measures multivariate analysis of variance
s	Second
SD	Standard deviation
SpO_2	Percentage of arterial oxygen saturation
T1/2	Half-life
V	Volume of distribution
VEMP	Vestibular Evoked Myogenic Potential
VNC	Vestibular nuclear complex
VOR	Vestibular ocular reflex
VsEP(s)	Vestibular sensory evoked potential(s)
τ	Time constant

CHAPTER I: REVIEW OF THE LITERATURE

Introduction

This work focused primarily on an attempt to understand the generation of responses from vestibular sensors and neural pathways that are evoked by transient linear acceleration. In this case, the stimulus was head motion and the responses are referred to as vestibular sensory evoked potentials (VsEPs). Head motion is the natural adequate stimulus for vestibular receptors. The VsEP response has proven to be of use as an objective measure of vestibular function (e.g., S. Jones, 2008; T. Jones & S. Jones, 2007). However, the neural pathways generating VsEPs in mammals have not been fully characterized. Understanding the sensors and corresponding neural pathways generating VsEPs may improve considerably the usefulness of these responses in both clinical and basic research. VsEPs have been used to study vestibular function in several strains of mice and other rodents with various disease (e.g., demyelinating disorders, peripheral vestibular deficits), cerebellar disorders (i.e., cerebellar infarct) and genetic abnormalities (i.e., syndromic and non-syndromic hearing loss). These studies gave one new insight into what underlying structures are responsible for this electrical potential in the mammal and aid the understanding of VsEPs in general. With this new knowledge, a long-term goal is to further develop the VsEP for clinical utility and ultimately, these efforts have contributed to a better understanding of the genetic basis of hearing and balance disorders.

Background and Review of Literature

Evoked potentials are used both clinically and in basic science research to evaluate the electrical activity produced by neurons and sensory structures within the body. Auditory and vestibular evoked potentials are utilized to evaluate the physiological status of the inner ear and the central neural pathways/relays of the auditory and vestibular systems, respectively (e.g.,

Burkard, Don, & Eggermont, 2007; Jacobson & Shepard, 2008). Evoked potentials are often classified according to the recording distance of electrodes from the structure(s) measured and are often referred to as near-field or far-field based on this distance (e.g., Lutkenhoner & Mosher, 2007). Clinical evaluations and scientific study with the use of evoked potentials, both far-field and near-field, are essential for the evaluation of auditory and vestibular systems in difficult-to-test patients and in animals due to the inability to obtain behavioral responses. Near-field potentials are recorded with the use of invasive electrode placements on, in or in close proximity to neurons or anatomic structures of interest. Near-field potentials usually have large amplitudes [e.g., 100 - 400 microvolts (μV) for near field sternocleidomastoid muscle recording associated with acoustic stimuli or 70 - 80 millivolts for cell membrane potentials] and are used when one is trying to isolate specific areas of the nervous system.

With reference to assessment of the auditory and vestibular systems, examples of near-field potentials include the cochlear microphonic recorded from electrodes at the round window or electrodes recording from the inside of single neurons of the vestibular portion of the eighth nerve. Far-field potentials are recorded with the use of non-invasive electrodes or needle electrodes placed on or beneath the skin at strategic locations to record neural activity generated a considerable distance from the recording electrodes. Far-field recordings are useful for studying activity in major pathways of the nervous system with scalp electrodes. Far-field potentials usually have small amplitudes (e.g., 1 - 5 μV for auditory brainstem responses [ABRs] and VsEPs in animals, < 1 μV for humans [ABRs only]) and are commonly used when one is trying to record compound action potentials as they course centrally via neural tracts and relays.

With reference to measurement of the auditory and vestibular systems, examples of far-field potentials include ABRs and VsEPs, respectively. Although near-field and far-field evoked

potentials have their own advantages, there are observations that are consistent across both types of recordings. As the recording electrode placement moves closer in proximity to the site of electrical potential generator (e.g., an electric dipole), various changes occur in the morphology of the recorded waveforms (Eggermont, 2007). For example, as an electrode moves closer to an electric dipole generator source (e.g., a central nucleus), amplitudes become less positive and eventually invert and become negative. As noted with far-field potentials, larger distances from the dipole source are common and the nature of the recording enables the recording of large numbers of cells over large areas of electrical activity. This causes lower signal-to-noise ratios and typically requires a larger number averages to resolve evoked potentials of interest.

Far-field type of recording is often used to gain information about the physiological status of auditory and vestibular pathways. Although the neural generators are well understood for ABRs, little is currently known about the neural generators of VsEPs. To better understand the clinical capabilities of VsEPs as far-field evoked potentials, studies of VsEPs in conjunction with anatomical verification of its neural generators are warranted. An in depth discussion of VsEPs and ABRs is given in the subsequent sections.

Clinical Measures of Vestibular Function

The vestibular system contributes to the maintenance of balance, posture and visual stabilization on targets of interest. This system contains sensory organs that are sensitive to both angular acceleration (semicircular canals) and linear acceleration (utricle and saccule). Clinical evaluation of this system may be warranted in cases where patients experience certain symptoms (e.g., dizziness or vertigo). Both indirect and direct evaluation methods are currently available for assessing the function of the vestibular system. Indirect evaluations of sensory systems are completed by evaluating the function of physiologic systems (e.g., muscular, respiratory, renal,

etc.) that may be influenced by the sensory system of interest. Examples of the indirect clinical vestibular evaluation are vestibular evoked myogenic potentials (VEMPs) and the vestibulo-ocular reflexes (VOR).

Vestibular evoked myogenic potentials (VEMPs) are generally thought to arise from stimulation of the vestibular periphery by intense sounds (Jacobson & McCaslin, 2007). Assessment of the vestibular periphery using the VEMP depends on the activation of peripheral, central and motor systems. In the case of the VEMP, activation of the vestibular periphery by an intense acoustic transient, leads to the activation of vestibulospinal reflex pathways (Colebatch, 2001; Zhou & Cox, 2004; Murofushi & Kaga, 2009). The pathways mediating vestibulospinal reflexes and thus presumably mediating VEMPs are summarized in Figure 1. Vestibulospinal reflexes are initiated with the activation of primary afferent neurons projecting from the vestibular sensors in the labyrinth to central vestibular relays in the brainstem (e.g., the medial and lateral vestibular nuclei; Carpenter, 1976). Second order cells of these vestibular nuclei give rise to the medial and lateral vestibulospinal tracts. Vestibulospinal tracts project to alpha and gamma motor neuron pools of the spinal cord (Burke & Edgerton, 1975). Vestibulospinal tracts generally activate some alpha motor neuron pools and inhibit other pools, particularly those that innervate opposing muscle groups (e.g., opposing extensor and flexor muscle groups; Akin & Murnane, 2008; Murofushi & Kaga, 2009). Activation of alpha motor neurons causes the corresponding muscle to contract. Inhibition of alpha motor pools can occur directly by vestibulospinal axon terminals (Kushiro, Zakir, Ogawa, Sato, & Uchino, 1999) or indirectly via interneurons and results in a reduction in muscle activity. The vestibulospinal pathways innervate alpha and gamma motor neurons of neck and trunk musculature both ipsilateral and contralateral to the vestibular stimulus (e.g., Pompeiano & Brodal, 1957; Wilson & Yoshida,

1969). Gamma motor neurons regulate muscle tone indirectly by adjusting the sensitivity of the muscle spindle. In contrast, alpha motor neurons send neural impulses directly to the motor end plates of individual muscle fibers, which cause muscle contraction that can be recorded using electromyography (EMG; Latash, 2008). A motor unit can be defined as the alpha motor neuron and all muscle fibers innervated by it. Further, groups of motor units typically work together to coordinate the contraction of a single muscle. Neural pathways thought to mediate the vestibulocollic reflexes are summarized schematically in Figure 1.

Similar to VEMPs, the vestibulo-ocular reflex (VOR) is an indirect assessment of the vestibular periphery via the measurement of eye movements (e.g., Hain & Rudisill, 2008; Baloh & Honrubia, 2001). As the head is turned in one direction, the VOR is responsible for compensatory eye movements in the opposite direction of the head turn in order to maintain stable vision. Both semicircular canals (e.g., superior, posterior and lateral) and macular organs (e.g., saccule and utricle) are stimulated during different directions of head movement (Baloh & Honrubia, 2001).

Head movements are defined as "rotational" or "translational". Rotational head motion causes an inertial shift of endolymph within the semicircular canals whereas the macular organs are activated by a combination of translational head motion and the gravity vector. Endolymph movement mechanically deforms the ampullary cupula causing the activation or inhibition of hair cells within the ampula of the semicircular canals. Hair cell activation in turn activates vestibular primary afferents. Translational head motion or head tilt (stimulation by gravity) gives rise to the direct displacement of the otoconial layer and activation or inhibition of hair cells of the macular organs, and this gives rise to the activation of vestibular primary afferent neurons. The VOR also requires activation of central and motor systems.

Vestibular primary afferent neurons transmit signals to the medial, lateral, superior and inferior vestibular nuclei (Figure 2). The vestibular nuclei are located on either side of the brainstem and receive signals from both vestibular peripheries. Midline-crossed and uncrossed projections from the vestibular nuclei innervate the oculomotor nuclei (e.g., III-Oculomotor, IV-Trochlear, VI-Abducens). The oculomotor nuclei innervate the muscles of the eye (e.g., extraocular muscles: superior, lateral, medial, inferior rectus muscles and superior and inferior oblique muscles). These muscles are responsible for vertical, horizontal and torsional movements of the eyes. Activation or inhibition of the motor nuclei cause contraction or enable relaxation of opposite pairs of eye muscles to allow movement in the opposite direction of the head movement (e.g., Baloh & Honrubia, 2001). Ultimately, the eye movements initiated by the VOR are measured by eye-tracking cameras. Clinically, VOR is used to assess function using various tests (e.g., rotary chair, calorics, and oculomotor evaluation strategies).

Currently, indirect tests of vestibular function are the only methods available for assessing the vestibular periphery (i.e., evaluating vestibular function via the VOR). A direct method would be useful since it could provide a means to evaluate the vestibular periphery alone without potentially confounding contributions from portions of the central nervous system (i.e., evaluating only primary afferent and second order projections).

The VsEP provides a direct measure of vestibular function. For this reason it provides important advantages over other indirect methods of vestibular assessment. Although the distinction between the neural generators of the early and late peaks of the VsEP have been established in the bird (e.g., Nazareth & T. Jones, 1998), the precise neural generators of later peaks have yet to be described. Further, little is known about the neural generators of the VsEP in the mammal. Identifying the central neural generators of the VsEP will permit more accurate

assessments regarding the functional status of specific central vestibular pathways; something that is not possible now. More precise knowledge about specific generator structures will increase what one can learn from VsEP testing. Further development of the VsEP will contribute to the knowledge of the vestibular system and may lead to new strategies of clinical evaluation and treatment of vestibular disorders.

Vestibular Sensory Evoked Potentials

Linear VsEPs can be recorded from the surface of the skull and are composed of four to six positive and negative electric response peaks that occur within approximately six milliseconds (ms) of the stimulus onset (Figure 3). The stimulus used to elicit the response is a transient linear acceleration of the head (T. Jones, S. Jones, & Colbert, 1998). Response amplitudes are a function of stimulus level and are in the range of 1 - 2 μV at moderate stimulus levels (Figure 4). Responses depend critically on the integrity of the inner ear and disappear following labyrinthectomy (e.g., T. Jones, 1992; T. Jones & Pedersen, 1989; S. Jones & T. Jones, 1996; S. Jones, T. Jones, & Shukla, 1997; Plotnik, Elidan, Mager, & Sohmer, 1997; Plotnik, Sichel, Elidan, Honrubia, & Sohmer, 1999; Weisleder, T. Jones, & Rubel, 1990). They are not responses generated by the cochlea since they are resistant to intense acoustic masking and are unaffected by cochlear ablation (T. Jones, 1992; S. Jones & T. Jones, 1996; S. Jones et al., 1997; Weisleder et al., 1990). They are initiated within the macular organs since they are absent in otoconia-deficient animals (S. Jones, Erway, Bergstrom, Schimenti, & T. Jones, 1999) and have amplitudes directly proportional to the amount of otoconial matrix present (S. Jones, Erway, Yu, Johnson, & T. Jones, 2004). Thus, the linear VsEP is a compound action potential that is initiated within macular sensors (saccule and utricle), which then propagates to vestibular and cerebellar structures in the central nervous system. Presumably, vestibular afferent action

potential volleys lead to the generation of action potentials in post synaptic cells in the brainstem vestibular nuclear complex (VNC; e.g., superior, lateral, medial and inferior nuclei) and cerebellum. These in turn lead to the activation and inhibition of other vestibular circuits. The objective of the proposed work is to identify what aspect of central neural activity and associated structures contributes to the VsEP waveform. The neural pathways and nuclei mediating central response activity are therefore candidate neural generators of the VsEP.

Vestibular Pathways

Two reviews of the VNC's afferent and efferent connections have been offered recently (Barmack, 2003; Newlands & Perachio, 2003). The following is a brief account drawn in part from information offered in these reviews. Vestibular primary afferents of the eighth nerve synapse with the macular organs peripherally. The superior vestibular nerve innervates the neuroepithelia of the anterior (superior) and horizontal canals, the utricle and about one third of the saccule (anterosuperior portion), while the inferior vestibular nerve innervates the posterior canal and the remaining two-thirds of the saccule (e.g., Gacek, 1969; Honrubia, Kuruvilla, Mamikunian, & Wichel, 1987; T. Jones, S. Jones, & Hoffman, 2008). Vestibular primary afferents project from all vestibular end organs (i.e., maculae and ampulae) to the VNC of the brainstem as well as to the cerebellum where the majority of primary afferent projections terminate in the uvula and nodulus (cerebellar lobules IXd and X, respectively; e.g., Barmack, Baughman, Errico, & Shojaku, 1993; Gerrits, Epema, van Linge, & Dalm, 1989; Newlands & Perachio, 2003). The vestibular nuclei also receive afferents from the cerebellum, reticular formation, spinal cord, contralateral vestibular nuclei as well as other sensory systems including: visual, auditory and somatosensory (e.g., Barmack, 2003). Vestibular peripheral and central connections are summarized in Figure 2.

Various neural tracts are formed from the outflow of the vestibular nuclei. Ascending projections from vestibular nuclei make up portions of the medial longitudinal fasciculus (MLF) and have bilateral projections to thalamus (e.g., Blum, Day, Carpenter, & Gilman, 1979; Shiroyama, Kayahara, Yasui, Nomura, & Nakano, 1999), the interstitial nucleus of Cajal, unilateral and bilateral projections to the oculomotor (III), abducens (VI) and trochlear (IV) cranial nerve nuclei and the cerebellum (e.g., Barmack, 2003; Parent, 1996). The second order cells of the VNC project as mossy fibers bilaterally to the granule layer of cerebellar lobules IXd and X as well as to the flocculus, paraflocculus, and folium I in the anterior lobe. These same cerebellar regions send reciprocal projections back to the medial vestibular nuclei.

Descending projections from the lateral vestibular nuclei are somatotopically organized and project to the spinal cord as the lateral vestibulospinal tract, while descending efferents from the medial vestibular nucleus project as the medial vestibulospinal tract. The vestibulospinal tracts activate and inhibit alpha motor neuron pools throughout the spinal cord, which have direct influence on head, neck, and trunk musculature and contribute to the maintenance of balance and gaze during head movement.

The thalamus is the major relay point for vestibulo-cortical projections. Outflow of the vestibular nuclei projects to the ventrobasal thalamus and thalamic neurons project to the cortex where vestibular sensation is processed (e.g., Shiroyama et al., 1999). Projections to the sensory cortices from the thalamus include vestibular, visual, somatosensory, gustatory and auditory fibers. Connections between the sensory and motor cortices exist. Descending fibers project to the cerebellum and the vestibular nuclei. Vestibular nuclei also project to the limbic system (Balaban, 1999), which is responsible for integrating various inputs, including emotions, storing memory, and regulating autonomic activity. Modification of sympathetic activity (e.g., systems

controlling arterial blood pressure) is also initiated by projections from the vestibular nuclei to the medulla, solitary nucleus, and parabrachial nucleus (e.g., Balaban & Porter, 1998; Yates & Miller, 1998). These actions initiated by the vestibular system have been termed the "vestibulosympathethic reflex". Other projections from vestibular nuclei include commissural fibers, which make reciprocal connections between the left and right VNC. Thus, vestibular input influences numerous motor and sensory systems.

Many of the above structures represent candidate neural generators for the linear VsEP. The intent herein was to use neural sectioning to interrupt specific projections from the sensory organs to the VNC and cerebellum as well as between the VNC and the cerebellum. This was consistent with previous procedures conducted in the bird (Nazareth & T. Jones, 1998). In addition, selected regions of the cerebellum were aspirated to identify regions critical to VsEP components (e.g., nodulus, uvula, flocculus, etc.)

Expectations Based on Linear VsEPs in Birds and Rotary VsEPs in Mammals

VsEPs elicited by transient rotary stimuli have also been described (e.g., Elidan, Langhofer, & Honrubia, 1987a). They have been shown to be dependent on the inner ear (e.g., Elidan, Lin, & Honrubia, 1986; Elidan, Langhofer, & Honrubia, 1987b; Li, Elidan, & Sohmer, 1993; Elidan et al., 1987b; Li et al., 1993) and are thought to be generated in large part by ampular sensors but also reflect activity from macular organs (Li, Elidan, & Sohmer, 1995; Trimble & S. Jones, 2001). Generator studies reported by Li and colleagues provide evidence that P1 of rotary VsEP reflects peripheral whereas later peaks reflect central brainstem nuclei (e.g., Li et al., 1993; Li, Elidan, Meyler, & Sohmer, 1997; Li et al., 1997).

In the case of linear VsEPs, Nazareth and T. Jones (1998) demonstrated in the bird (i.e., chicken, *Gallus domesticus*) that P1 remains intact and P2 amplitude decreases after a proximal

isolation of the eighth nerve from the brainstem, while peaks beyond P2 are abolished. With this type of lesion, only the ipsilateral eighth nerve remains as a candidate generator for P1 while generators of later peaks must arise from central vestibular projections. This includes brainstem and/or cerebellar structures. Based on these studies, it was hypothesized that in the mouse P1 of the linear VsEP reflects peripheral activity whereas peaks beyond P2 reflect central activity. The present studies critically tested this hypothesis in mice. Although there is some evidence in the bird (Nazareth & T. Jones, 1998), virtually nothing definitive is known regarding the role of the cerebellum in generating VsEP components. The effects of cerebellar lesions were evaluated on VsEPs to identify its' contributions.

Auditory Brainstem Response and its Neural Generators

The auditory system can be activated by various levels and types of acoustic stimuli. The ABR is an electroencephalographic (EEG) recording of the electrical activity of the auditory system generated in response to transient auditory stimuli (e.g., Durrant & Boston, 2007). It consists of compound action potentials produced by neurons of the auditory pathways from the peripheral nerve (e.g. eighth nerve) and relays up to the level of the midbrain (e.g. inferior colliculus). The response has five positive and negative peaks that occur within 10 ms after the onset of an adequate stimulus. Commonly, human ABR peaks are referred to with roman numerals (I, II, III, IV and V) set in place by Jewett (1970) and four peaks in animal work are typically referred to with a “P” for positive and an “N” for negative followed by the peak number (e.g. P1, N1, P2, N2, P3, N3, etc.). Peaks occur from I-V and P1-N5. For the ABR, acoustic stimuli are presented to the mastoid bone or to the external auditory meatus and are referred to as bone-conducted or air-conducted stimuli, respectively. Clicks and brief tone bursts are common stimuli utilized to evoke the ABR. Action potentials are generated in the auditory nerve

following stimulation of the hair cells within the cochlea. Action potentials course through the brainstem and thalamic auditory relay nuclei to arrive ultimately in the auditory cortex located in the temporal lobe. Latencies of the five response peaks of the ABR have been associated with latencies of near-field recordings of various sites throughout the auditory pathway. These neural generation sites will be discussed in further detail below.

Many investigators have studied the neural generators of the ABR P1 through P5 (Figure 5) in various species (Table 1). Although there are some disagreements on exact locations of generators for some peaks across species, a general consensus exists throughout the literature and that is that earlier peaks are generated by the auditory periphery and auditory nerve whereas later peaks are generated by second, third and four order cells of the auditory pathway. The purpose of the following discussion is to describe and review various candidate neural generators of the respective ABR peaks in various species. For the purposes of this discussion, the terms "ipsilateral" and "contralateral" refer to the stimulus ear.

Positive ABR Peak I

Latencies of eighth nerve compound action potentials recorded from the round window of the mouse, cat and rat are similar to latencies of P1 of the ABR (i.e. 1-2 ms; e.g., Henry, 1979a; Jewett, 1970; Jewett & Romano, 1972). Henry (1979a) and Buchwald and Huang (1975) demonstrated that isolation of the eighth nerve from the brainstem abolishes all ABR peaks after P1 in the mouse and cat, respectively. Additionally, P1 was abolished post-mortem. Eighth nerve recordings in the human have also isolated the eighth nerve as a sole contributor to P1 (e.g., Sohmer, Feinmesser, & Szabo, 1974; Starr & Hamilton, 1976). Case studies of patients with unilateral brainstem pathology showed normal ABR Wave I latencies and amplitudes, whereas later peaks are either abolished completely or were lowered in amplitude (Musiek &

Geurkink, 1982). In summary, P1 and Wave I of the ABR arises from the ipsilateral auditory nerve due to evidence that P2 is abolished once the nerve is sectioned from the ipsilateral cochlear nucleus and that P1 latency is similar to latencies of proximal auditory nerve and round window recordings of potentials associated with acoustic stimuli.

ABR Peak II

There is some controversy over the exact origin of ABR P2 throughout the literature. Two conflicting arguments present interesting cases for its origin. Some investigators have suggested that P2 arises from the ipsilateral cochlear nucleus (e.g., Jewett, 1970; Jewett & Romano, 1972; Henry, 1979a; Huang & Buchwald, 1977; Goldenberg & Derbyshire, 1975) while others have suggested that P2 arises from the proximal portion of the auditory nerve (e.g., Møller & Jannetta, 1983; Musiek & Baran, 2006). There is evidence to support both claims. Jewett and Romano (1972) inserted recording electrodes into the cochlear nucleus of both rats and cats and demonstrated an increase in responses amplitude and peak inversions as seen when recording electrodes are placed close to dipole locations. The latencies of these responses were comparable to the latency of P2 of the ABR. Buchwald and Huang (1975) demonstrated that P2 remained intact in the cat after interrupting the crossing fibers from the contralateral auditory nerve (i.e., ruling out contralateral cochlear nucleus contributions) and that P2 is abolished by sectioning the auditory nerve from the ipsilateral cochlear nucleus. These observations suggested that P2 is generated by neurons of the cochlear nucleus ipsilateral to the stimulus in the cat. Huang and Buchwald (1977) demonstrated that the onset latencies of time-locked single unit neural activity within the ipsilateral cochlear nucleus were consistent with the latency of P2 of the surface recorded ABR. Henry (1979a) demonstrated that the peaks with latencies consistent with the first three peaks of the ABR were visible when recording from the ipsilateral

cochlear nucleus of the mouse. He noted that ABR latencies of the largest peak, the second peak, were directly correlated to the latency of P2 of the ABR. In summary, P2 of the ABR is thought to arise from the proximal portion of the auditory nerve as it enters the ipsilateral cochlear nucleus or from the ipsilateral cochlear nucleus based on evidence that response latencies in the region of the cochlear nucleus are similar to ABR P2 and P2 is abolished when the input from the ipsilateral auditory nerve is not present.

ABR Peak III

At the level of P3, P4, and P5 of the ABR, candidates of neural generation become somewhat complex due to the nature of innervation from the cochlear nucleus with higher order central auditory system structures. In the human, the ipsilateral cochlear nucleus has three divisions: anterior ventral cochlear nucleus, posterior ventral cochlear nucleus and the dorsal cochlear nucleus (e.g., Webster & Fay, 1992). These three divisions share connections with the ipsilateral and contralateral medial superior olive, the ipsilateral lateral olive, the lateral nucleus of the trapezoid body, the contralateral ventral nucleus of the lateral lemniscus, and both ipsilateral and contralateral inferior colliculus (e.g., Webster & Fay, 1992). Auditory information flows primarily contralaterally once crossing the midline after exiting the ipsilateral cochlear nucleus. There is a consensus that P3 is generated in the area of the pons by the contralateral superior olivary complex/trapezoid body of the mouse, rat, guinea pig, and cat (e.g., Henry, 1979a; Wada & Starr, 1983a; Wada & Starr, 1983b; Wada & Starr, 1983c). Henry (1979a) demonstrated that contralateral brainstem and cortical lesions, which did not involve the superior olivary complex, did not affect P3. Buchwald and Huang (1975) demonstrated that P3 is abolished post midsagittal section of the brainstem of the cat, thus eliminating auditory input to the contralateral superior olivary complex. Additionally with the use of multiple electrode

montages, Allen and Starr (1978) reported amplitudes and latencies of P3 of the ABR in the monkey with neural generation sites located in the brainstem and correlated latency with that of other mammals (i.e. cat, rat and human), which supports evidence that P3 is generated by the superior olivary complex. Wada and Starr (1983a; 1983b; 1983c) demonstrated that both surgical isolation and neural blockade the activity of the contralateral superior olivary complex and trapezoid body in the guinea pig abolished and/or reduced amplitude responses of P4 and P5, while P3 remained unaffected. In summary, P3 of the ABR arises from the contralateral superior olivary complex due to evidence that when brainstem crossed auditory pathways are severed, P3 of the ABR is abolished whereas P3 is unaffected by lesions to the auditory pathways central to the contralateral superior olivary complex.

ABR Peak IV

P4 of the ABR has been described as having both ipsilateral and contralateral neural generators (e.g., Buchwald & Huang, 1975; Henry, 1979a; Huang et al., 1977; T. Jones, Stockard, Rossier, & Bickford, 1976; Jewett, 1970). The right and left tracts of lateral lemniscus are comprised of projections from crossed and uncrossed fibers of the lower auditory structures (e.g., superior olive and cochlear nucleus). Jewett (1970) recorded near-field potentials in close proximity to the lateral lemniscus during his ABR experiments. He reported an inversion of peaks with latencies consistent with peak IV of the ABR when recording electrodes were placed in the vicinity of the lateral lemniscus tract fibers.

Evidence from Buchwald and Huang (1975) supports a summed response from the ipsilateral and contralateral lateral lemniscus. They reported a decrease (~50%) in P4 amplitude after a complete midline sagittal brainstem section. Subsequent destruction of the ventral nucleus of the lateral lemniscus and pre-olivary structures eliminated the remaining P4 response

peak, thus providing the first evidence that P4 is generated bilaterally from regions at the level of the lateral lemniscus. Huang and Buckwald (1977) demonstrated that single units recorded from the area of the lateral lemniscus in the cat exhibited latencies consistent with those of P4.

T. Jones et al. (1976) inserted cooling probes in the right and left rostro-lateral pons of the cat. This anatomical location is in close proximity to both the right and left lateral lemniscus tracts respectively. Cooling the brain locally near the lateral lemniscus delayed the generation of responses in the region. Unilateral cooling on the contralateral side reduced P4 amplitude (by about 50%) and increased P5 latency (Figure 6). In contrast, during bilateral cooling P4 amplitudes were essentially unaffected whereas the latencies of P4 and P5 were increased. Based on these results the investigators proposed that P4 is dependent upon the bilateral activation of the lateral lemniscus, indicating that P4 has multiple generators; one on the contralateral side and one on the ipsilateral side. During unilateral contralateral cooling only one P4 generator was delayed and broadened to merge with P5, whereas the ipsilateral uncooled generator was activated at its usual latency and appears as P4 with reduced amplitude. However, during bilateral cooling both the ipsilateral and contralateral generators were shifted in latency together. Thus P4 amplitude remained little affected whereas the peak was slightly broader and latency increased substantially. Such findings are consistent with the work of others (e.g., Buchwald & Huang, 1975; Henry, 1979a; Huang & Buchwald, 1977; Jewett, 1970).

Henry (1979a) observed that lesions of the contralateral nuclei of the lateral lemniscus in the mouse caused a single P4 peak to become triphasic, but it did not completely disappear. The latency of the center of the peak morphology was comparable to latencies of ABR wave IV. Since P4 was not completely abolished, the findings were consistent with earlier work suggesting there is more than one generator for P4 of the ABR in the mouse. In summary, P4 of the ABR

arises from both ipsilateral and contralateral lateral lemniscus based on evidence that when partial regions of lateral lemniscus pathways are damaged or otherwise physiologically altered P4 of the ABR is affected whereas peak P3 is unaffected.

ABR Peak V

Wave V of the human ABR is often easily identified for its large peak amplitude and it is commonly used for behavioral auditory threshold estimation (e.g., Sininger & Don, 1989). A general consensus throughout the literature is that P5 of the ABR is generated by the contralateral inferior colliculus (e.g., Buchwald & Huang, 1975; Henry, 1979a; Jewett, 1970; Musiek & Baran, 2006). Jewett (1970) reported ABR peaks in the cat with latencies consistent with that of P5 at the superior regions of the inferior colliculus and at locations between the inferior colliculus and its more central projection to the medial geniculate body. Huang and Buchwald (1977) demonstrated that P5 was abolished after the surgical aspiration of the inferior colliculi as well as post-midsagittal brainstem section. Recording techniques and anatomical descriptions across laboratories may make it difficult to compare some findings. For example, Goldenberg and Derbyshire (1975) performed lesions to the ipsilateral and contralateral inferior colliculi, but they showed no changes in P5 of the ABR although these investigators may not have caused sufficient lesions to the inferior colliculi to cause noticeable changes in P5. Henry (1979a) demonstrated that near-field potentials with latencies consistent with P5 of the ABR had greater amplitude when recorded from the lateral most portions of the contralateral inferior colliculus in the mouse, while amplitudes were lower in medial areas of contralateral inferior colliculus and in the ipsilateral inferior colliculus.

Based on the above observations, the generators of ABR peaks can be summarized as follows. P1 is generated by the ipsilateral auditory nerve. P2 is generated by the ipsilateral

cochlear nucleus. P3 is generated by the contralateral superior olivary complex. P4 is generated by both the ipsilateral and contralateral lateral lemniscus. P5 is generated by the contralateral inferior colliculus.

Although this ABR neural generator information is well known (e.g., Hall, 2007; Møller, 2006), the intent was to include ABR recordings during studies of the neural generators of VsEPs. Vestibular neural pathways do not course through the exact same anatomic structures as those generating the ABR. However, the ABR can be utilized to measure general alterations in the physiological status of the brainstem and can be used to monitor the physiological stability of the animal while vestibular structures are lesioned and evaluated.

Experimental Design and Hypothesis

In recent years, numerous genes have been discovered that play essential roles in the normal inner ear. Mutations in many of these genes have been linked to human deafness and vestibular dysfunction (e.g., Evans, Sainio, & Baser, 2000; Keats & Corey, 1999; Rabionet, Gasparini, & Estivill, 2000). In mice, it is often the case that the same genetic mutation produces similar otological pathologies as humans (e.g., Di Palma et al., 2001; Hampton, Wright, Alagramam, Battey, & Noben-Trauth, 2003), thus providing an important animal model for in depth study. Understanding the functional deficits associated with these genetic changes is an important part of understanding the disease process itself. The linear VsEP was developed to provide a noninvasive direct assessment of vestibular function and it is used to study genetic models of human disease (S. Jones, 2008). The VsEP is the vestibular analog to the auditory ABR.

As noted above, VsEPs are vestibular compound action potentials that are recorded in response to head translation (Figure 3). The VsEP waveform is a series of peaks that are thought to be generated by neurons making up the vestibular peripheral and central pathways. Although

work in birds (Nazareth & T. Jones, 1998) has demonstrated that the earliest response peaks are dependent on the integrity of the vestibular nerve (P1 and N1), the exact origin of the later peaks (beyond P2) have yet to be described. In general, the main objective of this research is to better understand which structures among the vestibular pathways make substantial contributions to the VsEP waveform. The hypothesis of this study was that each respective peak of the VsEP is associated with specific peripheral or central vestibular structures. The first specific aim was to distinguish components of VsEPs in the mouse that were generated by peripheral neurons from those generated by central vestibular structures including the cerebellum. This was done by surgically interrupting the vestibular nerve as it enters the vestibular nuclei and cerebellum. The second specific aim was to distinguish brainstem versus cerebellar generators of the VsEP. This was done by inducing lesions in the cerebellum. In this case in separate experiments, specific regions of the cerebellum (e.g., flocculus or lobules IXd or X, etc.) or major pathways between brainstem and cerebellum were sectioned or aspirated. VsEPs were recorded before and after surgical manipulations. Histology was used to characterize the site and extent of lesions in all studies. The third specific aim was to characterize effects of vestibular pathway lesions on the ABR. There has been a substantial amount of work done on the generators of the ABR. Although, the generators of the ABR are well known and are distinct from the vestibular pathways, brainstem lesions of the vestibular pathway may overlap and intersect auditory structures or lead to a general decline in brainstem function and thus also affect the ABR waveform. Changes in ABR waveforms following surgical manipulations were evaluated and used to help identify the functional limits of injury induced by lesions and provided a measure of the general physiological status of brainstem structures.

Preliminary Studies

Ketorolac

The non-steroidal anti-inflammatory drug (NSAID) ketorolac (Toradol) is a candidate for use as a supplemental analgesic during major surgery in anesthetized rodents. The use of ketorolac during surgery is believed to reduce the anesthetic dose required to achieve and maintain an adequate surgical plane and thus improve the physiological conditions and survival of animals during long experimental procedures. Ketorolac has reported side effects of dizziness, "ear pain", hearing loss, tinnitus and vertigo in humans (e.g., Bauman, 2003; Otti, Weindel, & Bastani, 1997; Reinhart, 2000; Schaab, Dickinson, & Setzen, 1995), but there has been no report of ketorolac's effect on the auditory and vestibular system in animal models. Thus the use of ketorolac during studies of the inner ear in anesthetized animals is subject to question. The aim was to evaluate the effect of ketorolac on vestibular and auditory compound action potentials in the mouse (c57BL/6J). Further detail on the study of the effects of Ketorolac can be found in Chapter 2.

Brain Temperature and Response Morphology

Temperature alters response latencies and amplitudes of VsEPs and ABRs (e.g., Henry, 1979a; T. Jones & Pedersen, 1989; T. Jones, Stockard, & Weidner, 1980; Marsh, Yamane, & Potsic, 1984; Nazareth & T. Jones, 1998). In the following studies it was necessary to maintain a constant brain temperature to prevent substantial latency variation. The rate of change in latency as a function of temperature has been characterized for the bird (T. Jones & Pedersen, 1989; Nazareth & T. Jones, 1998). The relationship between temperature and VsEP peak latencies and peak amplitudes has not been described for the mammal. In general, the findings demonstrated that latencies decrease systematically as brain temperature is increased whereas amplitudes had

large variation with peaks beyond P1-N1, and P1-N1 demonstrated little variation. Due to variations of peak latencies, it was necessary to maintain brain temperature at a consistent level throughout all subsequent studies.

Establishing Histological Methods

Histology of lesion studies is important to document the location and extent of the induced lesion. In the proposed studies, histology was required to document areas of the brain that have been lesioned to rule those in or out as possible neural generators of the VsEP. Initial histological methods were established based on methods utilized by Franklin and Paxinos (2007). These investigators documented the brain stereotaxically with the use of sagittal and coronal sections. Additionally, they used a nissl stain to assist in the location of specific neural structures throughout the brain.

In the initial histological trails, the animal was perfused with 4% paraformaldehyde (PFA), the skull was decalcified with Cal-EX (Fisher Scientific) for 24 hours, imbedded in paraffin (Brody School of Medicine Facilities by Ms. Joani Zary), cut into 10-20 micron sections, slide mounted and stained with cresyl violet (e.g., a nissl stain). It was noted that the tissue would initially take the stain, but the majority of the stain would wash away after the final steps of the staining protocol. Success was found with a hemotoxilin and eosin stain (Figure 7) following the 24-hour Cal-EX decalcification; however, the coloring was not directly comparable to the stereotaxic atlas and made it somewhat difficult to identify key auditory and vestibular pathways and structures from the sectioned tissue. At a later time, 10-day decalcification with Ethylenediaminetetraacetic acid (EDTA) was attempted followed by the cresyl violet stain and proved to be successful. It was subsequently concluded that the hydrochloric acid in Cal-Ex somehow inhibited the stain from taking to the tissues in earlier trials. The ensuing protocols

consisted of animal perfusion (4% PFA) immediately after the study, 10-day decalcification in EDTA, the skull blocked behind the eyes, imbedded in paraffin, microtome sectioning from 10-20 micron sections, sections are slide mounted, stained with cresyl violet and cover-slipped. Further detail of the histological protocol can be found in Chapter 4.

Table 1

Various researchers that have evaluated the neural generators of the ABR.

Investigator(s)	Species
Allen & Starr, 1978	Human and Monkey
Achor & Starr, 1980a	Cat
Achor & Starr, 1980b	Cat
Beck, Brown-Borg, & T. Jones, 1987	White Leghorn Chicken
Beck & T. Jones, 1984	White Leghorn Chicken
Brown-Borg, Beck, & T. Jones, 1987	White Leghorn Chicken
Buchwald & Huang, 1975	Cat
Bullock, Grinnell, et al. 1968	Porpoise
Goldenberg & Derbyshire, 1975	Cat
Grinnell, 1963	Bat
Hamill, McGinn, et al. 1989	Ground Squirrel
Henry, 1979a	Mouse
Henry, Symanski, et al. 1999	Killer Whale
Huang & Buchwald, 1977	Cat
Jewett, 1970	Cat
Jewett & Romano, 1972	Rat and Cat
Jewett & Williston, 1971	Human
T. Jones, Beck, Brown-Borg, & Burger, 1987	White Leghorn Chicken
T. Jones & Stockard, 1976	Cat
T. Jones et al., 1980	Cat

T. Jones & Weidner, 1986	Dog
Lev & Sohmer, 1972	Human
Picton, Hillyard, Krausz, & Galambos, 1974	Human
Sohmer et al., 1974	Human
Starr & Hamilton, 1976	Human
Vaughan & Ritter, 1970	Human
Wada et al., 1983a	Guinea Pig and Cat
Wada et al., 1983b	Guinea Pig and Cat
Wada et al., 1983c	Guinea Pig and Cat

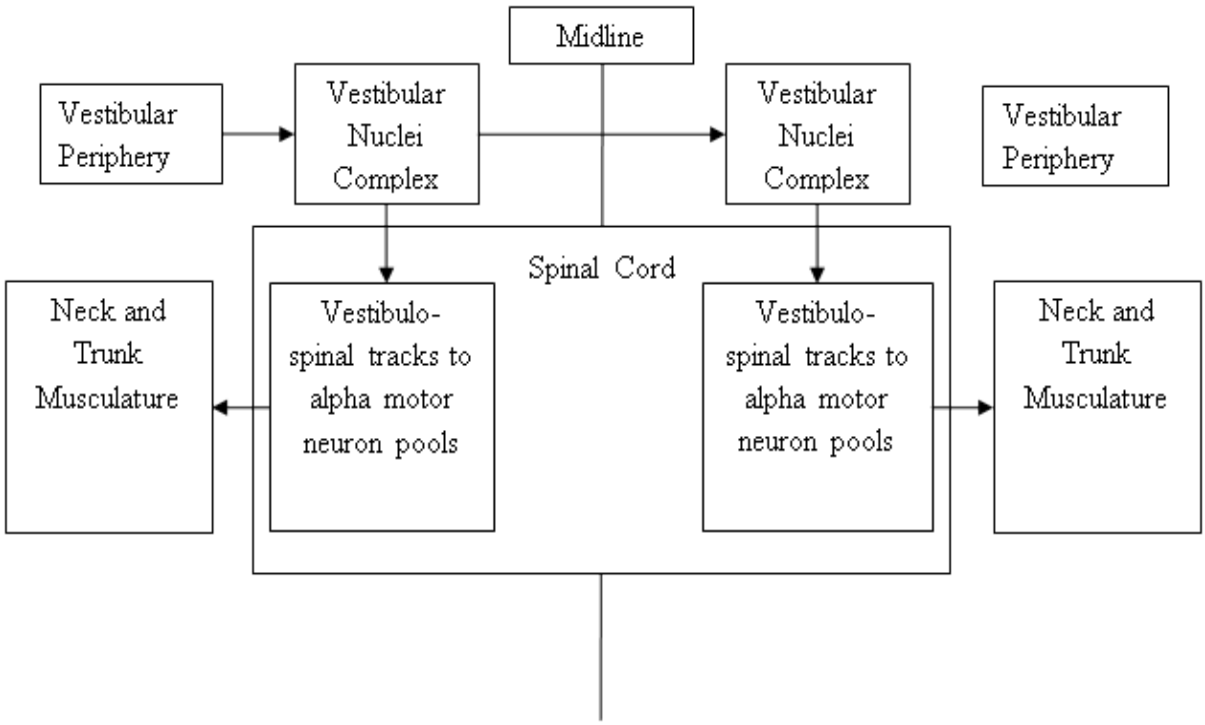

Figure 1. Descending vestibulospinal pathway from a single labyrinth.

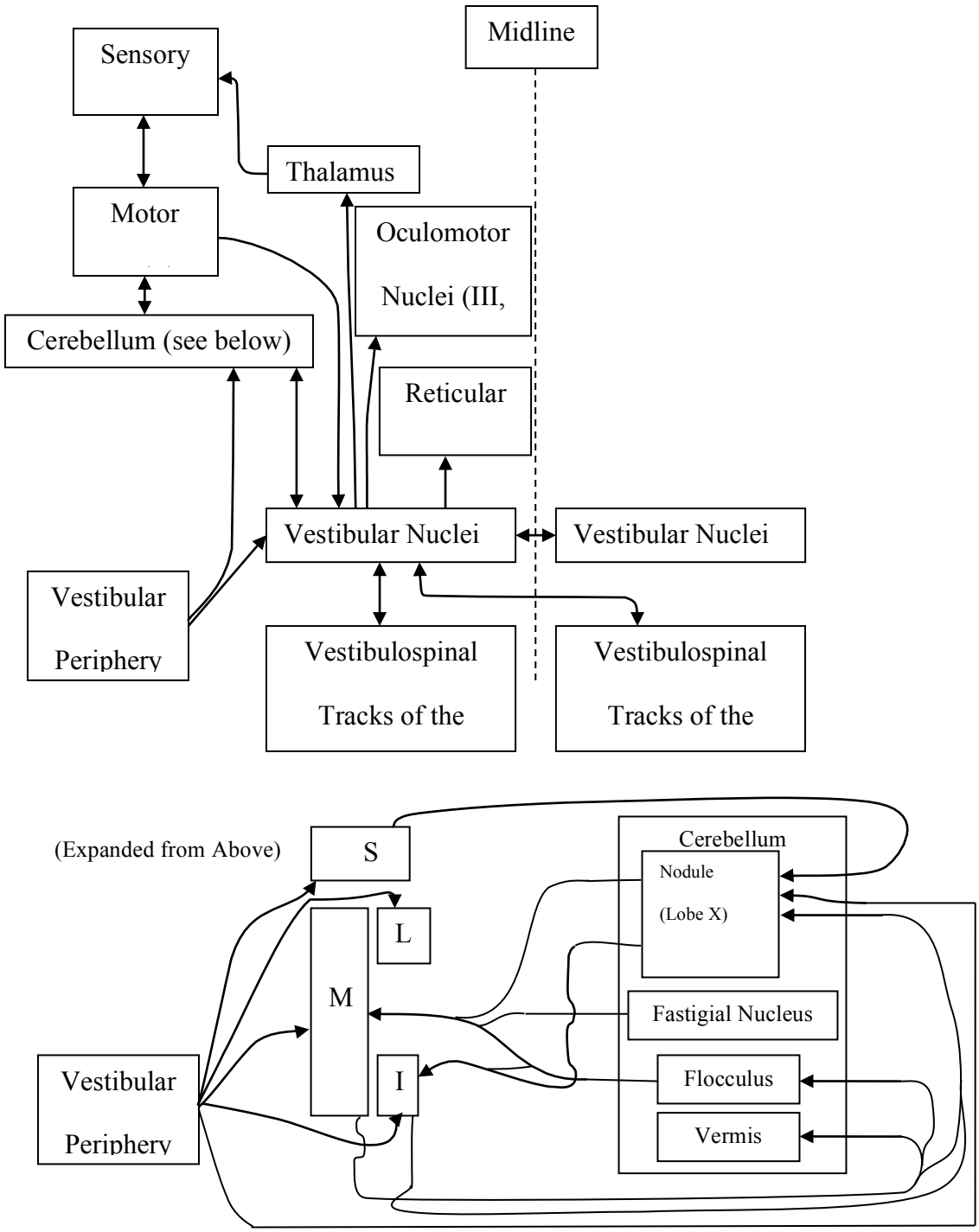

Figure 2. Above: Peripheral and central vestibular projections. Arrows indicate neuronal tracks and arrowheads indicate direction action potentials flow from peripheral to central projections. Below: An expanded diagram of projections between the vestibular periphery, vestibular nuclei (S-Superior, M-Medial, L-Lateral, I-Inferior), and the cerebellum. These diagrams are merely schematic and do not accurately depict anatomical structures or locations.

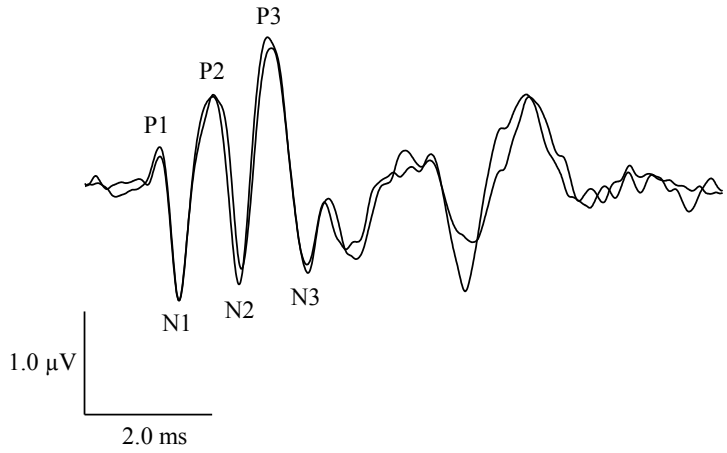

Figure 3. VsEP waveforms recorded from a c57BL/6J mouse. Positive peaks are labeled as P1, P2 and P3 as they occur in order within 10 ms of the stimulus onset. VsEP response was elicited with a stimulus level of +6.0 $dB_{re: 1.0g/ms}$.

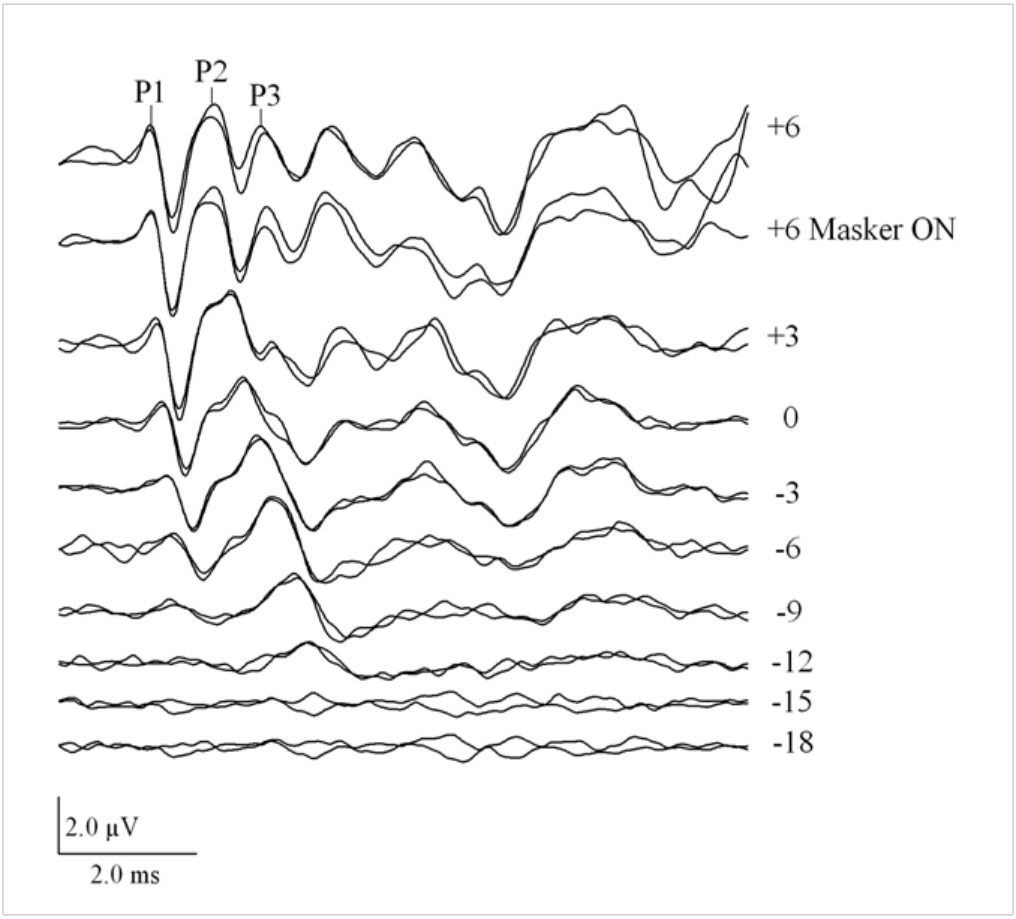

Figure 4. Linear VsEP stimulus level series obtained from an anesthetized mouse using subcutaneous and cortical electrodes with direct coupling of the skull to the stimulus platform. Stimulus level is given in $dB_{re: 1.0g/ms}$. Threshold for this animal was scored at -13.5 $dB_{re: 1.0g/ms}$. A wide-band (50 Hz-50 KHz) 90 dB SPL forward masker was presented during the recording of the second pair of traces (Masker ON) to demonstrate the absence of auditory components.

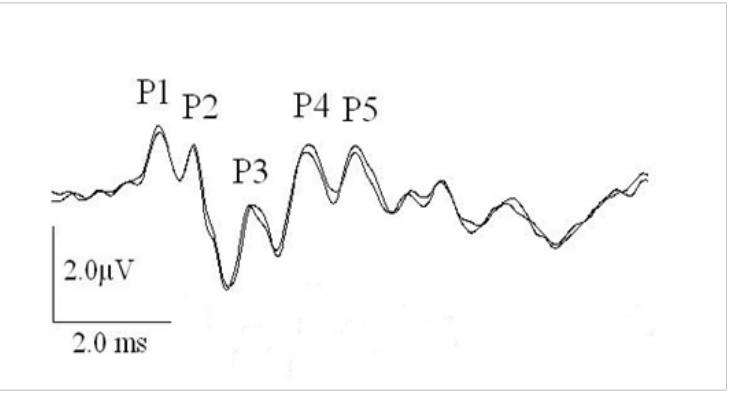

Figure 5. ABR waveform recorded from a c57BL/6J mouse. Positive peaks are labeled as P1, P2, P3, P4 and P5 as they occur in order within 10 ms of the stimulus onset. ABR response was elicited stimulus with 60 dB peSPL.

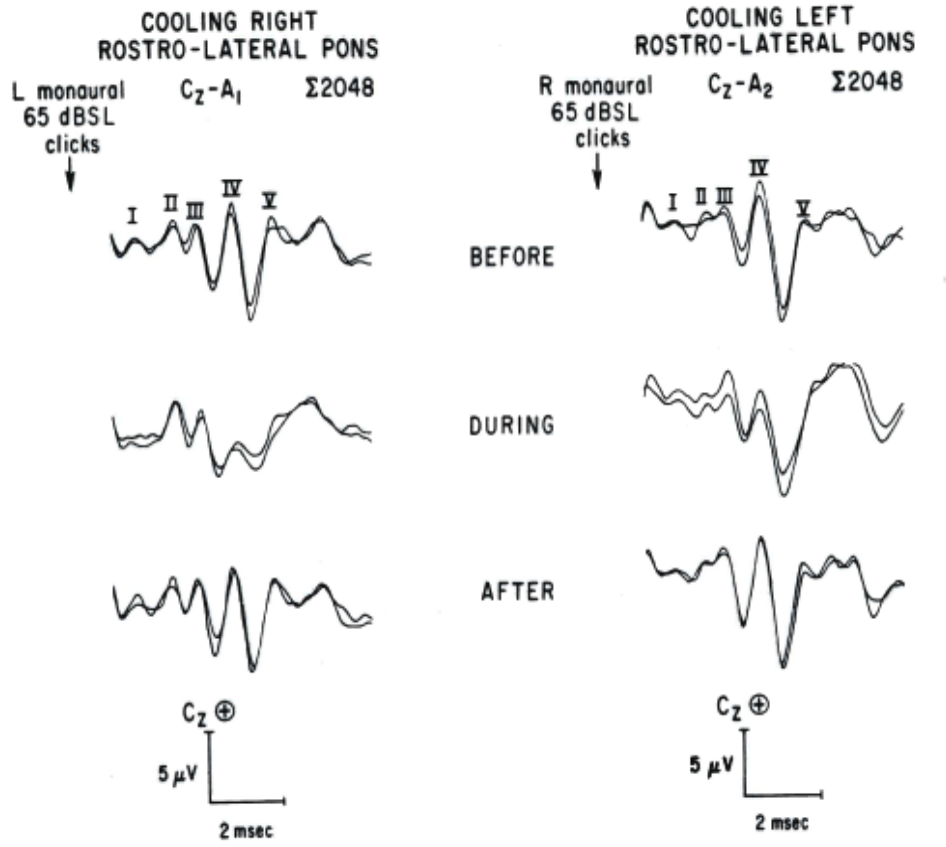

Figure 6. "Brainstem auditory evoked responses taken before, during and after unilateral cooling. Four cooling experiments are represented." Reprinted from "Application of Cryogenic Techniques in the Evaluation of Afferent Pathways and Coma Mechanisms," by T. A. Jones, J. J. Stockard, V. S. Rossier, and R. G. Bickford, 1976, *Proceedings of the San Diego Biomedical Symposium*, *15*, p. 252. Copyright 1976 by Academic Press, INC.

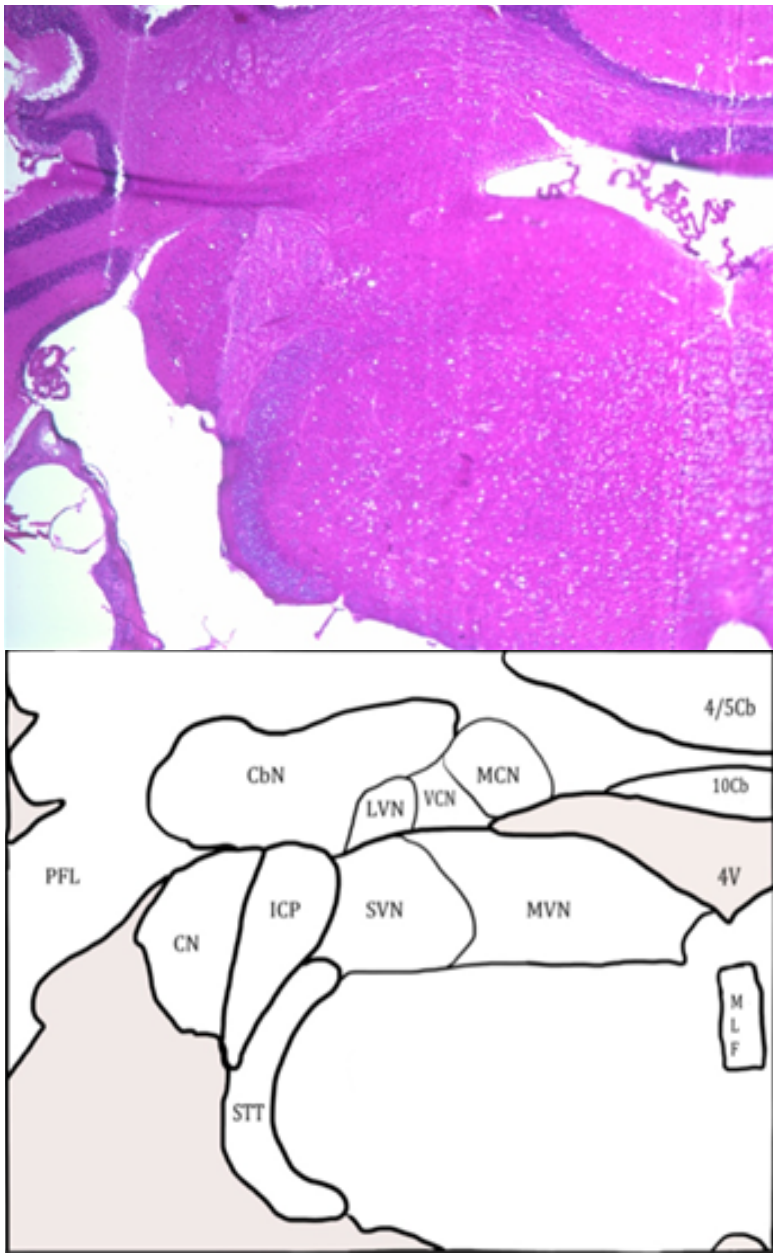

Figure 7. Histological brain section at the level of the pons of a normal mouse (hematoxylin and eosin stain). Structures were traced (Bamboo bit pad, Wacom) from the original digital image taken under the microscope. Labels for structures were made according to Franklin and Paxinos (2007). Labels: 4V-4th ventricle; CbN-cerebellar nuclei (interposed and lateral); CN-cochlear nuclei (dorsal and ventral); ICP-inferior cerebellar peduncle; 4/5Cb-cerebellar lobules 4 and 5; 10Cb-cerebellar lobule 10; LVN-lateral vestibular nucleus; M-medial longitudinal fasciculus; MCN-medial cerebellar nucleus; MVN-medial vestibular nucleus; PFL-paraflocculus; STT-spinal trigeminal tract; SVN spinal vestibular nucleus; VCN-vestibulocerebellar nucleus

CHAPTER II: EFFECTS OF KETOROLAC (TORADOL) ON MAMMALIAN AUDITORY AND VESTIBULAR SENSORY EVOKED POTENTIALS

Abstract

The NSAID ketorolac (Toradol) is a candidate for use as a supplemental analgesic during major surgery in anesthetized rodents. The use of ketorolac during surgery is believed to reduce the anesthetic dose required to achieve and maintain an adequate surgical plane and thus improve the physiological conditions and survival of animals during long experimental procedures. Ketorolac has reported side effects that include dizziness, "ear pain", hearing loss, tinnitus and vertigo in humans, but there has been no report of ketorolac's effect on the auditory and vestibular system in animal models. Thus, the use of ketorolac during studies of the inner ear in anesthetized animals is subject to question. The aim was to evaluate the acute effects of ketorolac on vestibular and auditory compound action potentials in the mouse (c57BL/6). This was accomplished by recording linear VsEPs and ABRs during administration of ketorolac at doses three to fourteen times the effective analgesic dose. VsEP and ABR results for ketorolac were compared to those from a control group maintained under anesthesia for the same period. There were no significant ketorolac-dependent effects on the temporal profiles of response latencies and amplitudes and no significant difference in the rate of change in response measures over time between controls and ketorolac-treated animals. These findings demonstrate that ketorolac can be used as an analgesic to supplement anesthesia in mice without concerns of modifying the linear VsEP or ABR.

Introduction

Prostaglandins are synthesized in cells throughout the body (Campbell & Halushka, 1996). Release of prostaglandins promotes inflammation, pain, and clotting function of platelets. Prostaglandins are produced by the enzyme cyclooxygenase (COX). NSAIDs block COX enzymes and reduce prostaglandin release and for that reason reduce inflammation, pain, and fever. NSAIDs thus are commonly used as systemic analgesics. Ketorolac (Toradol) is an NSAID that is commonly used by veterinarians to reduce "mild to moderate pain in rodents" (Plumb, 2008). Ketorolac has reported side effects including dizziness, ear pain, hearing loss, tinnitus and vertigo in humans (Bauman, 2003; Otti et al., 1997; Reinhart, 2000; Schaab et al., 1995). The anti-inflammatory properties of ketorolac have been shown to help prevent hearing loss during experimentally induced pneumococcal meningitis (Braunstein, Crenshaw, Morrow, & Adams, 2008) and its analgesic properties make it a candidate for use as a supplement to anesthesia in rodents. However, there have been no reports evaluating potential direct effects that ketorolac may have on vestibular or auditory function. Given the reported side effects in humans, it is reasonable to ask the question of whether acute administration of ketorolac alters vestibular and auditory function directly. The purpose of the present study was to evaluate this question using VsEPs (S. Jones et al., 1999) and ABRs as direct measures of peripheral and central vestibular and auditory function, respectively. VsEPs and ABRs were measured in control mice and in mice injected with increasing doses of ketorolac (i.e., 5, 10, 20, 40, 80 and 160 mg/kg).

Materials and Methods

The care and use of animals in the present study was approved by the Institutional Care and Use Committee of East Carolina University and conformed to all guideline of the National

Institutes of Health. Seventeen c57BL/6 mice weighing 23.0 g to 29.4 g (M = 27.1, SD = 1.8) were utilized in this study. They were obtained from The Jackson Laboratory (Bar Harbor, ME) or Charles River (Raleigh, NC). The mice were anesthetized [Ketamine (18 mg/mL)/Xylazine (2 mg/mL): 7 μL per gram of body weight], tracheotomized and intubated. Animals were ventilated with oxygen rich air [29% Nitrogen in Oxygen, 125 to 135 breaths per minute, 175-225 μL per stroke]. The percentage of arterial oxygen saturation (SpO_2) was measured using a clip light emitting diode sensor (TDR-43C) and monitored by a pulse oximeter [MED Associates Model: CANL-425SV-A (St. Albans, VT)]. Blood/gas levels were maintained with SpO_2 above 90%. A brain thermistor [Cole Parmer (Vernon Hills, IL)] was placed in the caudal cerebrum. Brain and rectal temperature were monitored and maintained between 36.8 and 37.5º C by a heat lamp and homeothermic heating pad (FHC Inc, Bowdoin, ME), respectively. Electrocardiographic (EKG) activity was monitored on an oscilloscope (rates ranged from 218 to 480 beats per minute (bpm), M = 354, SD = 75, n = 17). A lactated Ringer's solution was administered as needed subcutaneously to prevent dehydration. Animals evidencing poor physiological status (e.g., erratic or low heart rates) were excluded from the study. Animals were included provided they were recorded for at least one hour after baseline recordings and were given at least three increasing doses of drug.

Tissue overlying the skull was shaved, incised and retracted. Two stainless steel anchor screws (#00 x 4.7625 mm) were placed in the bone overlying the frontal sinus. A small hole was made parasagittally over the caudal cerebrum near the intersection of the sagittal and caudal coronal (lamdoid) sutures to access the dura. A bare stainless steel electrode was placed in the epidural space and the hole was sealed with bone wax. Plaster was poured to encase the anchor screws, the insulated portion of the electrode and a stainless steel thumbnut (1 cm diameter, 4-40

thread) placed on the midline. The thumbnut was used to secure the skull to an aluminum plate. The aluminum plate was attached to a mechanical shaker [LabWorks, INC Model: ET-132-203 (Costa Mesa, CA)]. The mechanical shaker was used to deliver linear acceleration stimuli in the naso-occipital axis (Figure 8). The motion of the shaker was monitored by an accelerometer [Vibra-Metrics Model: 1018 (Princeton Junction, NJ)] and adjusted to produce the acceleration and jerk stimulus waveforms.

ABR stimuli were delivered using a calibrated free-field speaker driver [Tucker Davis Technologies Model: FF1 (Alachua, FL)] placed 10.8 cm laterally from the right ear. Tone bursts were used to elicit auditory responses (8 kHz sine wave with a 3 ms onset ramp, 3 ms plateau and 3 ms offset ramp envelope). Sound levels were measured in decibels peak equivalent sound pressure level (dB peSPL). A calibrated microphone [Etymotic Research Model: ER7 (Elk Grove Village, IL)] was utilized to monitor sound pressure level at the external auditory meatus (EAM). The amplitude of the monitored stimulus waveform was visualized on an oscilloscope and the stimulus output voltage was adjusted using an attenuator [Tucker Davis Technologies Model: PA5 (Alachua, FL)] to obtain a stimulus level at the EAM of 60 dB peSPL for each animal.

VsEP stimuli were produced by applying a linear ramp voltage waveform (digital-to-analog conversion: 2 μs/point) to a power amplifier that in turn drove movements of the shaker and coupling platform. The amplitude of the applied waveform was adjusted using an attenuator to increase or decrease stimulus level. A linear ramp acceleration of 2 ms duration was utilized for the stimulus. The accelerometer output was routed to a calibrated electronic differentiator, which converted acceleration to jerk, the first derivative of acceleration (T. Jones et al., 2011; T. Jones et al., 1998). Jerk magnitude was determined from the output of the differentiator using an

oscilloscope. The amplitude of the jerk stimuli was measured as the mean peak jerk level and expressed in units of g/ms, where g = 9.81 m/s^2 and expressed in dB relative to 1.0 g/ms (S. Jones et al., 2002). A stimulus level of +6 $dB_{re:1.0g/ms}$ (i.e., 2.0 g/ms) was used throughout the study.

The electrode placed over the caudal cerebrum (noted above) was connected to the non-inverting input of a biological amplifier. The inverting electrode was placed subcutaneously below and behind the right pinna and the ground electrode was placed subcutaneously on the ventral neck. Electrophysiological signals were amplified [GRASS P511 Model: K, 200,000× (West Warwick, RI)] and filtered [300-3000 Hz, (-6 dB amplitude points)] for all ABR and VsEP recordings. Signal averaging was used to resolve responses in electrophysiological recordings. Stimuli were presented at a rate of 17/s. Analog-to-digital conversion was triggered at the onset of each stimulus (1024 points at 10 μs/point). Responses to normal and inverted stimulus polarities were collected and summed for a total of 256 sweeps per waveform. A binaural 90 dB SPL wide band (50 Hz to 50 kHz) forward masker (T. Jones & S. Jones, 1999) was presented during initial VsEP recordings of each study with a free field speaker driver [Tucker Davis Technologies Model: FF1 (Alachua, FL)] to confirm the absence of auditory components in VsEPs. After masking assessment was completed, the left ear was fully occluded with stopcock grease.

Ketorolac dose regimen and estimated drug levels:

Ketorolac is rapidly and completely absorbed, the maximum plasma concentration (Cmax) is achieved within ~15 minutes of administration, the pharmacokinetics are linear, it has a half-life (T1/2) of about 186 min and a reported plasma clearance rate (CL) of 0.43 ml/min/kg in the mouse (Mroszczak et al., 1987). The effective analgesic dose range for ketorolac is reportedly

between 0.5 and 10 mg/kg (Domer, 1990; Plumb, 2008; Jett et al., 1999; Rooks, Tomolonis, Maloney, Wallach, & Schuler, 1982; Pasloske, Renaud, Burger, & Conlon, 1999; Hillier, 1981; Rooks et al., 1985) and a dose of 200 mg/kg reportedly produces a 50% mortality rate (lethal-dose 50%, LD50; Plumb, 2008). Animals in the drug treatment group (n = 6), received a series of three to six incremental subcutaneous doses of ketorolac (5, 10, 20, 40, 80 and 160 mg/kg), where each successive dose was given at twenty-minute intervals. The treatment group included one animal that received the first three doses (maximum 20 mg/kg), one animal that received four doses (maximum 40 mg/kg), three animals that received five doses (maximum 80 mg/kg) and one animal that received a sixth dose (maximum 160 mg/kg). Thus all animals received cumulative doses well above the effective dose levels for analgesia (see Table 2). The volume injected was kept less than 400 μL. Ringer's solution was administered to the sham group (n = 5) at the same volumes and time intervals as the treatment group. A control group (n = 6) was given Ringer's solution once per hour to prevent dehydration. VsEP and ABR responses were recorded at approximately ten-minute intervals for all animals throughout each study thus including periods before and after each dose of ketorolac.

Using the CL (0.43 ml/min/kg) and T1/2 (186 min) values reported for the mouse (Mroszczak et al., 1987), one can provide estimates of the cumulative dose (D(t)), volume of distribution (V) and plasma concentrations (C(t)) resulting from the dose regimen in a mouse weighing 0.0275 kg (average weight of drug group). The estimates rely on the assumption that the drug is completely absorbed with subcutaneous injection, that the pharmacokinetics of ketorolac remains linear over the entire dose range and behave in accordance with a simple single compartment model. Volume of distribution can be calculated from CL and T1/2 using Equation 1:

Eq1: $V = (CL/k)* \text{weight}$,

where k is the rate of elimination constant and is given by $k = 0.69315/(T1/2)$ and "weight" is the weight of the “test” animal.

For a 0.0275 kg mouse, the estimated volume of distribution is:

$V = [0.43/(0.00373)]* 0.0275 = 3.17$ ml.

The maximum concentration for each dose is given by Equation 2:

Eq2: $C_{max} = Dose/V = Dose/3.17$ in mg/ml

After each dose (in mg), Cmax is achieved within 15 minutes and thereafter plasma levels decrease at a rate set by the rate of elimination constant, k. Estimated plasma concentration over time, C(t), is then given by Equation 3:

Eq3: $C(t) = (Dose/V) * e^{-kt}$, in mg/ml.

The dose per kg (mg/kg) as a function of time (D(t)) can also be written:

Eq4: $D(t) = (Dose/weight) * e^{-kt}$, where k is the elimination constant calculated above, "weight" is the mean weight of animals receiving drug (0.027 kg) and Dose is in mg.

Using Equations 3 and 4, drug levels remaining after each initial dose over time at each 20-minute time interval following injection were estimated. The remaining levels were summed from each injection at each 20-minute interval to produce an estimate of the total remaining dose at time, t. Table 2 summarizes the estimates for dose by weight (mg/kg) and plasma concentration levels (mg/ml) at each 20-minute interval over the time period of study.

Scoring response latencies and amplitudes:

For ABRs, three positive response peaks (i.e., P1, P4, and P5) and three negative response peaks (i.e., N1, N4, and N5) were used to quantify ABR responses and were identified as shown in Figure 5. These peaks represent neural responses generated by both peripheral (P1 and N1)

and central components (P2 and later) of the auditory sensory projections (Buchwald & Huang, 1975; Henry, 1979a). As illustrated in Figure 5, the appearance of P2 of the ABR was highly variable across study groups and in many cases was difficult to distinguish or was absent. P3 and N3 were also absent in one animal. Therefore, response peaks P2, N2, P3, and N3 were not used to quantify drug effects on the ABR. Peaks P4, N4, P5, and N5 were used as measures of central auditory function (i.e., brainstem). For VsEPs, three positive response peaks (i.e., P1, P2, and P3) and two negative response peaks (i.e., N1 and N2) were consistently present and were thus scored and used to measure effects (see Figure 3). P1 and N1 of the VsEP reflect peripheral vestibular nerve activity whereas peaks beyond N1 reflect the activation of central vestibular pathways (Nazareth & T. Jones, 1998). Peaks beyond P3 are highly variable and are thought to be myogenic and labile to anesthesia (T. Jones, 1992).

Response peak latencies were defined as the time, in μs, from the onset of the stimulus to the onset of the response peak. Peak-to-peak amplitudes were measured in μV and represent the difference in amplitude between a positive peak and a negative peak (e.g., P1-N1). Response amplitudes and latencies were documented before and after each dose administered. Normalized response values were calculated as the ratio of measured post-drug values to mean baseline value prior to drug administration.

Since drug levels were estimated to increase monotonically with time (e.g., Table 2), dose-dependent changes in response amplitude and latency would be expected to manifest as systematic changes with time were therefore evaluated. The change in response latencies and amplitude as a function of time. The single global hypothesis was as follows: ketorolac administration has no effect on vestibular and auditory responses. This was tested using repeated measures multivariate analysis of variance (RM MANOVA; SPSS 19.0; Ludbrook, 1998). The

RM MANOVA limited the number of animals that could be included from the sample (i.e., 5 shams, 6 controls and 5 drug-treated animals) and thus restricted the number of treatment doses analyzed to four (estimated cumulative dose: 33.6 mg/kg; estimated plasma level: 0.29 mg/ml). Thus for RM MANOVA, response measures were evaluated at four dose/time levels for within-subjects factors and contrasted across control and drug treatment groups for between-subjects factors. To include all animals and doses, a second quantitative test was also completed. In this case, the linear regression slope was used as a single metric for characterizing the drug effects over time on each response peak tracked (latency and amplitude versus time). Regression slopes were then compared between control, sham and drug treatment groups using MANOVA to determine the presence of drug or time effects. For MANOVA, response measures were evaluated across control and drug treatment groups as fixed factors.

Results

All animals had robust VsEP and ABR waveforms (e.g., Figure 9 and Figure 10). There were no significant differences between sham and control animals for VsEP and ABR response profiles over time with RM MANOVA for VsEP amplitudes, $F(2, 9) = 1.50$, $p = 0.29$, VsEP latencies, $F(4, 7) = 1.83$, $p = 0.26$, ABR amplitudes, $F(3, 8) = 2.12$, $p = 0.20$, and ABR latencies, $F(3, 8) = 4.23$, $p = 0.06$. There also were no significant differences between linear regression slopes of sham and control groups for any VsEP and ABR response component with MANOVA for VsEPs amplitudes, $F(4, 7) = 1.51$, $p = 0.31$, VsEP latencies, $F(5 ,6) = 2.24$, $p = 0.20$, ABRs amplitudes, $F(4, 7) = 1.38$, $p = 0.35$, and ABR latencies, $F(6, 5) = 0.28$, $p = 0.92$. Therefore, the sham and control groups were combined into one control group ($n = 11$) and the results for this control group were compared to those of the drug treatment group ($n = 6$) using RM MANOVA and MANOVA.

Response amplitude and latency profiles over time and dose level:

VsEP and ABR responses remained relatively stable over time despite the administration of high doses of ketorolac. Figures 11 and 12 illustrate the stability of VsEP and ABR waveforms recorded before and after the administration of ketorolac at cumulative doses of approximately 0, 33, and 135 mg/kg (0, 1, and 2 hours respectively). Response profiles over time are also presented for all animals in Figures 11 and 12. Normalized amplitudes and latencies for representative peripheral and central response peaks are shown in Figures 13 and 14 for both control and drug-treated animals. Baseline periods are represented to the left of the vertical dashed line, which marks time zero (t = 0 minutes). The first dose of ketorolac was administered at time zero. All response profiles were relatively flat over time indicating no general trend or major systematic influence of time or drug. This impression was confirmed quantitatively. Ketorolac administration had no significant effect on VsEP and ABR response amplitude and latency profiles (RM MANOVA). For both VsEPs and ABRs, there was no effect of treatment group (drug versus control) with Between-Subject Factor for VsEP amplitudes, $F(3, 13) = 2.95$, $p = 0.08$, ABR amplitudes, $F(3, 13) = 0.27$, $p = 0.84$, VsEP latencies, $F(4, 12) = 0.59$, $p = 0.68$, ABR latencies, $F(4, 12) = 0.61$, $p = 0.66$. For latencies and amplitudes of VsEPs, there were no effects of dose (time) with Within-Subject Factor for VsEP amplitudes, $F(9, 7) = 0.84$, $p = 0.62$, VsEP latencies, $F(12, 4) = 3.15$, $p = 0.27$, and no interaction between treatment groups and dose level for VsEP, $F(9, 7) = 2.92$, $p = 0.13$, and VsEP latencies, $F(12, 4) = 9.16$, $p = 0.10$. Similarly, there were no effects of dose/time for ABR amplitudes, $F(9, 7) = 1.55$, $p = 0.33$, and no interaction between dose and treatment groups, $F(9, 7) = 4.103$, $p = 0.07$. Interestingly, there was a small dose/time effect for ABR latencies. Latencies changed slightly over time during studies with Multivariate Within Subjects dose/time effects, $F(12, 4) = 2.62$, $p = 0.01$. However,

these reached significance only for some peaks (Greenhouse-Geisser Univariate Test: P1, p = 0.01, and P4, p = 0.05). This small effect can be appreciated from Figures 13 and 14. However, it should be noted that this was not a drug effect since the effect appeared in both treatment groups and there was no interaction between treatment groups and dose level, $F(12, 4) = 1.22$, p = 0.54.

Linear regression and response latency and amplitude as a function of time:

Regression slopes for amplitude and latency as a function of time were computed for all animals. The mean values of regression slopes for representative peripheral and central peaks are illustrated in Figures 15 and 16. There were no significant differences between the regression slopes of control and drug treatment groups with MANOVA for VsEP amplitudes, $F(4, 12) = 0.23$, p = 0.91, ABR amplitudes, $F(4, 12) = 0.86$, p = 0.52, VsEP latencies, $F(5, 11)$ = 0.91, p = 0.51, and ABR latencies, $F(6, 10) = 1.59$, p = 0.25.

Discussion

The present results clearly demonstrated that VsEP and ABR response parameters are unaffected by sequential administration of increasing doses of ketorolac. There were no significant differences in response profiles over time between the two treatment groups. Responses changed little over the period of drug administration despite estimated cumulative doses approaching or exceeding 146 mg/kg in most animals (4 of 6). Given the reported effective analgesic dose range of 0.5 to 10 mg/kg, the range of doses used in the present study represents levels of drug 3 to 14 times greater than those used for effective analgesia. There was no evidence of a drug-specific effect since there were no significant interactions between control and drug treated animals. These findings support the hypothesis that ketorolac has no

appreciable direct action on the auditory and vestibular sensory apparatus of the inner ear or on central neural relays.

As noted in the introduction, symptoms reported by humans during ketorolac administration include dizziness, ear pain, hearing loss, tinnitus and vertigo (Bauman, 2003; Otti et al., 1997; Reinhart, 2000; Schaab et al., 1995). The findings in animals lead one to question the likelihood of a direct acute action of ketorolac on neurosensory function in the inner ear of the human. It is possible that other effects of the drug mediate symptoms reported. The time frame for the appearance of symptoms in humans is not apparent from the literature. The effects of ketorolac acutely were evaluated over a period of about two hours. It is not possible to rule out effects of ketorolac that may require longer time to develop. There also may be subtle actions on the inner ear to which the VsEP and ABR are insensitive.

The subtle changes in latency observed herein might be due to a gradual change in temperature at the level of the inner ear or to minor adjustments in other physiological variables over the two-hour recording session. Although brain temperature was carefully monitored and controlled throughout all studies, the exact temperature of the inner ear during these studies was unknown.

The analgesic properties of ketorolac make it a candidate for use as a supplement to anesthesia in rodents. The present findings indicate that ketorolac may be used for that purpose acutely without producing significant changes in VsEP and ABR inner ear functional measures. Its use, however, should also take into consideration other drug effects especially those leading to longer clotting times.

Table 2

Dose schedules and resulting estimated cumulative dose and plasma concentration.

Time (min)	Dose (mg/lg)	Est. Cumulative Dose (mg/kg)	Est. Plasma Conc (mg/ml)
0	5	0.00	0.00
20	10	5.00	0.04
40	20	14.64	0.13
60	40	33.59	0.29
80	80	71.17	0.62
100		146.06	1.27
120		135.56	1.18
140		125.81	1.09

Note. The sequence presented represents five sequential doses at 20-minute intervals. Assumptions: Volume of distribution V = 3.17 mls. Weight = 0.028 kg (mean of treatment group). k = 0.0037 (half-life 3.1 hr).

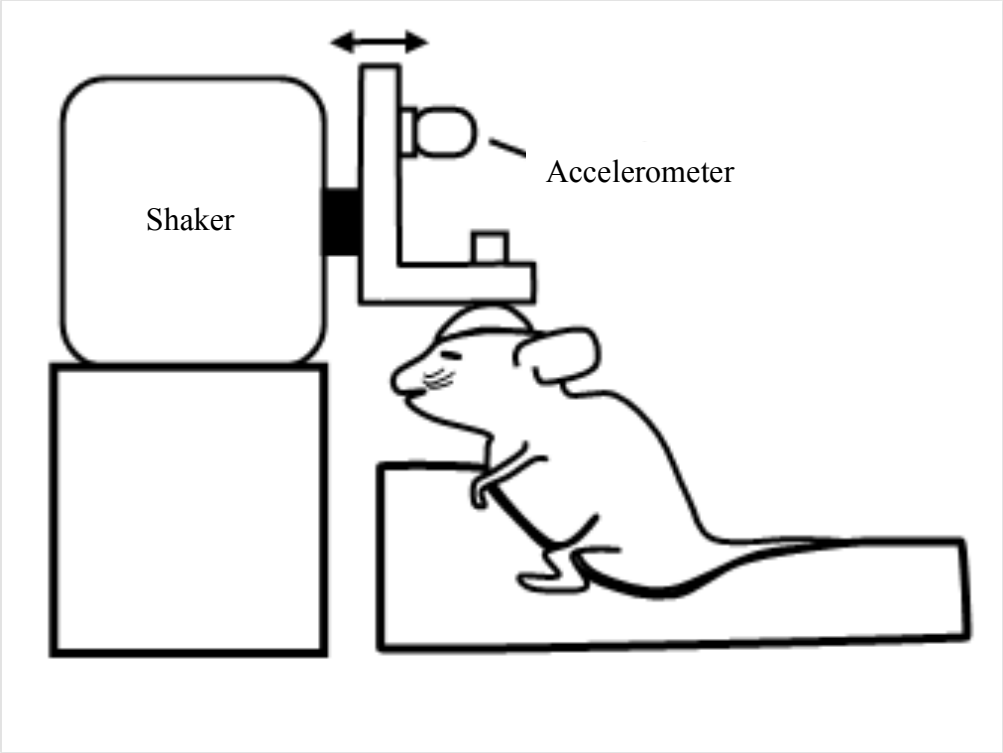

Figure 8. Schematic illustration of the coupling of the skull to the stimulus platform. The shaker shaft produces a transient head translation in the naso-occipital axis in the direction of the arrows. An accelerometer is mounted to the "L" bracket to monitor acceleration. The accelerometer output is electronically differentiated to monitor jerk levels in g/ms.

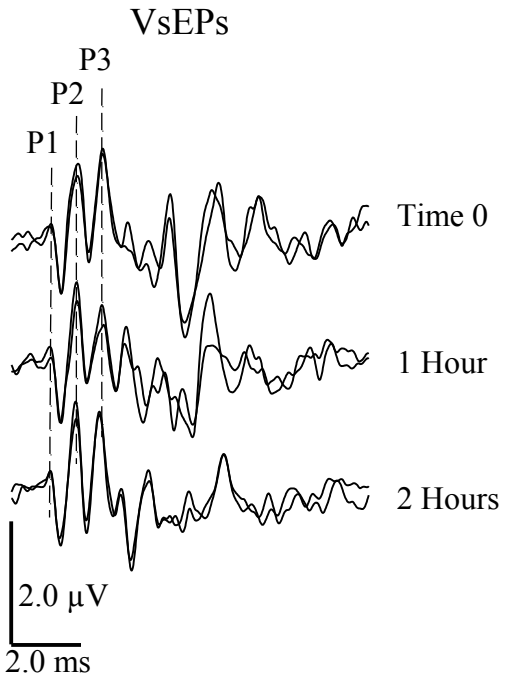

Figure 9. VsEPs stability over time. VsEPs were recorded over a period of two hours in a c57 BL/6 mouse with brain and rectal temperature stabilized at 37.0° C using a stimulus level of +6 dBre: 1.0g/ms. SpO_2 was maintained between 95-100% and heart rate remained above 300 beats per minute. Animal KET14. Positive peaks are labeled as P1, P2, and P3. Negative peaks (N1 and N2) are not marked here but represent the next negative minimum or peak voltage amplitude following the corresponding positive peak. Negative peaks are used to form response peak-to-peak amplitudes P1-N1, P2-N2, and P3-N2.

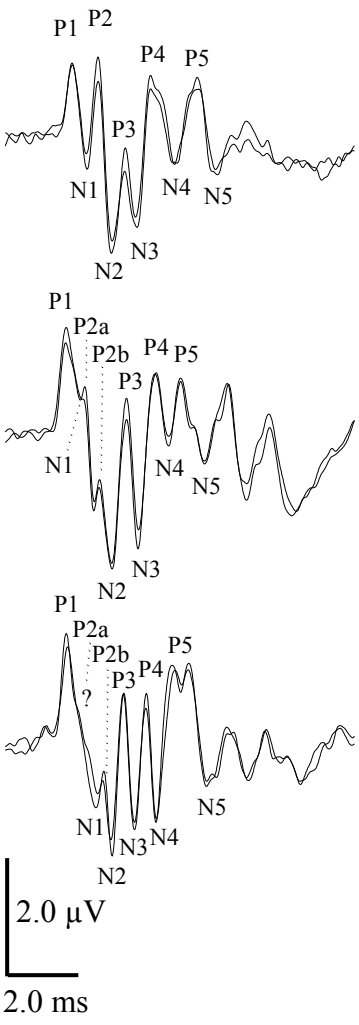

Figure 10. ABRs recorded from three mice (KET03, KET04, and KET11). All ABR responses shown demonstrate robust amplitudes for positive peaks P1, P3, P4, and P5. Positive peak P2 is clearly distinguished in the top waveform, but is only poorly formed or is missing components in the two lower sets of waveforms. This type of variability for P2 was common among animals, and for that reason, P2 was not included in quantitative assessments.

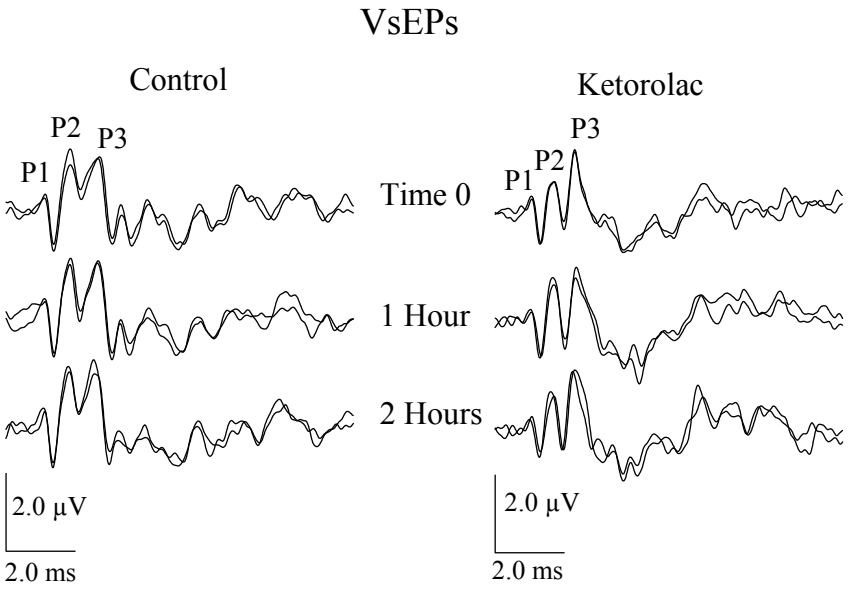

Figure 11. VsEP waveforms for one representative control mouse (left, KET11) and one representative mouse from the ketorolac treatment group (right, KET24). Waveforms demonstrate the stability of the VsEP over time in both control and drug treatment groups. Estimated cumulative doses of ketorolac were 0, 33, and 135 mg/kg at times 0, 1 and 2 hours, respectively. Positive peaks P1 through P3 are labeled.

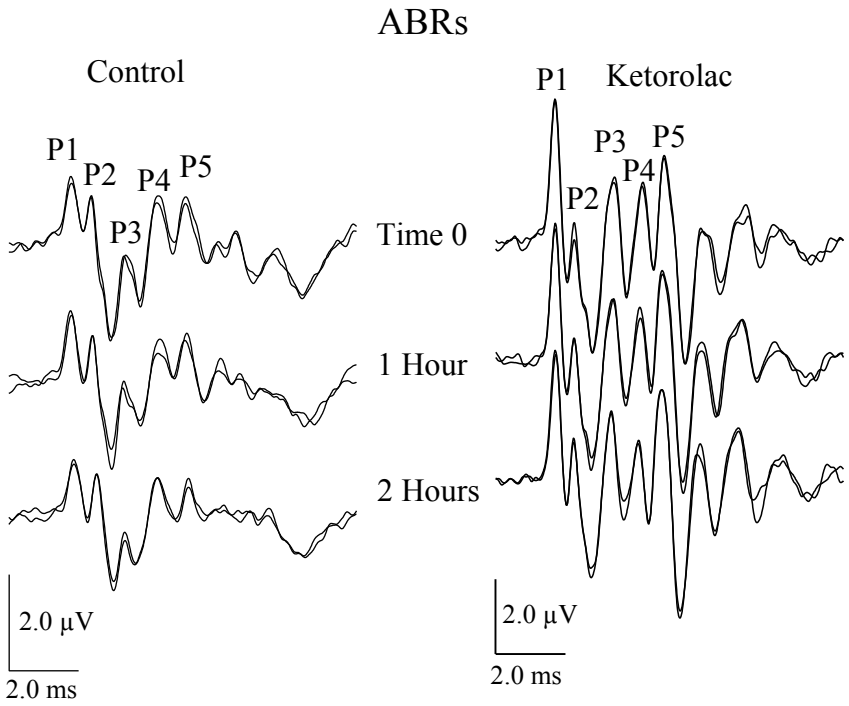

Figure 12. ABR waveforms for one representative control mouse (left, KET4) and one representative mouse from the ketorolac treatment group (right, KET26). Responses demonstrate the stability of the ABR over time in both control and drug treatment groups. Estimated cumulative doses of ketorolac were 0, 33, and 135 mg/kg at times 0, 1, and 2 hours, respectively. Positive peaks P1 through P5 are labeled.

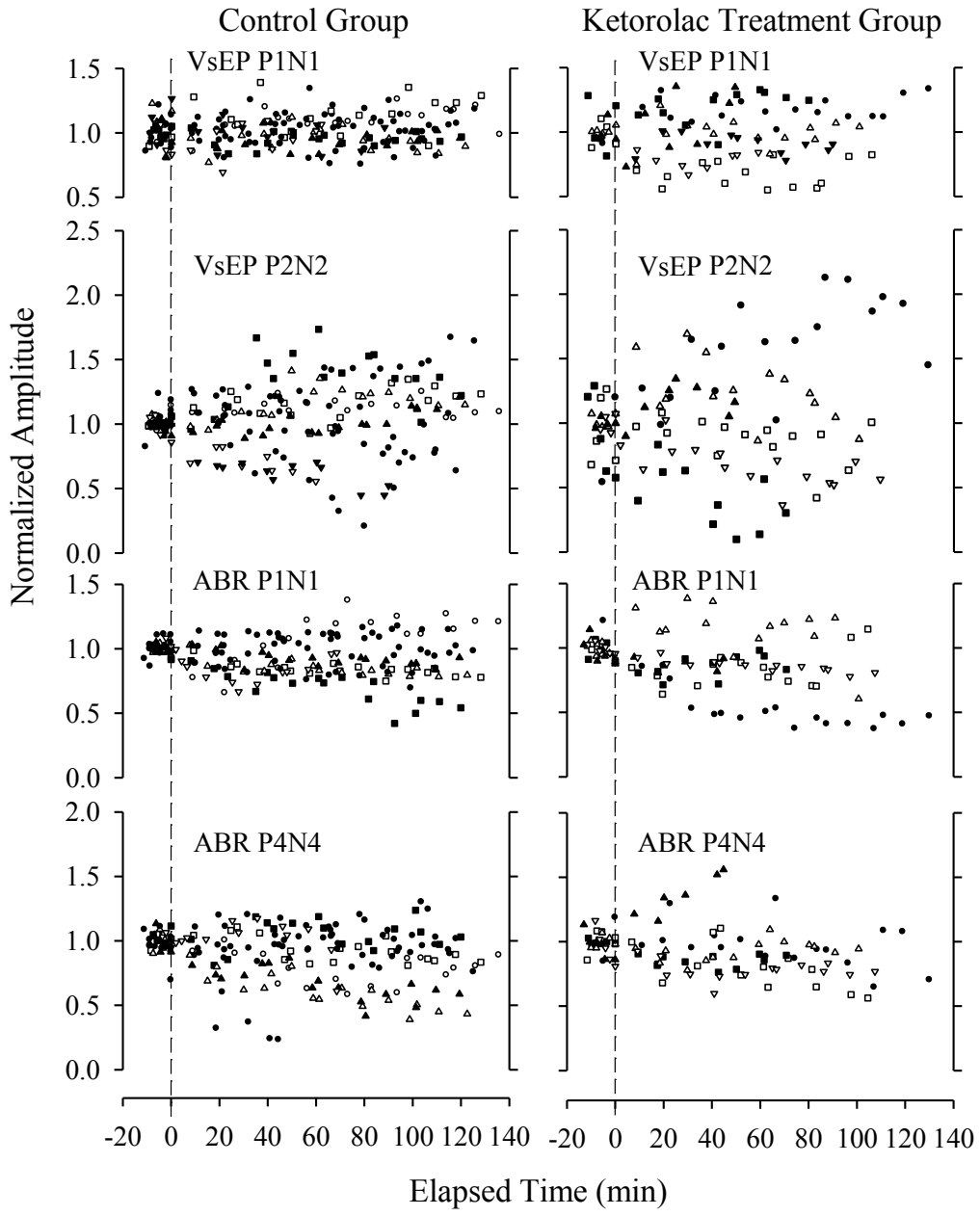

Figure 13. VsEP (above) and ABR (below) normalized response amplitudes as a function of time (in minutes) for control and ketorolac treatment groups. Data reflect response amplitude profiles over time/dose and includes data from all animals. Respective symbols represent individual animals. Cumulative maximum doses of ketorolac ranged from approximately 33 to more than 146 mg/kg. Time zero is the time of the initial dose of ketorolac. Data to the left of the vertical dashed line represent baseline recordings before drug administration.

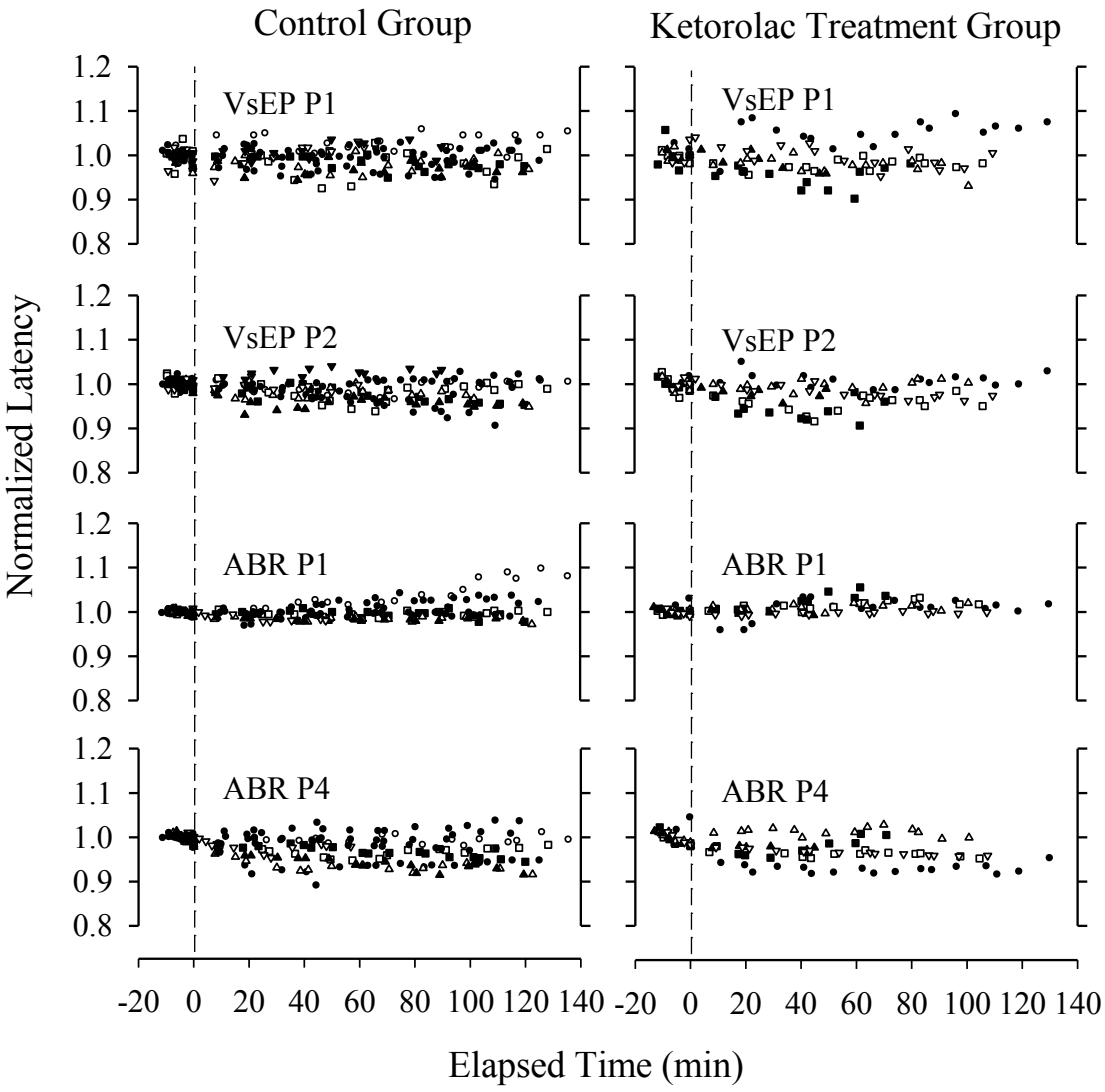

Figure 14. VsEP (above) and ABR (below) normalized response latencies as a function of time (in minutes) for control and ketorolac treatment groups. Data reflect response latency profiles over time/dose and includes data from all animals. Cumulative maximum doses of ketorolac ranged from approximately 33 to more than 146 mg/kg. Time zero is the time of the initial dose of ketorolac. Data to the left of the vertical dashed line represent baseline recordings before drug administration.

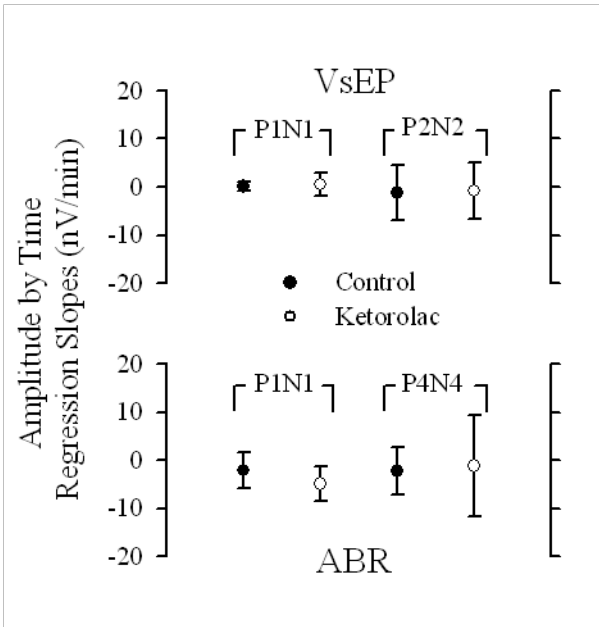

Figure 15. Mean linear regression slopes for amplitudes as a function of time expressed in nanovolts per minute. Two response peaks represent peripheral (P1-N1) and central (P2-N2 and P4-N4) components of the VsEP (top) and ABR (bottom) amplitudes. Solid black circles = control group. Open circles = drug group. Error bars represent one standard deviation from the mean.

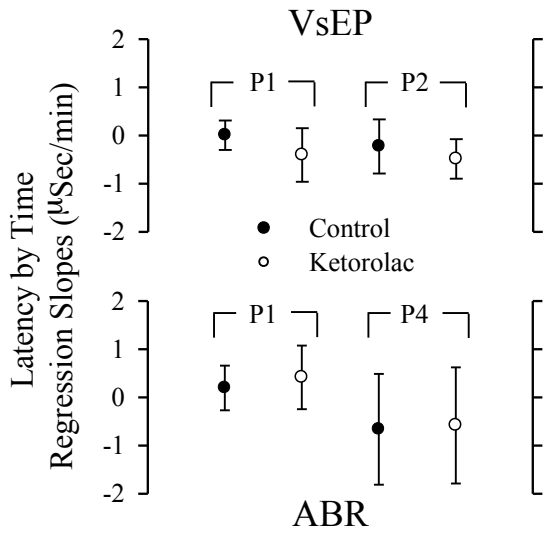

Figure 16. Mean linear regression slopes for latencies as a function of time expressed in microseconds per minute. Two response peaks represent peripheral (P1) and central (P2 and P4) components of the VsEP (top) and ABR (bottom) latencies. Solid black circles = control group. Open circles = drug group. Error bars represent one standard deviation from the mean.

CHAPTER III: EFFECTS OF STIMULUS DURATION ON MAMMALIAN LINEAR VESTIBULAR SENSORY EVOKED POTENTIALS

Abstract

Linear VsEP voltage ramp stimulus durations less than 1.0 ms altered the thresholds and amplitudes of the response (T. Jones et al., 2011; T. Jones et al., 1998). However, this effect has not been studied in detail and the effects on threshold have not been evaluated in the mammal. To better understand the stimulus duration effects on linear VsEPs, thresholds with durations shorter than 1.0 ms (i.e., 0.25, 0.50 and 0.75 ms) were evaluated and compared to thresholds of stimulus durations of commonly used stimuli (i.e., 1.0 and 2.0 ms). The present results revealed that stimulus durations less than 1.0 ms can increase VsEP thresholds in mammals. Durations of 1.0 and 2.0 ms produced thresholds similar to those reported for normal mice. The relationship between stimulus duration and threshold may provide insight into the transfer function of jerk stimuli from skull to the vestibular macular sensory epithelium. These results provide an estimate for the time constant for such transfer in mice. The time constant (τ) appears to be between 0.20 and 0.50 ms. This corresponds to frequency cutoffs (-3 dB) between 574 and 753 Hz.

Introduction

Short latency responses to pulsed linear head acceleration have been described in both mammals (e.g., Lange, 1988; Lange & T. Jones, 1989; Lange & T. Jones, 1990; Bohmer, Hoffman, & Honrubia, 1995; S. Jones et al., 1999; T. Jones & S. Jones, 1999; S. Jones, T. Jones, Bell, & Taylor, 2001; S. Jones et al., 2004; Mock, S. Jones, & T. Jones, 2011; T. Jones et al., 2011; Plotnik et al., 1997; Plotnik et al., 1999) and aves (e.g., T. Jones & Pedersen, 1989; Jones, 1992; S. Jones et al., 1997; S. Jones & T. Jones, 1996) and have been shown to be compound

responses from neurons innervating the macular epithelia. When a pulsed linear acceleration stimulus is applied to the skull, it activates vestibular receptors by causing shearing motion of the otolith structures overlying the macular sensory epithelium. The shearing motion in turn activates hair cells, which lead to a synchronous activation of vestibular primary afferents (e.g., De Vries, 1950; Fernandez & Goldberg, 1976). The VsEP is a physiological measurement of peripheral vestibular activation and the central volleys of the generated compound action potential (e.g., T. Jones & S. Jones, 2007; S. Jones, 2008). The VsEP is elicited by a pulsed linear acceleration of the head. VsEPs are composed of up to 6 peaks, which occur within 10 ms of stimulus onset. Early peaks, P1 and N1 of the VsEP reflect peripheral vestibular nerve activity whereas peaks beyond N1 reflect the activation of central vestibular pathways (Nazareth & T. Jones, 1991a; Nazareth & T. Jones, 1991b; Nazareth & T. Jones, 1998) excluding those projecting to the cerebellum and flocculus (see Chapter 4). Peaks beyond P3 are highly variable and are thought to be myogenic and labile to anesthesia (T. Jones, 1992).

Several studies have analyzed the effects of altering the properties of the adequate stimulus on VsEPs (T. Jones et al., 1998; T. Jones & Pedersen, 1989; T. Jones, 1992; S. Jones et al., 2001; T. Jones et al., 2011). Notably, the first four kinematic elements of linear head motion are: displacement, velocity, acceleration and jerk. "Jerk" is the primary kinematic element associated with linear VsEP response parameters in both birds (T. Jones et al., 1998) and mammals (T. Jones et al., 2011).

To produce the adequate VsEP stimulus, an acceleration ramp was used. The mathematical time derivative of this ramp (da/dt) is a rectangular pulse of kinematic jerk (Figure 17). Stimulus duration refers to the duration of the onset acceleration ramp and corresponding jerk pulse. T. Jones, et al. (2011) evaluated the effects of using stimulus durations of 0.50, 1.0, 2.0, and 4.0 ms

on response amplitudes in mice. They reported relatively constant amplitudes for durations of 1.0, 2.0 and 4.0 ms and a decrease in response amplitude for the shortest stimulus (0.50 ms). VsEP activation thresholds were not evaluated. Similar results were obtained in the bird where response amplitudes decreased and thresholds increased for the shortest stimulus (0.50 ms). The working hypothesis explaining a decrease in response amplitudes and elevated thresholds for 0.50 ms stimuli is that the time constant for stimulus transfer from skull to macular epithelium is on the order of 0.50 ms and hence a stimulus duration of 0.50 ms is too short to develop full stimulus force at the sensory epithelium. The purpose of the present study was to characterize mammalian VsEP activation thresholds at short durations (i.e., < 1.0 ms) for the first time. VsEP thresholds for stimulus durations of 2.0, 1.0, 0.75, 0.50 and 0.25 ms in mice were evaluated. The hypothesis was that VsEP thresholds would increase at stimulus durations less than 1.0 ms. The results provided insight regarding the temporal characteristics of jerk transfer from the skull to inner ear gravity receptors in mammals.

Materials and Methods

Eight c57BL/6 mice weighing 22.3 g to 26.1 g (M = 24.4, SD = 1.2) with ages 68 to 71 days-old (M = 69.4, SD = 0.92) were utilized in this study. They were obtained from Charles River (Raleigh, NC). The mice were anesthetized [Ketamine (18 mg/mL)/Xylazine (2 mg/mL): 7 μL per gram of body weight]. SpO_2 was measured using a clip light emitting diode sensor (TDR-43C) and monitored by a pulse oximeter (MED Associates Model: CANL-425SV-A). Blood/gas levels were maintained with SpO_2 above 90%. A brain thermistor [Cole Parmer (Vernon Hills, IL)] was placed in the caudal cerebrum. Brain and rectal temperature were monitored and maintained by a heat lamp and homeothermic heating pad (FHC Inc, Bowdoin, ME), respectively. EKG activity was monitored on an oscilloscope (rates ranged from 380 to

420 bpm; M = 392.5, SD = 16.1). Lactated Ringer's solution was administered as needed subcutaneously to prevent dehydration.

Tissue overlying the skull was shaved, incised and retracted. Two anchor screws were placed in the bone overlying the frontal sinus. A small hole was made parasagittally over the caudal cerebrum near the intersection of the sagittal and caudal coronal sutures to access the dura. A bare stainless steel electrode was placed in the epidural space and the hole was sealed with bone wax. Plaster was poured to encase the anchor screws, the insulated portion of the electrode and a thumbnut placed on the midline. The thumbnut was used to secure the skull to an aluminum plate. The aluminum plate was attached to a mechanical shaker [LabWorks, INC Model: ET-132-203 (Costa Mesa, CA)]. This mechanical shaker was used to deliver VsEP stimuli in the naso-occipital axis (Figure 8). The motion of the shaker was monitored by an accelerometer [Vibra-Metrics Model: 1018 (Princeton Junction, NJ)] and adjusted to produce the acceleration and jerk stimulus waveforms.

VsEP stimuli were produced by applying a linear ramp voltage waveform (D/A conversion 2 μs/point) to a power amplifier that in turn drove movements of the shaker and coupling platform (with attached accelerometer for stimulus monitoring). The amplitude of the applied waveform was adjusted using an attenuator to increase or decrease stimulus level. Linear ramp accelerations of 0.25, 0.50, 0.75, 1.0 and 2.0 ms duration were utilized for the stimuli. The accelerometer output was routed to a calibrated electronic differentiator, which converted acceleration to its first derivative (i.e., jerk; T. Jones et al., 1998). Jerk magnitude was determined from the output of the differentiator using an oscilloscope. Ringing at the onset of the stimulus is commonly reported and was apparent in the present study. The amplitude of all jerk stimuli were adjusted such that the amplitude of the first peak was 1.0 g/ms at 0 dB

attenuation, where g = 9.81 m/s^2 and all stimulus levels were expressed in dB relative to 1.0 g/ms (S. Jones et al., 2002). For stimulus durations of 0.50 and 0.25 ms, this adjustment resulted in maximum peak jerk levels that were 2.7 dB below those of longer duration stimuli (Figure 18). This difference in peak amplitude was taken into consideration and corrected in the final calculations of threshold (i.e., scored thresholds for 0.50 and 0.25 ms stimuli were lowered by 2.7 dB).

VsEP responses were recorded for stimuli initially at +6 $dB_{re: 1.0 g/ms}$, then decreased to -18 dB and then increased successively in 3 dB steps (i.e., threshold seeking protocol). Each animal received five stimulus duration threshold-seeking protocols where VsEP threshold was documented for the five stimulus durations.

The electrode placed over the caudal cerebrum (noted above) was connected to the non-inverting input of the preamplifier. The inverting electrode was placed subcutaneously below and behind the right pinna and the ground electrode was placed subcutaneously on the ventral neck. Electrophysiological signals were amplified (GRASS P511 Model: K, gain = 200,000) and filtered [300-3000 Hz, (-6 dB amplitude points) VsEP recordings. Signal averaging was used to resolve responses in electrophysiological recordings. Stimuli were presented at a rate of 17/s. Analog-to-digital conversion was triggered at the onset of each stimulus (1024 points at 10 μs/point). Responses to normal and inverted stimulus polarities were collected and summed for a total of 256 sweeps per waveform. For each study, a binaural 90 dB SPL wide band (50 Hz to 50 kHz) forward masker (T. Jones & S. Jones, 1999) was presented during initial VsEP recordings [free field speaker driver (Tucker Davis Technologies Model: FF1, Alachua, FL)] to confirm the absence of auditory components in VsEPs.

VsEP Response Characteristics: Two positive response peaks (i.e., P1 and P2) and two negative response peaks (i.e., N1 and N2) were consistently present (see Figure 19). P1 and N1 of the VsEP reflect peripheral vestibular nerve activity whereas peaks beyond N1 reflect the activation of central vestibular pathways (Nazareth & T. Jones, 1998) excluding those to the cerebellum and flocculus (see Chapter 4). Peaks beyond P3 are highly variable and are thought to be myogenic and labile to anesthesia (T. Jones, 1992). Threshold was defined as the stimulus intensity between two levels of stimuli, one that produced minimal vestibular activation and the second where vestibular activation could not be detected in the VsEP waveform. Thresholds are reported in dB relative to 1.0 g per ms. Response thresholds were documented in each animal for all five rise times (i.e., 0.25, 0.50, 0.75, 1.0, and 2.0 ms).

Threshold Comparisons: Three individuals scored thresholds and results were compared between individuals for interrater reliability (intraclass correlation coefficient = 0.84, CI: 0.75-0.91; Shrout & Fleiss, 1979). Scores were highly correlated and therefore the mean value across scores was calculated and used for comparisons. Data were grouped according to stimulus duration.

Results

Threshold results are summarized in Figure 20 and Table 3. Stimulus duration had a significant effect on VSEP thresholds with one-way ANOVA, $F(4, 4) = 24.23$, $p < 0.01$. The mean threshold for the 0.25 ms duration stimulus was significantly higher than means for 1.0 and 2.0 duration stimuli (~3.5 dB, Fisher's Least Significant Difference, $p < 0.01$). Mean thresholds for 0.50 and 0.75 ms stimuli were not significantly different than those of 1.0 and 2.0 ms (Fisher's Least Significant Difference, $p > 0.05$). Thresholds values for stimulus durations (dB re: 1.0 g/ms) of 1.0 and 2.0 ms (1.0 ms: $M = -12.06$, $SD = 1.32$; 2.0 ms: $M = -12.16$, $SD = 1.49$)

were comparable to those reported for VsEP thresholds in normal mice (e.g., T. Jones & S. Jones, 1999; S. Jones et al., 2002). Thresholds varied for 0.25, 0.50 and 0.75 ms (0.25 ms: *M* = -8.54, *SD* = 3.26; 0.50 ms: -10.22, *SD* = 0.32; 0.75 ms: *M* = -10.38, *SD* = 1.27).

Discussion

The present findings demonstrate that VsEP response thresholds in mice are dependent on stimulus durations less than 1.0 ms. VsEP thresholds or amplitudes for durations of 1.0 ms and longer have been shown to be independent of stimulus duration in the mammal (T. Jones, et al. 2011) and in the bird (T. Jones et al. 1998). These observations are consistent with these findings and provide new evidence for altered thresholds at stimulus durations of 0.25 ms. In the earlier reports reduced amplitudes (mammal) or elevated thresholds (bird) were described for a stimulus duration of 0.50 ms. These findings indicate that vestibular activation in otoconial organs evidences a preference for stimulus durations 1.0 ms or greater and such stimuli appear to be therefore most suitable for functional vestibular assessment in mice.

The time constant for the transfer of mechanical stimuli from the surface of the skull to the macular sensors in the inner ear of mammals and birds is unknown. The activation of the VsEP is dependent upon such transfer and therefore is subject to any temporal transfer restrictions in the activation process. Transfer functions are often represented by their corresponding time constants, which specify the time required to achieve 63% of full transfer (-3 dB). The results of the present study are consistent with the idea of a timing limit in the transfer of the jerk stimulus to sensors and suggest further that this limit begins to elevate thresholds for stimulus durations less than 0.50 ms. Although more detailed studies would be required to carefully define the transfer timing, one can suggest based on data from the mouse here and bird previously that the transfer time constant is likely on the order of 0.20 to 0.50 ms. This corresponds to a frequency

cutoff (-3 dB) between 574 and 753 Hz, where $f = 1/(2\pi\tau)$ and $\tau = 0.5 \times 10^{-3}$ and 0.2×10^{-3} s respectively. These values are slightly higher than those reported for the turtle recently (e.g., 328-397 Hz; Dunlap, Spoon, & Grant, 2012) and raise the question of whether transfer of translational energy to sensory epithelia in mammalian and perhaps avian systems accommodates higher frequencies than those of poikilotherms.

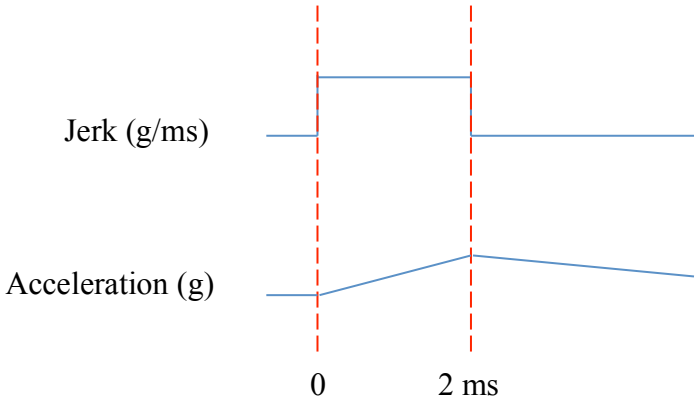

Figure 17. Stimuli. A standard onset acceleration ramp is used to produce a rectangular jerk stimulus of 2.0 ms duration. Jerk is the rate of change in acceleration, da/dt.

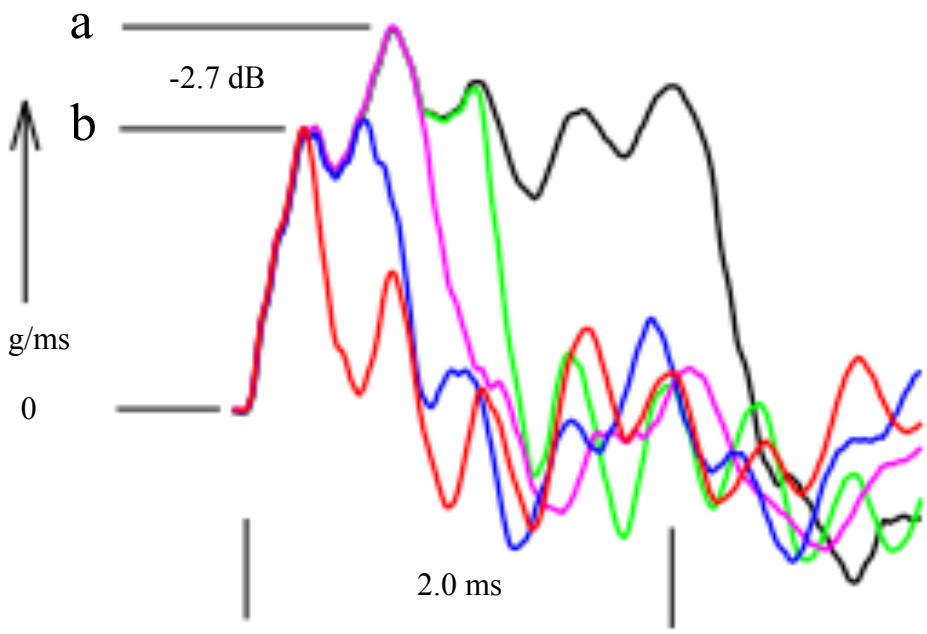

Figure 18. Recordings of stimulus jerk (in g/ms) used in the present study (i.e., 2.0 ms-black, 1.0 ms-green, 0.75 ms-pink, 0.50 ms-blue, 0.25 ms-red). For stimulus durations of 2.0, 1.0 and 0.75 ms peak amplitude was constant and equivalent (i.e., level "a"). For durations of 0.50 and 0.25 ms, peak amplitude was 2.7 dB less (i.e., level "b"). To correct for lower stimulus amplitude thresholds were corrected (i.e., lowered 0.50 and 0.25 ms by 2.7 dB).

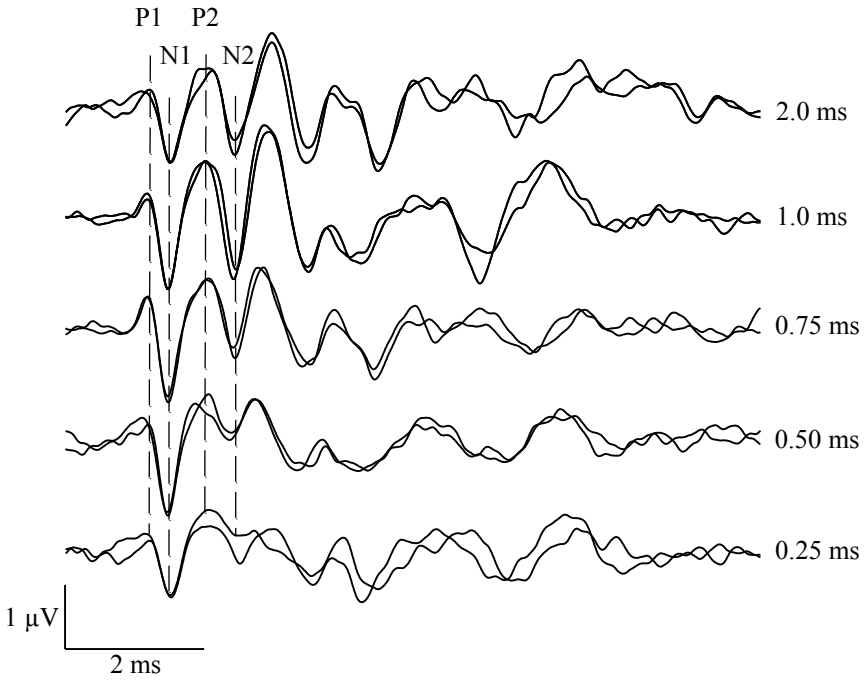

Figure 19. Representative VsEP waveforms recorded at various stimulus durations (i.e., 2.0, 1.0, 0.75, 0.50, and 0.25 ms). Two positive response peaks (i.e., P1 and P2) and two negative response peaks (i.e., N1 and N2) were consistently present and were thus scored and used to measure effects.

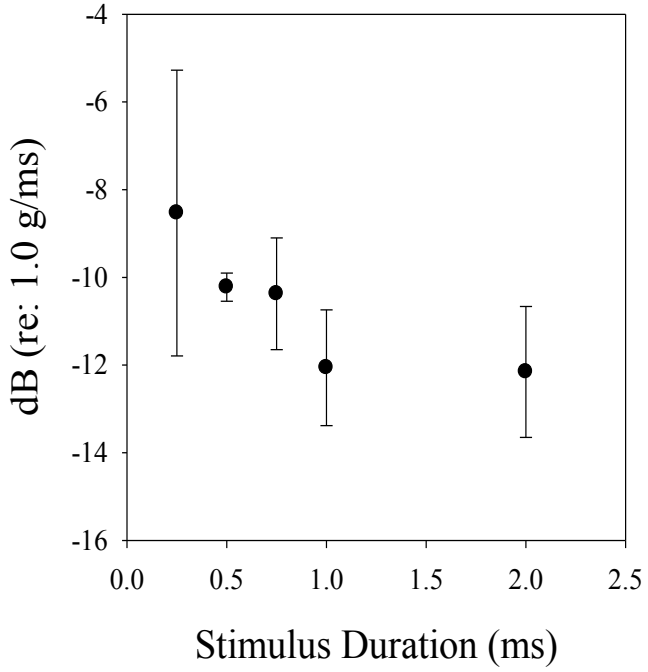

Figure 20. Mean VsEP thresholds measured for five stimulus durations in c57BL/6J mice. Stimulus duration (rise time) had a significant effect on threshold (RM MANOVA, $p = 0.01$). Error bars represent one standard deviation from the mean.

Table 3

VsEP thresholds means and standard deviations during various stimulus duration studies in c57BL/6J mice.

Stimulus Duration (ms)	VsEP Threshold $M \pm SD$ ($n = 8$)
2.0	-12.16 ± 1.49
1.0	-12.06 ± 1.32
0.75	-10.38 ± 1.27
0.50	-10.22 ± 0.32
0.25	-8.54 ± 3.26

CHAPTER IV: NEURAL GENERATORS OF MAMMALIAN LINEAR VESTIBULAR SENSORY EVOKED POTENTIALS

Abstract

The linear VsEP is thought to be the compound electrical response of peripheral macular neurons and central neural relays and as such, is used to directly assess macular function. The VsEP is used in animal research to study, among other things, the genetic basis of deafness and balance disorders. Although the neural generators of the linear VsEP have been described in the bird (Nazareth & T. Jones, 1998), the precise central neural generators have not been documented for the mouse model. Because the mouse is such a valuable model in vestibular research, it was important to clearly identify the peripheral and central generators of VsEPs in mice. VsEPs were recorded before and after strategic surgical manipulations of vestibular pathways. This included isolation of the eighth nerve from central relays and destruction of central candidate neural generators. The extent of lesions was characterized histologically and changes in response components were documented. Response components critically dependent on particular peripheral and central structures were identified. Findings confirmed that the VsEP is critically dependent on the labyrinth bilaterally, that each labyrinth contributes approximately equally to amplitudes (~50%) and that key central structures including the cerebellum and flocculus do not contribute appreciably to the VsEP response. These studies have increased the understanding of the neural generators of the VsEP, and in turn, enhanced the ability to assess peripheral and central vestibular function and detect vestibular disease.

Introduction

In recent years, numerous genes have been discovered that play essential roles in the normal inner ear. Mutations in many of these genes have been linked to human deafness and vestibular

dysfunction. In mice, it is often the case that the same genetic mutation produces similar otological pathologies thus providing an important animal model for in depth study. Understanding the functional deficits associated with these genetic changes is an important part of understanding the disease process itself. The linear VsEP was developed to provide a noninvasive direct assessment of vestibular function and it is used to study genetic models of human disease (S. Jones, 2008). The VsEP is the vestibular analog to the auditory ABR.

VsEPs are vestibular compound action potentials that are recorded in response to head translation. The VsEP waveform is comprised of a series of positive and negative peaks that are believed to be generated by neurons making up the vestibular peripheral and central pathways (Figure 3). Although, work in birds (Nazareth & T. Jones, 1998) has demonstrated that the earliest response peaks are dependent on the integrity of the vestibular nerve (P1 and N1), the exact origin of the later peaks (beyond P2) have yet to be described. Presumably, vestibular afferent action potential volleys lead to the generation of action potentials in post-synaptic cells in the brainstem VNC (e.g., superior, lateral, medial, and inferior nuclei) and cerebellum. These in turn lead to the activation and inhibition of other vestibular circuits. In the proposed work, central neural activity and associated structures contributing to the VsEP waveform were sought. The neural pathways and nuclei mediating central response activity are therefore candidate neural generators of the VsEP.

Vestibular Pathways:

Two reviews of the VNC's afferent and efferent connection have been offered recently (Barmack, 2003; Newlands & Perachio, 2003). The following is a brief account drawn in part from information offered in these reviews. Vestibular primary afferents of the eighth nerve synapse with the macular and ampular organs peripherally. The superior vestibular nerve

innervates the neuroepithelia of the anterior (superior) and horizontal canals, the utricle and about one third of the saccule (anterosuperior portion), while the inferior vestibular nerve innervates the posterior canal and the other two-thirds of the saccule (e.g., cat: Gacek, 1969; squirrel monkey: Honrubia et al., 1987; and mouse: T. Jones et al., 2008). Vestibular primary afferents project from all vestibular end organs (i.e., maculae and ampulae) to the VNC of the brainstem as well as to the cerebellum where the majority of primary afferent projections terminate in the uvula and nodulus (cerebellar lobules IXd and X respectively; e.g., Barmack et al., 1993; Gerrits et al., 1989; Newlands & Perachio, 2003). The vestibular nuclei also receive afferents from the cerebellum, reticular formation, spinal cord, contralateral vestibular nuclei as well as other sensory systems (e.g., Barmack, 2003). Thus, the outflow of the vestibular nuclei reflects the integration of many motor and sensory systems including visual and somatosensory systems. Various neural tracts are formed from the outflow of the vestibular nuclei. Ascending projections from vestibular nuclei make up portions of the medial longitudinal fasciculus (MLF) and have bilateral projections to thalamus (e.g., Blum et al., 1979; Shiroyama et al., 1999), the interstitial nucleus of Cajal, unilateral and bilateral projections to the oculomotor (III), abducens (VI) and trochlear (IV) cranial nerve nuclei and the cerebellum (e.g., Barmack, 2003; Parent, 1996).

Descending projections from the lateral vestibular nuclei are somatotopically organized and project to the spinal cord as the lateral vestibulospinal tract, while descending efferents of the medial vestibular nucleus project as the medial vestibulospinal tract. The vestibulospinal tracts activate and inhibit alpha motor neuron pools throughout the spinal cord, which have direct influence on head, neck and trunk musculature and contribute to the maintenance of balance.

The thalamus is the major relay point for vestibular-cortical projections. Outflow of the vestibular nuclei projects to the ventrobasal thalamus and thalamic neurons project to the cortex where vestibular sensation is processed (e.g., Shiroyama et al., 1999). Other projections from vestibular nuclei include commissural fibers, which make reciprocal connections between the left and right VNC.

Many of the above structures represent candidate neural generators for the linear VsEP. Neural sectioning was used to interrupt specific projections between the sensory organs and the VNC, as well as between the VNC and the cerebellum, as done previously (Nazareth & T. Jones, 1998). In addition, we aspirated selected regions of the cerebellum were aspirated to identify regions critical and not critical to VsEP components (e.g., nodulus, uvula, flocculus, etc.).

In general, the main objective of this research was to better understand which structures among the vestibular pathways make substantial contributions to the VsEP waveform. The hypothesis of this study was that each respective peak of the VsEP is associated with specific peripheral or central vestibular structures. The initial aim for this work was to distinguish components of VsEPs that are generated by peripheral neurons from those generated by central vestibular structures including the cerebellum. Based on work in the bird, the hypothesis was that P1 and N1 are generated by the vestibular nerve and that P2 and beyond are generated by the brainstem, cerebellum or other central structures. The proposed strategy was to surgically interrupt the vestibular nerve as it enters the vestibular nuclei and cerebellum. The second aim was to distinguish brainstem versus cerebellar generators of the VsEP. The hypothesis was that the cerebellum contributes significantly to the VsEP response. This was tested by aspiration and by inducing lesions in the cerebellum. In separate experiments, specific regions of the cerebellum (e.g., flocculus, lobules IXd, X, etc.) or major pathways between brainstem and

cerebellum were lesioned or sectioned. VsEPs were recorded before and after surgical manipulations. Histology was used to characterize site and extent of lesions in all studies. The third aim was to examine the individual contribution of each labyrinth to the VsEP. Research had demonstrated that the VsEP requires an intact vestibular labyrinth, however the contribution of each labyrinth has not been systematically evaluated. It was hypothesized that each labyrinth makes comparable contributions. To test this hypothesis, VsEPs were recorded before and after isolation of a single labyrinth and followed by ablation of the second labyrinth.

Expectations based on linear VsEPs in birds and rotary VsEPs in mammals:

VsEPs elicited by transient rotary stimuli have also been described (e.g., Elidan et al., 1987a). They have been shown to be dependent on the inner ear (e.g., Elidan et al., 1986; Elidan et al., 1987b; Li et al., 1993) and are thought to be generated in large part by ampular sensors but also reflect activity from macular organs (Li et al., 1995; Trimble & S. Jones, 2001). Generator studies reported by Li and colleagues provide evidence that P1 of rotary VsEP reflects peripheral whereas later peaks reflect central brainstem nuclei (e.g., Li et al., 1993; Li et al., 1997). In the case of linear VsEPs, Nazareth and T. Jones (1998) demonstrated in the bird (i.e., chicken, *Gallus domesticus*) that P1 remains intact and P2 amplitude decreases after a proximal isolation of the eighth nerve from the brainstem, while peaks beyond P2 are abolished. With this type of lesion, only the ipsilateral eighth nerve remains as a candidate generator for P1 while generators of later peaks must arise from central vestibular projections. This includes brainstem and/or cerebellar structures. Based on these studies, the expectation was to find evidence in the mouse that P1 of the linear VsEP reflects peripheral activity whereas peaks beyond P2 reflect central activity. These studies critically examined this hypothesis in mice. Virtually nothing to date was known regarding the role of the cerebellum in generating VsEP components. These studies

evaluated the effects of both cerebellar and brainstem lesions on VsEPs to identify their contributions or absence thereof.

Several studies had to be completed to evaluate the stability of the VsEP response under normal conditions. The effects of altering brain temperature had been shown to alter response latencies and amplitudes of VsEPs in the bird and ABRs in the mouse as well as other species (e.g., T. Jones & Pedersen, 1989; Nazareth & T. Jones, 1998; Henry, 1979b; T. Jones et al., 1980; Marsh et al., 1984; Lee, Suarez, Newman, & Honrubia, 1990). In the following studies brain temperature was maintained to prevent substantial latency variation. The relationship between temperature and VsEP peak latencies and peak amplitudes had not been described for the mammal although it has been reported for the bird (e.g., T. Jones & Pedersen, 1989; Nazareth & T. Jones, 1998). Additionally, the effects of stimulus duration were evaluated. The results are reported in Chapter 3.

Methods

Animals

Normal c57BL/6J mice (The Jackson Laboratory, Bar Harbor, ME) were used in the proposed studies. The care and use of the animals were approved by the East Carolina University Animal Care and Use Committee (protocol # P057) and can be found in Appendix A. Weights for the mice ranged from 25 to 30 grams.

Anesthesia and Physiological Support

Mice were injected intraperitoneally with a mixture of Ketamine (18mg/ml) and Xylazine (2 mg/ml) to induce anesthesia (0.07 cc/10 grams of body weight). Maintenance doses (one-half original dose) were given as needed to maintain a deep surgical plane of anesthesia. Rectal temperature was maintained at 37.0 ± 0.2º C by a direct current temperature regulation system

(i.e., servo-controlled heating pad, FHC Model: 40-90-8D). A tracheotomy and cannulation of the trachea was performed and oxygen enriched air was delivered via a mechanical ventilator. SpO_2 was measured via clip light emitting diode sensor (TDR-43C) and monitored by a pulse oximeter (MED Associates – Model: CANL-425SV-A). Blood/gas levels were maintained with SpO_2 at 95-100%. EKG was used to monitor heart rate. A lactated Ringer's solution was administered as needed subcutaneously to prevent dehydration.

The methods used to record VsEPs have been reported in detail (e.g., S. Jones & T. Jones, 1996; T. Jones & S. Jones, 1999; S. Jones & T. Jones, 2000; S. Jones et al., 1997; T. Jones et al., 1998). They are described here as well.

Skull Preparation and Coupling to Mechanical Shaker

Tissue overlying the skull was shaved, incised and retracted. Two anchor screws were placed in the bone overlying the frontal sinus (Figure 21). A small hole was made parasagittally over the caudal cerebrum near the intersection of the sagittal and caudal coronal sutures to access the dura. A bare stainless steel electrode was placed in the epidural space and the hole was sealed with bone wax. Plaster was poured to encase the anchor screws, the insulated portion of the electrode and a thumbnut placed on the midline. The thumbnut was used to secure the skull to an aluminum plate. The aluminum plate was attached to a mechanical shaker (Labworks, Inc. Model 132-203B). This mechanical shaker was used to deliver VsEP stimuli in the naso-occipital axis (Figure 8). The motion of the shaker was monitored by an accelerometer and adjusted to produce the acceleration and jerk stimulus waveforms. Bone was removed to expose the cerebellum and enable access to the medial surface of the temporal bone and brainstem for aspiration and sectioning experiments.

Vestibular Stimuli

Stimuli were produced by applying a linear ramp voltage waveform (D/A conversion 2 μs/point) to a power amplifier that in turn drove movements of the shaker and coupling platform (with attached accelerometer, Figure 8). The amplitude of the applied waveform was adjusted systematically [Tucker Davis Technologies (TDT) PA5 attenuators (Alachua, FL)] to increase or decrease stimulus level. Generally, a linear ramp acceleration of 2.0 ms duration was utilized. Shorter durations 1.0 and 0.50 ms were also used where noted. The accelerometer output was routed to a calibrated electronic differentiator, which converted acceleration to its first derivative (i.e., jerk; T. Jones et al., 1998). Jerk magnitude was determined from the output of the differentiator using an oscilloscope. The amplitude of jerk stimuli was measured as the mean peak jerk level and expressed in units of "g per ms", where g is 9.81 m/s^2 and expressed in dB relative to 1.0 g/ms (S. Jones et al., 2002). Generally a level of +6 $dB_{re:1.0g/ms}$ was used.

Acoustic Stimuli

ABR stimuli were delivered using a calibrated closed-field speaker driver (TDT Model: CF1) placed at the opening of the external auditory meatus (pinna removed previously) of the left ear. Tone bursts were used to elicit auditory responses (8 kHz sine wave with a 3 ms onset ramp, 3 ms plateau and 3 ms offset ramp envelope). Sound levels were measured in dB peSPL. A calibrated microphone [Etymotic Research Model: ER7 (Elk Grove Village, IL)] was utilized to monitor sound pressure level at the EAM. The amplitude of the monitored stimulus waveform was visualized on an oscilloscope and the stimulus output voltage was adjusted using an attenuator (TDT Model: PA5) to obtain a stimulus level at the EAM of 60 dB peSPL for each animal.

Electrophysiological Response Recording

The electrode placed over the caudal cerebrum (noted above) was connected to the non-inverting input of the preamplifier. The inverting electrode was placed subcutaneously below and behind the pinna and the ground electrode was placed subcutaneously on the ventral neck. Electrophysiological signals were amplified (GRASS P511 Model: K, gain = 200,000) and filtered [300-3000 Hz, (-6 dB amplitude points)] for all ABR and VsEP recordings. Signal averaging was used to resolve responses in electrophysiological recordings. ABR and VsEP stimuli were presented at a rate of 17 per second. Analog-to-digital conversion was triggered at the onset of each stimulus (1024 points at 10 μs/point). Normal and inverted stimulus polarities were collected for a total of 256 sweeps per waveform at +6 dB (2 g/ms). A binaural 90 dB SPL wide band (50 Hz to 50 KHz) forward masker was presented during initial VsEP recordings of each study to confirm the absence of auditory components. Masker levels were controlled using an attenuator (TDT PA5).

Surgical Manipulations

The VsEP is generated bilaterally by the vestibular end organ. Unilateral labyrinthectomies were performed to eliminate the contribution of one ear prior to other manipulations. Additional procedures included nerve section, unilateral and bilateral labyrinthectomy, unilateral and bilateral removal of the flocculus, and complete removal of the cerebellum. A craniotomy was performed in order to access the cerebellum, flocculus, vestibular nerves and brainstem. Aspiration was used to eliminate the flocculus and cerebellum. Mini pipettes were pulled and shaped (sub millimeter to millimeter diameter tips) and used to aspirate cerebellar structures. Surgical sectioning was performed with a blunt tip knife (1 mm tip) to interrupt neural pathways connecting primary afferents to brainstem while aspiration was used to interrupt neural pathways

between the brainstem and cerebellum nuclei as well as those interconnecting brainstem VNC to the cerebellum as described previously in the bird (Nazareth & T. Jones, 1998).

Middle Ear Access and Surgical Labyrinthectomy

Access for surgical labyrinthectomy was gained with removal of the tympanic membrane. A 0.6 mm drill bur was inserted into the middle ear space and utilized to destroy the contents of the otic capsule. Unilateral labyrinthectomy was verified by histology, absent ABR for the ablated side and bilateral labyrinthectomy was verified by histology and absent ABR and VsEP responses.

Histology

Following experiments all animals, while deeply anesthetized, underwent transcardial perfusion with 4% paraformaldehyde (pH 7.4). Skulls were decalcified in EDTA for 10 days. To ensure the stabilization of tissue during tissue processing, all decalcified tissues were embedded with paraffin and allowed to dry for 24 hours. Paraffin-embedded tissue was sectioned, mounted on glass slides and stained with Cresyl Violet. Slides were cover slipped and viewed under 4 to 20x magnification. Central nuclei and pathways were identified according to the mouse brain stereotaxic atlas of Franklin and Paximos (2007). Sections were digitally photographed (SPOT Insight CCD Camera and software, Diagnostic Instruments) and saved on computer hard drive. Electronic copies of the photographed tissue were scored to identify lesion sites and extent. Vestibular structures included in damaged regions were documented. Key features noted included all intact structures, interruption of major tracts, cellular damage within nuclei as well as the absence of portions or all of a nucleus.

Ensuring Good Physiological Conditions and Response Stability During Recording Sequences

Several steps were taken to insure that responses were recorded under stable conditions and that steps in preparing the animals (e.g., craniotomy, brain thermistor insertion, etc.) produced minimal changes in responses. Both ABR and VsEP baseline responses were recorded immediately after the animal was deeply anesthetized and for at least 20 minutes after each subsequent major manipulation to insure response stability under good systemic physiological conditions. Several factors were utilized to determine response and physiological status. In the absence of the VsEP, the presence of robust ABR responses indicated that peripheral and brainstem structures were generally intact. EKG and O_2 saturation were also recorded to monitor physiological standing. In cases where the heart rate fell transiently, animals were allowed to stabilize before proceeding. Brain temperature has been shown to affect ABR and VsEP latencies (e.g., alters axon conduction velocity and synapse transmission times); therefore it was necessary to maintain a stable brain temperature for all studies. When tissue was aspirated, the movement of air typically cooled the neural tissues locally. Brain temperature was allowed to stabilize before response recordings continued. Strategic surgical manipulations were carried out following baseline recordings and responses were compared before and after. Only one major target manipulation was done in each animal. Once a major response change was produced, stabilized and documented for the animal, the study was stopped and tissues were perfused, harvested and processed for histological evaluation. Site and extent of structural damage was established. Changes in response peak morphology (i.e., peak amplitude or peak latency) were correlated with structural damage.

Response Measures and Data Analysis

Three positive response peaks (i.e., P1, P2, and P3) and two negative response peaks (i.e., N1 and N2) are consistently present in the normal mouse VsEP. These are considered to be the principal response components. Response peak latencies were defined as the time, in ms, from the onset of the stimulus to the onset of the response peak. Peak-to-peak amplitudes were measured in μV and represent the difference in amplitude between a positive and a negative peak (e.g., P1-N1).

Statistics

Responses were evaluated using repeated measures multivariate analysis of variance (RM MANOVA; SPSS 19.0). Peak-to-peak amplitudes (i.e., P1-N1, P2-N1, and P3-N2) were evaluated before and after each manipulation to determine if the specific surgical manipulation had a significant effect on the VsEP response.

Results

General Response Features

VsEP and ABR waveforms were recorded from a total of 76 c57 BL/6 mice. Placement of the brain thermistor (n = 46) and craniotomy (n = 44) had no visible effect on VsEP response morphology (Figure 22). As reported in Chapter 3 in the intact animal, changing stimulus durations between 0.50, 1.0, and 2.0 ms had little effect on the threshold of the VsEP. Similarly, the morphology of principal response components of the VsEP (e.g., P1, P2 & P3) visibly changed little across the three stimulus durations in intact animals (Figure 23). Due to this variation, data utilizing the lab standard 2.0 ms stimulus duration was analyzed.

Effects of Labyrinthectomy

The purpose of surgical labyrinthectomy (n = 8) was to identify the contribution of each labyrinth to the VsEP. To isolate the right labyrinth, a labyrinthectomy was performed first on the left labyrinth in each animal. Responses were obtained and then a right labyrinthectomy was completed to confirm the destruction of the left labyrinth indicated by the elimination of responses. Responses were analyzed based on the recording of the lab standard 2.0 ms stimulus duration. Unilateral labyrinthectomy significantly reduced VsEP response amplitudes (see Table 4) in recordings of the right channel, $F(3, 4) = 7.53$, $p = 0.04$, and left channel, $F(3, 4) = 10.35$, $p = 0.02$, whereas bilateral labyrinthectomy eliminated responses in all but 1 of 8 animals where traces in the latter case, evidenced poorly resolved remnants of the response. Despite the presence of damage to the left labyrinth as revealed by histology, some function remained in this single case. Figures 24 and 25 provide general illustrations of the results of labyrinthectomy. Notice the absence of early principal response peaks after bilateral labyrinthectomy. It is notable that there is often a higher amount of background activity present in responses obtained with the 2.0 ms duration stimuli. Elevated background activity, especially at latencies beyond 3-4 ms, was a common observation in responses to longer duration stimuli. Stimulus-related activity is completely absent in traces for 1.0 ms and 0.50 ms of Figure 24. The late slow potential seen in the 2.0 ms traces after bilateral ablation (Figure 24) was reminiscent of stimulus wire artifact but was not reflected prominently after death. In these experiments, animals were repositioned for surgical procedures and then replaced. This often changes the shape of the stimulus artifacts where they exist and produces altered shapes after death (see also Figure 25).

Figure 25 provides another example where unilateral labyrinthectomy reduces responses and bilateral ablation virtually abolishes responses. Notice the absence of early principal response

peaks after bilateral ablation. Also evident was lingering late activity that was most prevalent in responses to the longest stimulus duration (2.0 ms). This late background activity bears little resemblance to the principal components of the normal VsEP. After death, stimulus artifact was maximal in the longest duration stimulus, 2.0 ms, and minimal or absent at shorter durations.

Effects of Flocculus Aspiration

Before the vestibular nerve could be accessed directly, it was necessary to remove the overlying flocculus. Vestibular second order cells project bilaterally to the flocculus (e.g., Goldberg et al., 2012). Therefore to evaluate flocculus contributions to VsEP waveform, it was necessary to remove the left and right flocculus. A blunt tip surgical knife was utilized to retract the intact cerebellum to allow access for aspiration of the flocculus. Both single (i.e., left side; n = 16) and bilateral (i.e., left followed by right side; n = 9) flocculus removal was confirmed by histology. There were no significant effects on VsEP amplitude (see Table 5) of removing the single left flocculus, $F(3, 13) = 2.58$, $p = 0.10$, or both left and right flocculus, $F(3, 6) = 0.42$, $p = 0.75$. Indeed, bilateral flocculus removal produced no remarkable changes in VsEP waveforms [Left (unilateral): Figure 26; Right (bilateral): Figure 27] provided no damage occurred to the vestibular nerve, brainstem or surrounding vasculature.

Effects of Cerebellum Aspiration

Following craniotomy and excision of the dura, the caudal cerebellum was exposed. Notably, some minor cerebellar aspiration took place in most studies, as this was the initial entry point to access other neural structures (e.g., flocculus, vestibular nerve, and brainstem). Focused aspiration of cerebellar lobules IX and X alone (n = 7) as well as the entire cerebellum (n = 7) was confirmed in all animals with histology (e.g., Figure 28). There was no significant change in VsEP amplitude following aspiration of cerebellar lobes IX and X (see Table 6) in recordings of

both right channel, $F(3, 4) = 2.34$, $p = 0.22$, and left channel, $F(3, 4) = 0.85$, $p = 0.53$, or after complete aspiration of all cerebellar tissues (including flocculus; see Table 7) in recordings of both right channel, $F(3, 4) = 2.34$, $p = 0.22$, and left channel, $F(3, 4) = 1.74$, $p = 0.30$.

Effects of Nerve Sectioning

It proved very difficult to functionally isolate the vestibular nerve. Numerous attempts were made to section the left vestibular nerve ($n = 10$) and spare its' function, which involved first sectioning the left nerve followed by sectioning or destruction of the right nerve for confirmation. In the majority of animals ($n = 8$), rather than spare function, the attempted left nerve section abolished vestibular nerve activity since subsequent right nerve destruction abolished all response peaks. A significant decrease in VsEP response amplitude was noted following section of the left nerve in these animals. VsEP response amplitudes appeared to decrease by approximately 40-50% (see Table 8 and Figure 29) in recordings of both right channel, $F(3, 5) = 11.23$, $p = 0.01$, and left channel, $F(3, 5) = 11.01$, $p = 0.01$. These findings were similar to those reported above for labyrinthectomy. In some cases ($n = 2$), response components remained after left and right sectioning. However, in these cases nerve sections were incomplete as histology showed the nerves to be intact.

Effects of Brainstem sectioning

In one case (GEN54), there was an attempt to section the vestibular nuclei within the brainstem in order to isolate the eighth nerve and its terminal fields in the brainstem. To access the brainstem, portions of the cerebellum were aspirated. Histological analysis revealed that the central portions of the cerebellum were successfully aspirated. Cerebellar regions aspirated included all of cerebellum lobules IX and X (Figure 30). Brainstem lesions were made with a custom circular tungsten needle electrode (tip width 1.5 mm). The left brainstem lesion appeared

to have altered vestibular nuclei including the left superior and medial nuclei and the left interstitial nucleus as well as portions of the auditory/vestibular nerve root as it enters the brainstem (Figure 31). The right brainstem lesion appeared to have altered vestibular nuclei including the right superior and medial nuclei only (Figure 31). Right and left flocculus, auditory and vestibular nerves remained completely intact in this study (Figure 32). VsEP waveform components of P3 and later were visibly decreased after right and left brainstem lesions (Figure 33). There was a reduced amount of activity later than P2/N2 in the 2.0 ms duration trace after the brainstem lesion and this activity was decreased further in the 1.0 ms duration trace.

Discussion

In general, these studies were performed to determine the origins of various peaks of the VsEP waveform in the mouse. Surgical ablation of key vestibular relays gave insight into the generators of this potential. Based on findings in the bird, it was hypothesized that one would have similar results in the mouse (i.e., the labyrinth and vestibular primary afferent are required). The cerebellum had little or no contribution to VsEP waveform morphology, which did not support the original hypothesis.

Cerebellum

It was originally hypothesized that the cerebellum made substantial contributions to the morphology of the VsEP waveform. However, the results presented evidence to the contrary. These results demonstrate that the cerebellum makes little or no contribution to the VsEP waveform as traces were unaltered after its complete removal. These findings are noteworthy in that primary afferents project directly to the cerebellum and second order cells project to and from the cerebellum from the vestibular nuclei (e.g., Goldberg et al., 2012). Vestibular nuclei in

this instance remained intact and thus remain as the primary candidate central generators of the VsEP in the mouse. This hypothesis is supported by data from the bird where (Nazareth & T. Jones, 1998) sectioned the brainstem in the area of the vestibular nuclei and demonstrated decreased VsEP response peak amplitudes post-section.

The nodulus and uvula are lobules IX and X of the cerebellum that were removed during several lesion studies in these experiments. These lobules receive primary vestibular afferent input and are involved in the vestibular velocity storage mechanism, which prolongs and integrates the neural signals from vestibular primary afferents and second order cells for purposes of visual stabilization (e.g., Leigh & Zee, 2006). This mechanism can be evaluated clinically with horizontal angular accelerations of the head (i.e., horizontal semicircular canal) through rotary chair testing (i.e., trapezoidal or velocity step testing). The linear VsEP stimulus is presented in such a manner that the macular organs are selectively activated (T. Jones et al. 1998). The central neural pathways differ substantially between those semicircular canal origin and those of macular origin (e.g., Goldberg et al., 2012). Nodular/Uvula lesion studies in the monkey have shown VOR deficits in post-rotary conditions (e.g., Angelaki & Hess, 1995). However, the VOR is a product of vestibular afferents, complex cerebellar influence on vestibular nuclei and second order cell output to cranial nerve nuclei. Although the cerebellum may have influence on vestibular nuclei output in the VOR, these studies demonstrate that the cerebellum has little to no contribution to the linear VsEP. These findings agree with work on the rotary VsEP in the cat by (Elidan, Li, & Sohmer, 1995) who provided evidence that the origins of response peaks P2 and beyond are associated with generators within the brainstem (e.g., cranial nerve nuclei III, VI and X).

Flocculus

It was expected that the flocculus would have contributions to the VsEP waveform. These results demonstrate that the flocculus makes little to no contribution to VsEP waveform morphology, as traces were not altered after complete removal. Interestingly, the flocculus receives bilateral vestibular second order cell projections. These include fibers from the caudal nucleus prepositus hypoglossi, superior vestibular nucleus, medial vestibular nucleus, dorsal/inferior vestibular nucleus and the ventral y group (e.g., Goldberg et al., 2012). The integration of these neural inputs gives rise to its complexity. The flocculus can be indirectly evaluated clinically through an oculomotor test battery (i.e., optokinetics and smooth pursuit), in that it makes up a portion of neural tissues, which allow clinical patients to follow visual targets (e.g., Goldberg et al., 2012). Optokinetic tests utilize a moving light stimulus, which elicits reflexive eye tracking movements (i.e., nystagmus). Effects of floccular and other cerebellar lesions might be evaluated in more depth by vestibular evoked potentials in unanesthetized animals. Studies in unanesthetized animals have been completed only in birds (Nazareth & T. Jones, 1998).

Vestibular Nerve Section and Labyrinthectomy

Previous findings (e.g., T. Jones, 1992; Nazareth & T. Jones, 1998) have demonstrated that P1 and N1 in the bird reflect activity from the vestibular nerve. The findings in the mammal (mouse) herein suggest that the VsEP waveform including P1 and N1 require vestibular labyrinth/vestibular nerve activity. An attempt was first made to isolate the vestibular nerve/labyrinth with unilateral nerve section. A decrease of 40-50% after unilateral nerve section followed by absence of the VsEP with successful bilateral nerve section was evidenced. These results show that both labyrinths make approximately equal contributions to the VsEP. It

was not possible to isolate the nerve without damage to the peripheral nerve stump, which may have provided further insight into early response components. Labyrinthectomy yielded clearer results without the high mortality rate associated with the nerve sectioning procedure described earlier. Similar to vestibular nerve section, post-bilateral labyrinthectomy VsEP responses were substantially reduced or abolished. Responses were decreased by approximately 40-50% when one labyrinth remained intact. These results confirmed the hypothesis that the VsEP depends on both labyrinths about equally in the mouse and are consistent with other work in the bird (e.g., T. Jones, 1992; Nazareth & T. Jones, 1998) and mammal (e.g., S. Jones, 2008; T. Jones & S. Jones, 2007).

In some cases, late components (> 4.0 ms) were present after bilateral labyrinectomies with no other identifiable peaks. It was concluded that this late activity must be physiological and not mechanical in nature because this activity is not present after death. This evidence shows that the late responses cannot be of vestibular origin because the late peaks often were present following bilateral labyrinthectomy in the absence of early vestibular peaks. In future studies, the origin of late components (> 4.0 ms) in VsEPs should be evaluated in more detail.

Isolated Case

Results from brainstem sectioning of the vestibular nuclei are consistent with previous evidence in the bird (Nazareth & T. Jones, 1998) that components P3 and later may be associated with central vestibular relays possibly including vestibular nuclei while P1, N1, and P2 may be associated with intact remaining structures including the vestibular nerve and/or remaining intact portions of the vestibular nuclei. Future studies might focus on brainstem lesions to further examine VsEP response components. With the use stereotaxic equipment there may be some uncertainty when lesions are induced into deep neural tissues. Therefore, it is essential to

remove some if not all of cerebellar structures to more accurately access and identify areas of interest for lesion studies. These type studies can be completed without concern of cerebellar manipulation having effects on VsEP responses.

Summary

VsEPs are a measurement of the compound action potential as it courses from peripheral to central vestibular structures. As primary afferents synapse in both the cerebellum and the vestibular nuclear complex, from these studies the cerebellum has no contribution to VsEP waveform. This finding is important in that it will steer future researchers to examine effects of other possible contributing structures (e.g., vestibulospinal tract fibers projections from vestibular nuclei). As previously seen in the bird and mouse, once a confirmed bilateral disruption of the labyrinth occurs, responses are abolished. However, in these studies of the mammal, it was somewhat difficult to determine ear specific information from left and right electrode derivations used. Future studies might examine this phenomenon in more detail.

Table 4

Pre- and post Labyrinthectomy means and standard deviations for various VsEP peak-to-peak amplitudes.

Peak	Post Labyrinthectomy Peak-Peak Amplitude μV *M* ± *SD* contralateral recording channel	Post Labyrinthectomy Peak-Peak Amplitude μV *M* ± *SD* ipsilateral recording channel	% of Baseline Post Labyrinthectomy ipsilateral recording channel
P1-N1	0.87 ± 0.27	0.71 ± 0.25	70.18
P2-N1	1.15 ± 0.23	0.85 ± 0.18	65.80
P3-N2	0.54 ± 0.30	0.57 ± 0.21	55.36

Peak	Baseline Peak-Peak Amplitude μV *M* ± *SD* ipsilateral recording channel	Baseline Peak-Peak Amplitude μV *M* ± *SD* ipsilateral recording channel	% of Baseline Post Labyrinhectomy contralateral recording channel
P1-N1	1.01 ± 0.19	1.005 ± 0.19	93.95
P2-N1	1.36 ± 0.45	1.362 ± 0.45	81.26
P3-N2	1.18 ± 0.43	1.184 ± 0.43	56.13

Table 5

Pre- and post Flocculus removal means and standard deviations for various VsEP peak-to-peak amplitudes.

Left Flocculus only (n = 16) Peaks	Peak-Peak Amplitude in μV $M \pm SD$ right Ch. Before	Peak-Peak Amplitude in μV $M \pm SD$ right Ch. After	% Change right Ch.
P1-N1	1.31 ± 0.34	1.23 ± 0.24	99.04
P2-N1	1.70 ± 0.41	1.67 ± 0.45	102.39
P3-N2	1.39 ± 0.79	0.86 ± 0.53	74.07

Left and Right Flocculus (n = 9) Peaks	Peak-Peak Amplitude in μV $M \pm SD$ right Ch. Before	Peak-Peak Amplitude in μV $M \pm SD$ right Ch. After	% Change right Ch.
P1-N1	1.12 ± 0.25	1.09 ± 0.36	97.10
P2-N1	1.26 ± 0.38	1.20 ± 0.45	95.48
P3-N2	0.82 ± 0.59	0.82 ± 0.43	141.56

Table 6

Pre- and post IX and X lobules of the cerebellum removal means and standard deviations for various VsEP peak-to-peak amplitudes.

Removal of Center only (i.e., lobes IX, X; *n* = 7) Peaks	Peak-Peak Amplitude in μV *M* ± *SD* right Ch. Before	Peak-Peak Amplitude in μV *M* ± *SD* right Ch. After	% Change right Ch.
P1-N1	1.18 ± 0.15	0.92 ± 0.27	78.22
P2-N1	1.71 ± 0.43	1.39 ± 0.32	85.68
P3-N2	1.74 ± 1.03	1.38 ± 0.57	88.67

Removal of Center only (i.e., lobes IX, X; *n* = 7) Peaks	Peak-Peak Amplitude in μV *M* ± *SD* left Ch. Before	Peak-Peak Amplitude in μV *M* ± *SD* left Ch. After	% Change left Ch.
P1-N1	1.39 ± 0.66	1.14 ± 0.45	86.86
P2-N1	1.83 ± 0.54	1.48 ± 0.42	85.38
P3-N2	1.82 ± 0.83	1.45 ± 0.65	86.63

Table 7

Pre- and post all of the cerebellum removal means and standard deviations for various VsEP peak-to-peak amplitudes.

All Cerebellum (n = 7) Peaks	Peak-Peak Amplitude in μV M ± SD right Ch. Before	Peak-Peak Amplitude in μV M ± SD right Ch. After	% Change right Ch.
P1-N1	1.04 ± 0.16	0.89 ± 0.17	86.34
P2-N1	1.25 ± 0.44	1.14 ± 0.36	94.24
P3-N2	1.38 ± 0.46	0.98 ± 0.37	73.81

All Cerebellum (n = 7) Peaks	Peak-Peak Amplitude in μV M ± SD left Ch. Before	Peak-Peak Amplitude in μV M ± SD left Ch. After	% Change left Ch.
P1-N1	0.85 ± 0.22	0.81 ± 0.15	98.14
P2-N1	1.18 ± 0.45	1.11 ± 0.38	97.82
P3-N2	1.57 ± 0.38	1.08 ± 0.42	71.49

Table 8

Pre- and post vestibular nerve section means and standard deviations for various VsEP peak-to-peak amplitudes.

Left Vestibular Nerve (n = 8) Peaks	Peak-Peak Amplitude in μV $M \pm SD$ right Ch. Before	Peak-Peak Amplitude in μV $M \pm SD$ right Ch. After	% Change right Ch.
P1-N1	1.26 ± 0.36	1.00 ± 0.29	77.72
P2-N1	1.78 ± 0.52	1.32 ± 0.33	79.33
P3-N2	1.12 ± 0.38	0.67 ± 0.35	61.23

Left Vestibular Nerve (n = 8) Peaks	Peak-Peak Amplitude in μV $M \pm SD$ left Ch. Before	Peak-Peak Amplitude in μV $M \pm SD$ left Ch. After	% Change left Ch.
P1-N1	1.00 ± 0.16	0.77 ± 0.21	77.20
P2-N1	1.55 ± 0.59	1.15 ± 0.26	74.14
P3-N2	1.11 ± 0.65	0.93 ± 0.65	83.87

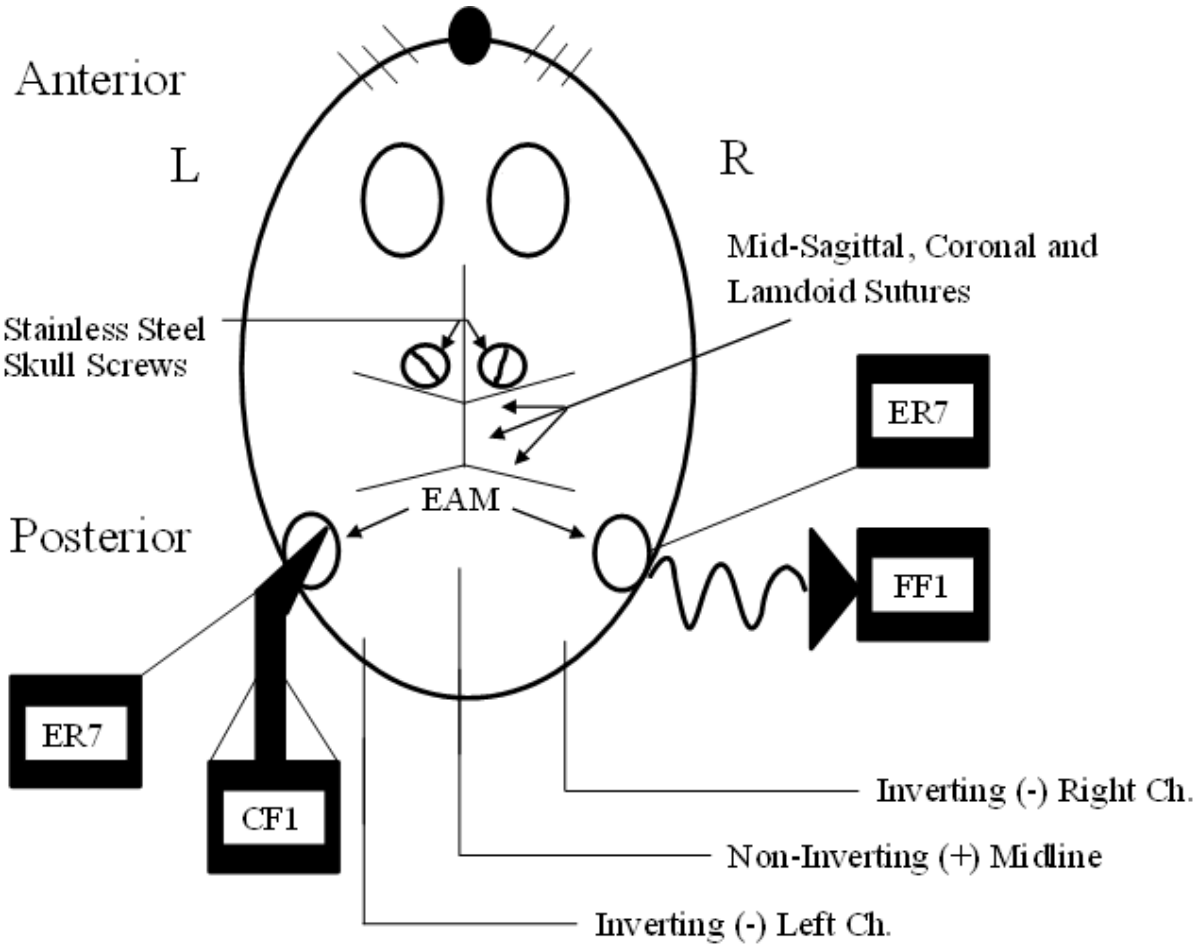

Figure 21. Skull preparation and coupling to mechanical shaker illustration. ER7 microphones were utilized to monitor ABR stimulus level. CF1 and FF1 were utilized to present ABR stimuli. EAM labeled as ear canal openings post pinnae removal.

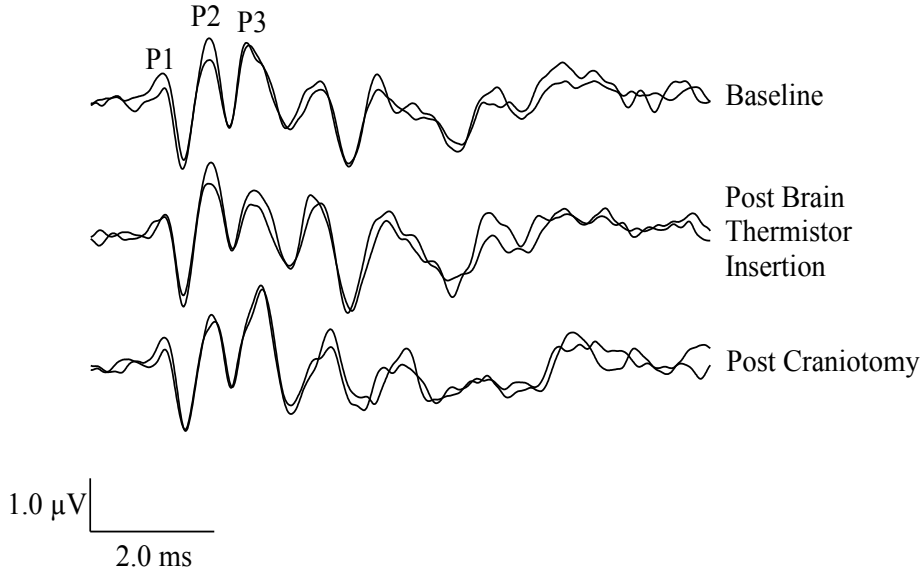

Figure 22. Linear VsEPs obtained from an anesthetized mouse after surgical preparation. Responses were recorded before and after each manipulation. Morphology of the VsEP waveform remained intact after brain thermistor insertion and craniotomy to access neural structures (i.e., cerebellum and vestibular nerve). Animal GEN33.

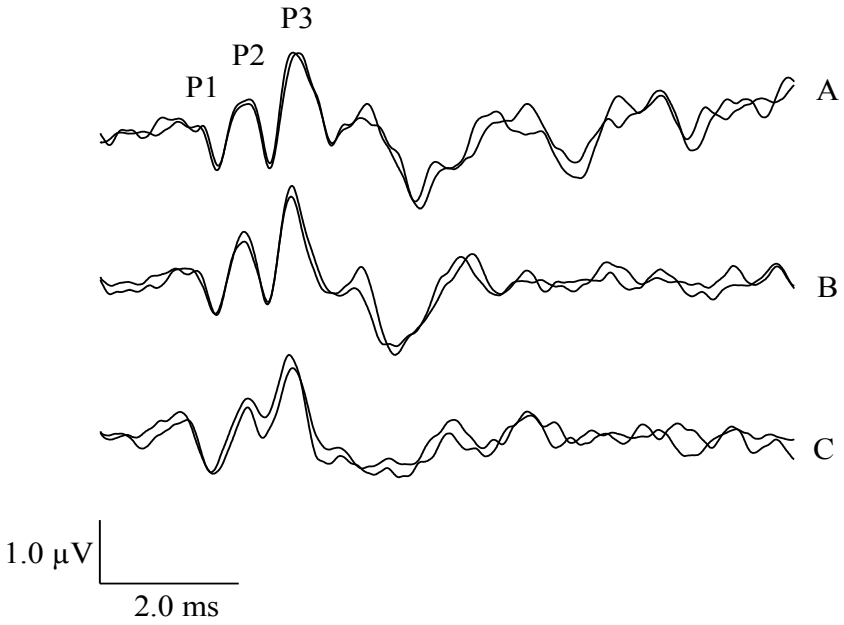

Figure 23. Effects of stimulus duration on VsEP waveform morphology (i.e., GEN74). Above, VsEPs are shown from a single representative animal, which were recorded with three variations in stimulus duration (A: 2.0 ms, B: 1.0 ms, and C: 0.50 ms).

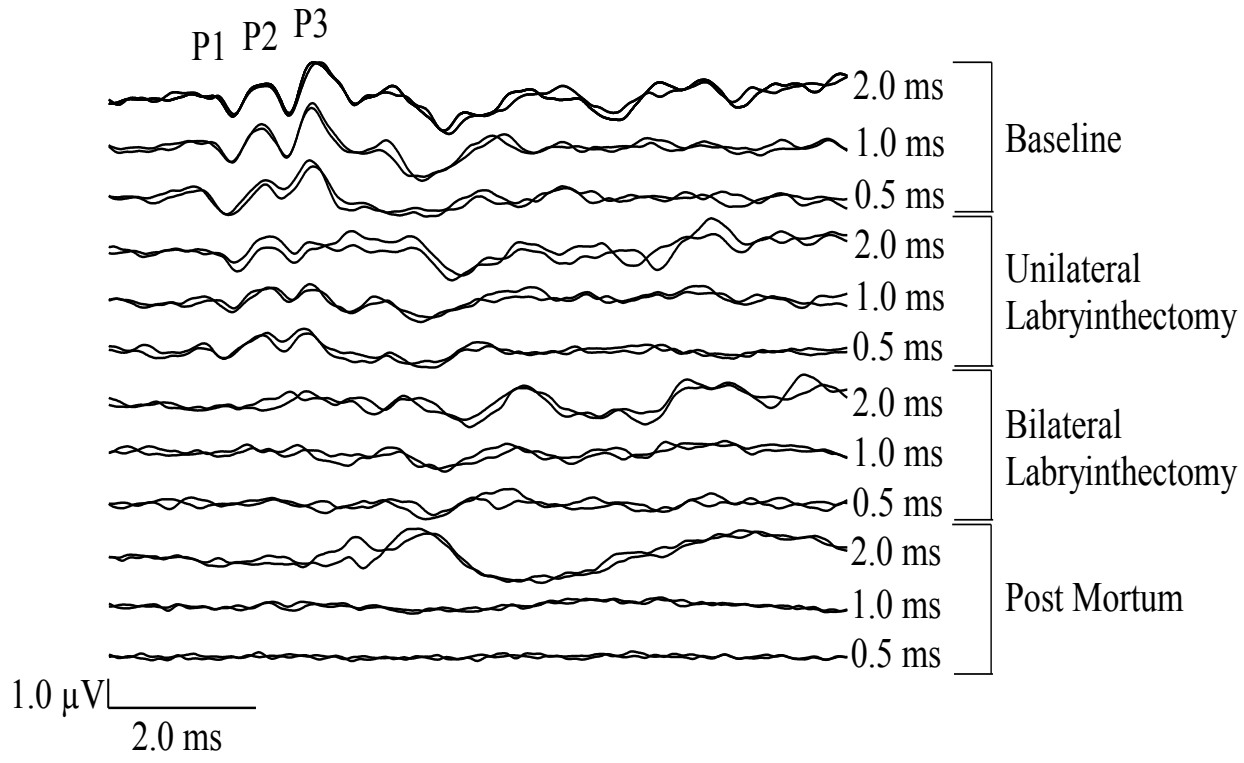

Figure 24. Illustration of typical VsEP recording sequence (GEN70). Three rise times (i.e., 2.0, 1.0, and 0.50 ms) were utilized in each of the four sequential conditions. It is notable that responses decrease by 40-50% following unilateral labyrinthectomy and are abolished following bilateral labyrinthectomy. From these waveforms, it is notable that higher amounts of background activity are present in the 2.0 ms rise time conditions.

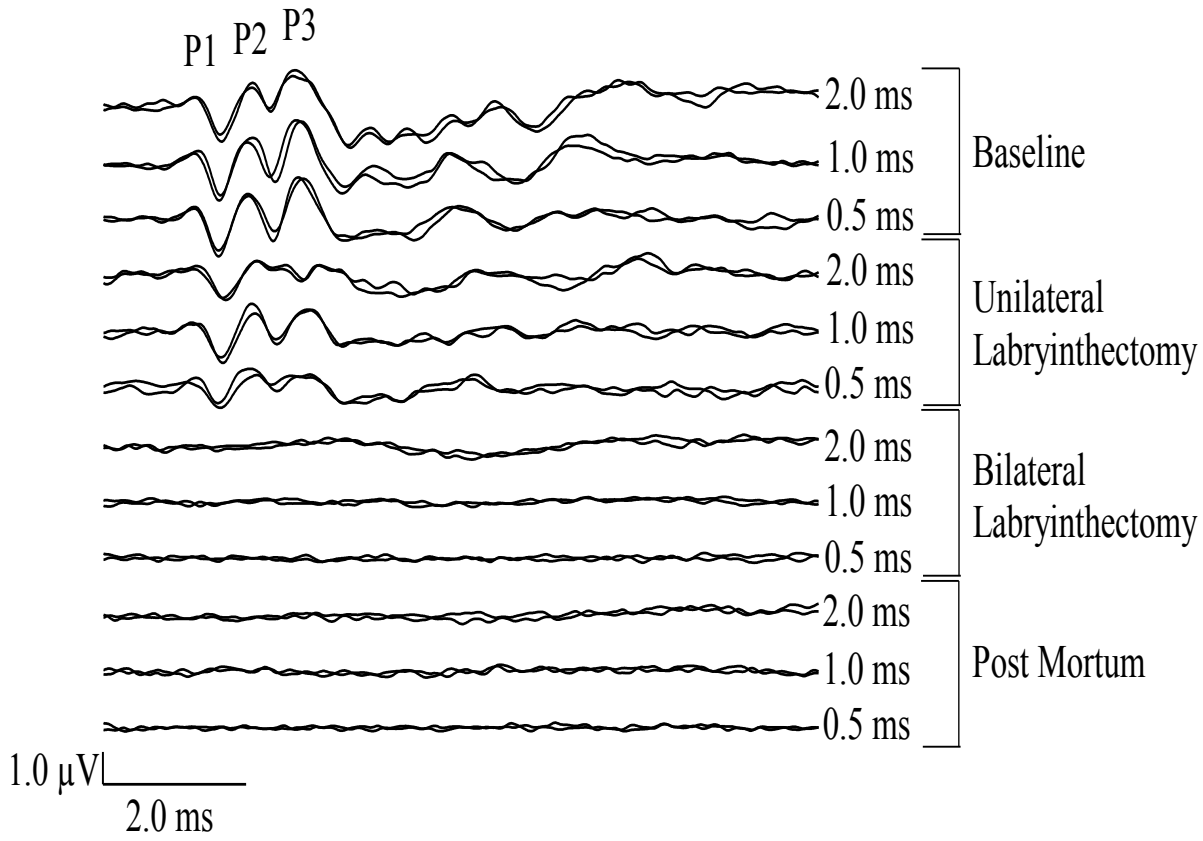

Figure 25. Illustration of typical VsEP recording sequence (GEN75). Three stimulus durations (i.e., 2.0, 1.0, and 0.50 ms) were utilized in each of the four sequential conditions. It is notable that responses decrease by 40-50% following unilateral labyrinthectomy and are abolished following bilateral labyrinthectomy.

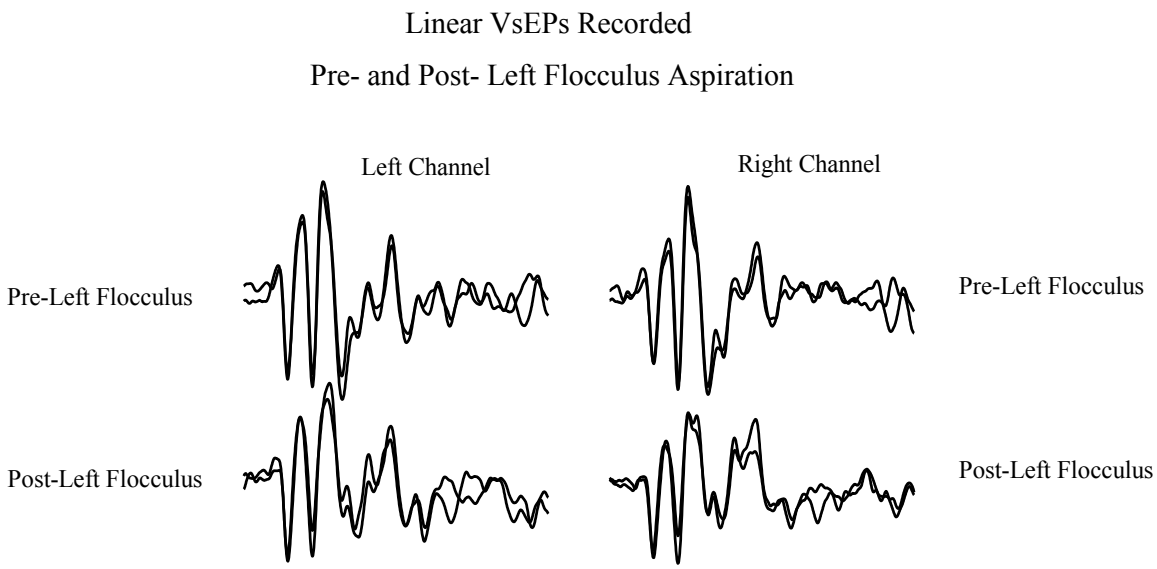

Figure 26. Left flocculus pre- and post-removal VsEP responses (Animal GEN37).

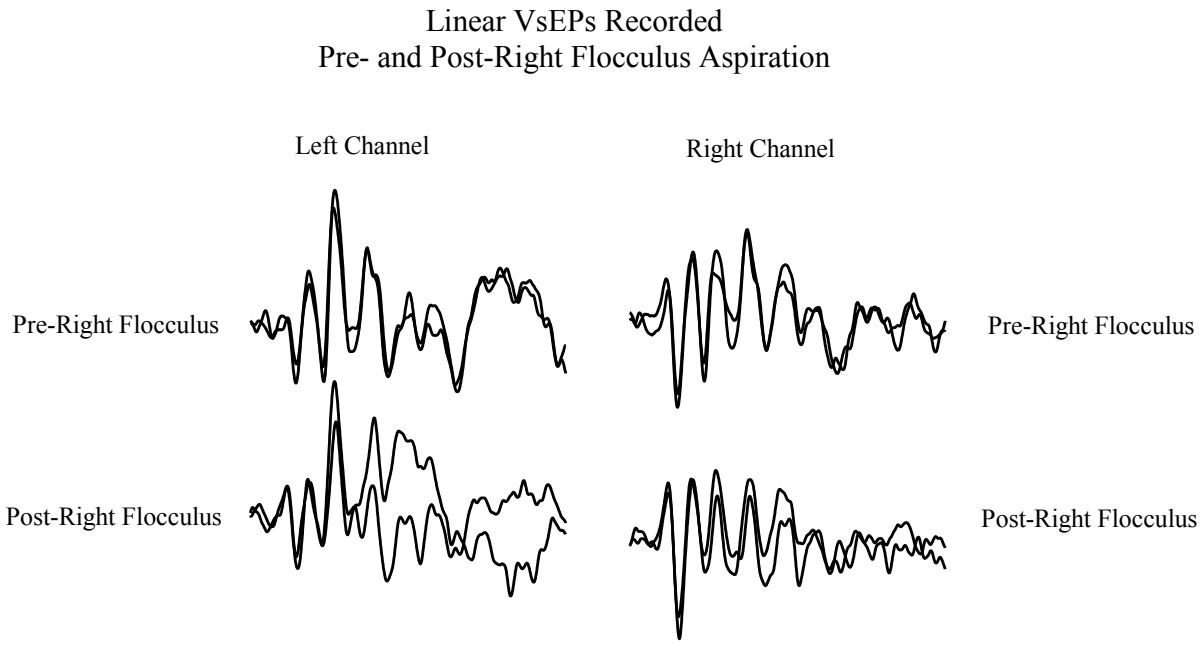

Figure 27. Right flocculus pre- and post-removal VsEP responses (Animal GEN33). Right flocculus was removed following aspiration of left floccus. Post-right flocculus thus represents bilateral removal of the flocculus.

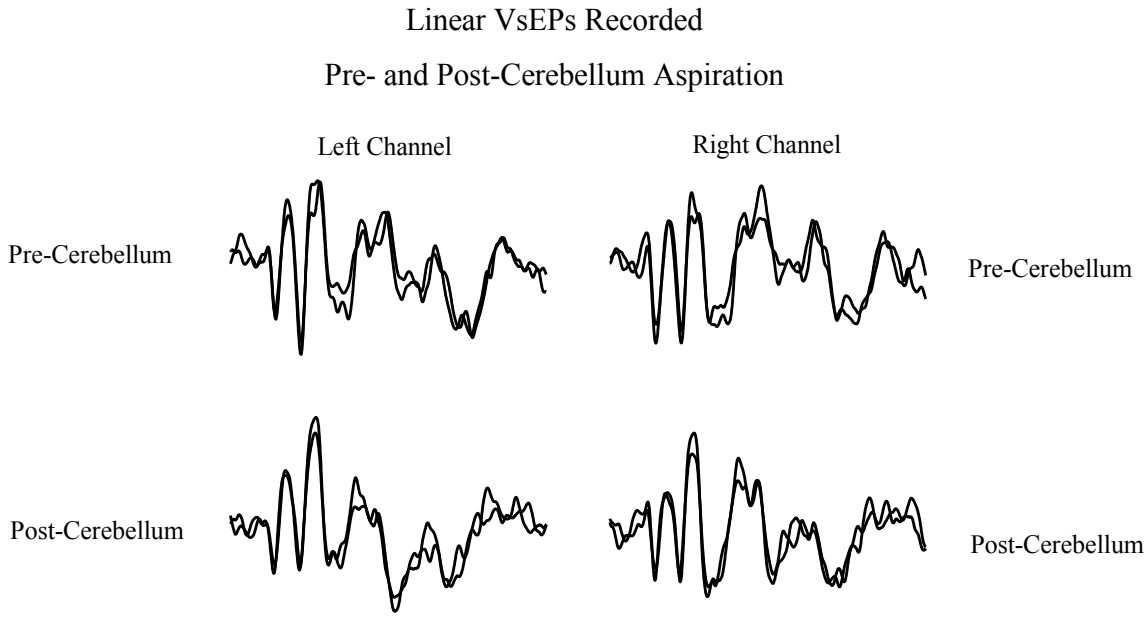

Figure 28. Cerebellum pre- and post-removal VsEP responses (Animal GEN37).

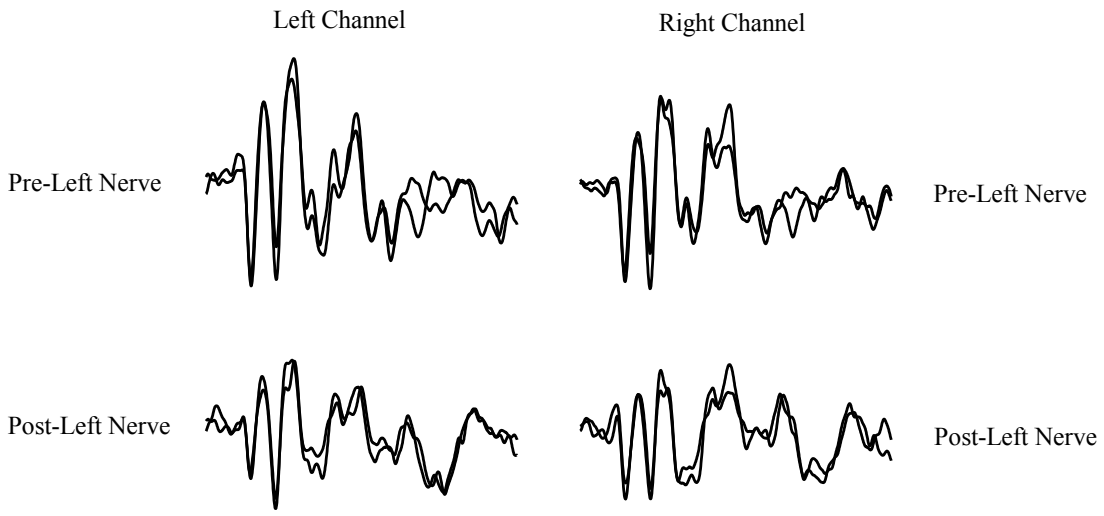

Figure 29. Left nerve pre- and post-sectioning VsEP responses (Animal GEN37).

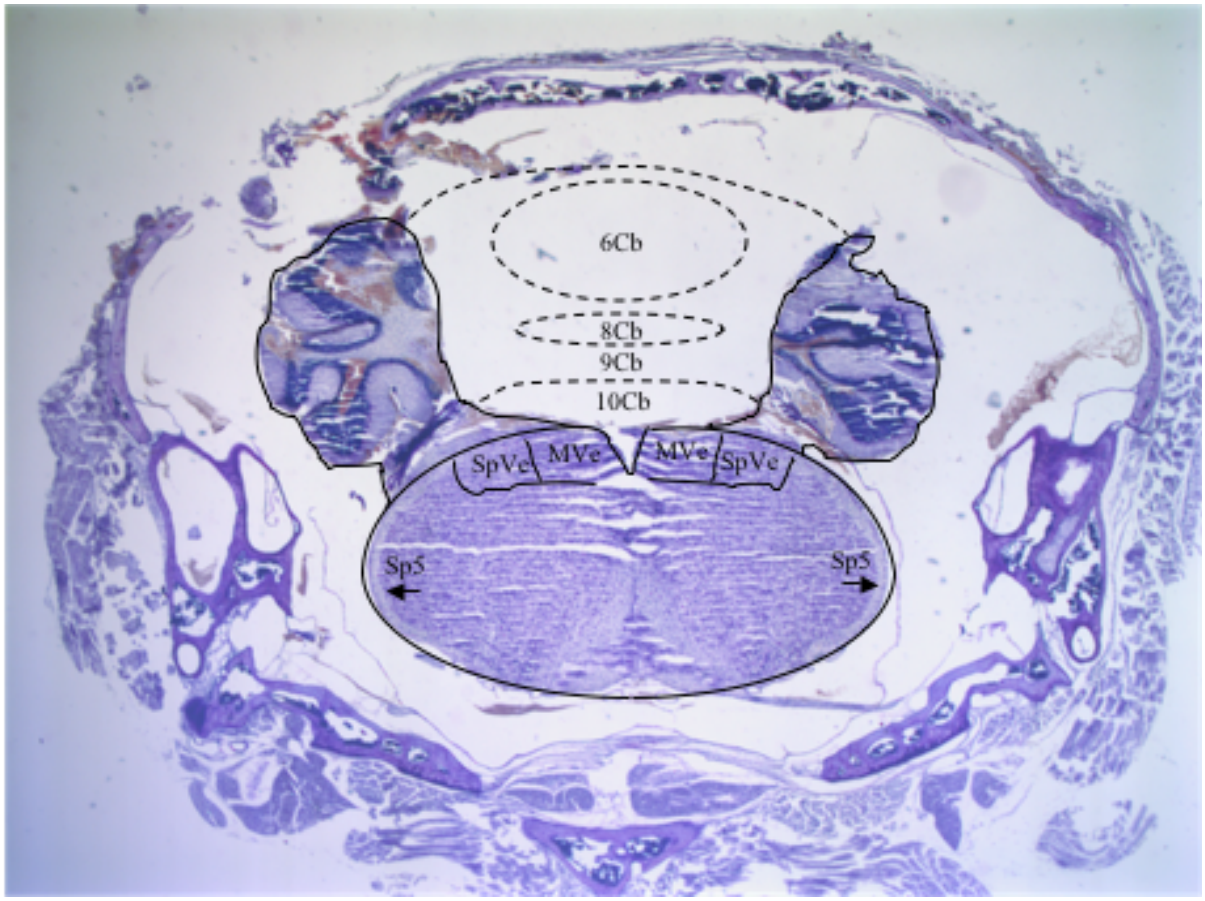

Figure 30. 6Cb-Lobule 6 of the cerebellar vermis; 8Cb-Lobule 8 of the cerebellar vermis; 9Cb-Lobule 9 of the cerebellar vermis; 10Cb-Lobule 10 of the cerebellar vermis; MVe-medial vestibular nucleus; Sp5-spinal trigeminal tract; SpVe-spinal vestibular nucleus. Animal GEN54.

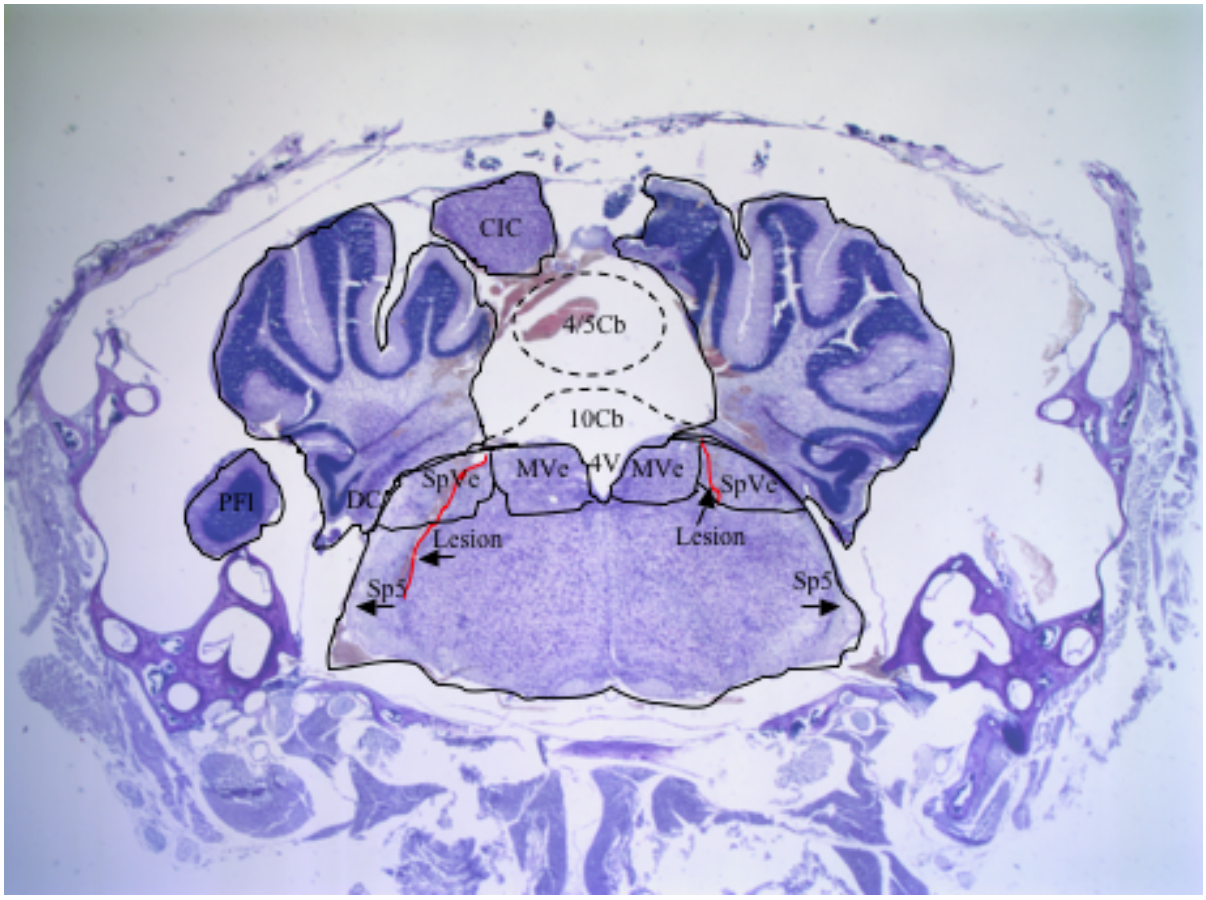

Figure 31. 4/5Cb-lobules 4 and 5 of the cerebellar vermis; 4V-4th ventricle; 10Cb-Lobule 10 of the cerebellar vermis; CIC-central nucleus of the inferior colliculus; DC-dorsal cochlear nucleus; MVe-medial vestibular nucleus; PFl-paraflocculus; Sp5-spinal trigeminal tract; SpVe-spinal vestibular nucleus; lesion indicated in red color. Animal GEN54.

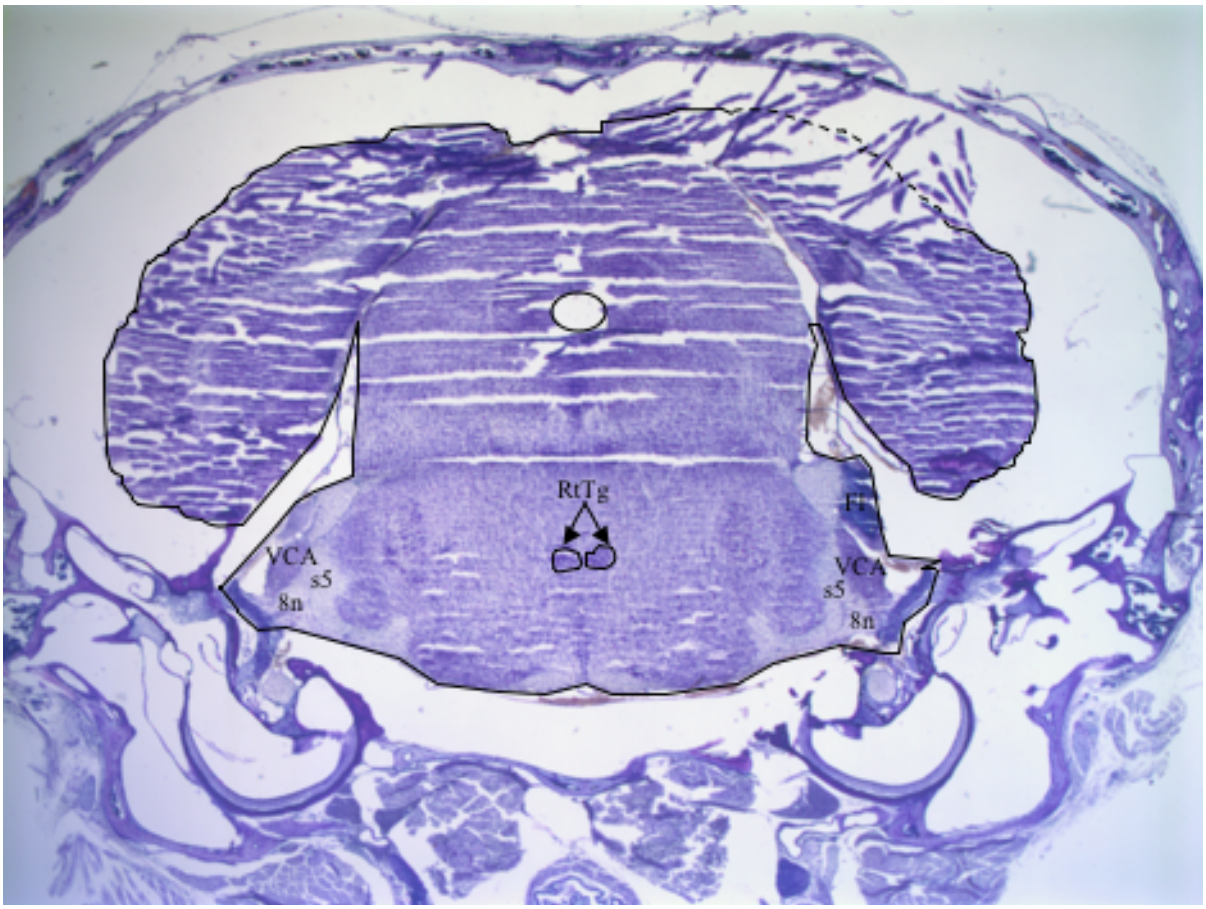

Figure 32. 8n-vestibulocochlear nerve; Fl-flocculus; RtTg-reticulotegmental nucleus of the pons; s5-sensory root of the trigeminal nerve; VCA-ventral cochlear nucleus, anterior part. Animal GEN54.

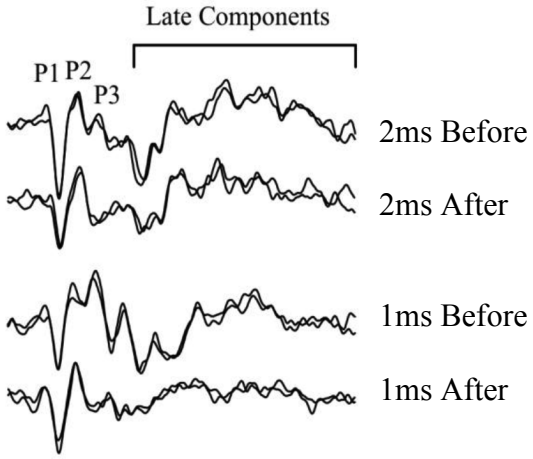

Figure 33. Brainstem section pre- and post-sectioning VsEP recordings. Animal GEN54 A demonstration of two stimulus durations (i.e., 2.0 ms and 1.0 ms) utilized before and after a surgical manipulation. Note that a greater amount "late component" residual activity is present in the 2.0 ms tracing. When utilizing the 1.0 ms stimulus duration, it was possible to remove/reduce this activity and concentrate on the principle VsEP response components.

CHAPTER V: GLOBAL DISSCUSSION

As noted previously, this work focused primarily on understanding the generation of responses from vestibular sensors and neural pathways that are evoked by transient linear acceleration. These studies included evaluation of VsEP response morphology with change in brain temperature, evaluation of drug on the VsEP response (i.e., Ketorolac), and the evaluation of stimulus duration on the VsEP response. During the generator studies, VsEPs were recorded before and after strategic surgical manipulations of vestibular pathways. This included isolation of the eighth nerve/labyrinth from central relays and destruction of central candidate neural generators (i.e., the cerebellum and flocculus).

In general, all of the studies have provided new information regarding the VsEP in the mammal and confirmed evidence from Nazareth and T. Jones (1998) in the bird. Interestingly, the hypothesis for Ketorolac was disproved and provided evidence that although labyrinthine related side effects are often reported with the drugs' use, there were no effect on the auditory or vestibular evoked potentials (i.e., tests that require an "intact" labyrinth). Ketorolac, was not utilized as planned in these generator studies due to decreased clotting function associated with NSAIDs. These studies on stimulus duration proved the hypothesis that VsEP thresholds could indeed be altered with various stimulus durations. The study on stimulus duration in particular has sparked an interest with the associated concept of the vestibular activation time constant. Studies have been completed to date in various models (i.e., turtle); however, there is no data at this point for the mouse, an important model for the study of the genetic basis of deafness and balance disorders. Future studies in the mouse might evaluate the vestibular time constant in more detail. The third interesting finding disproved the hypothesis of the cerebellum's contribution to the VsEP. It was found that the cerebellum and flocculus made little to no

contribution to VsEP waveform. This is an important finding in that the cerebellum receives primary afferents projecting from the vestibular system. Future studies in the mouse might examine further the contribution of brainstem nuclei in that morphological changes in the later components of the VsEP were observed in an isolated case.

In summary, it was verified that VsEP response components are critically dependent on both labyrinth and vestibular nerve function as well as ruled out the cerebellum as a possible contributor to the response. In general, these studies have increased the understanding of the neural generators of the VsEP, and in turn, enhanced one's ability to assess peripheral and central vestibular function and detect vestibular disease.

REFERENCES

Achor, L. J., & Starr, A. (1980a). Auditory brain stem responses in the cat. I. Intracranial and extracranial recordings. *Electroencephalography and Clinical Neurophysiology, 48,* 154-173.

Achor, L. J., & Starr, A. (1980b). Auditory brain stem responses in the cat. II. Effects of lesions. *Electroencephalography and Clinical Neurophysiology, 48,* 174-190.

Akin, F. W., & Murnane, O. D. (2008). Vestibular evoked myogenic potentials. In G. P. Jacobson & N. T. Shepard (Eds.), *Balance function assessment and management* (pp. 405-434). San Diego, CA: Plural publishing.

Allen, A. R., & Starr, A. (1978). Auditory brain stem potentials in monkey (*M. Mulatta*) and man. *Electroencephalography and Clinical Neurophysiology, 45,* 53-63.

Angelaki, D. E., & Hess, B. J. (1995). Lesion of nodulus and vestral uvula abolish steady-state off vertical axis otolith response. *Journal of Neurophysiology, 73,* 1716-1720.

Balaban, C. D. (1999). Vestibular autonomic regulation (including motion sickness and the mechanism of vomiting). *Current Opinion in Neurology, 12,* 29-33.

Balaban, C. D., & Porter, J. D. (1998). Neuroanatomic substrates for vestibulo-autonomic interactions. *Journal of Vestibular Research, 8,* 7-16.

Baloh, R. W., & Honrubia, V. (2001). Laboratory examination of the vestibular system. In *Clinical neurophysiology of the vestibular system* (pp. 152-199). New York, NY: Oxford University Press.

Barmack, N. H. (2003). Central vestibular system: vestibular nuclei and posterior cerebellum. *Brain Research Bulletin, 60,* 511-541.

Barmack, N. H., Baughman, R. W., Errico, P., & Shojaku, H. (1993). Vestibular primary afferent projection to the cerebellum of the rabbit. *The Journal of Comparative Neurology, 327,* 521-534.

Bauman, N. G. (2003). *Ototoxic drugs exposed.* (2 ed.) Stewartstown, PA: GuidePost Publications.

Beck, M. M., Brown-Borg, H. M., & Jones, T. A. (1987). Peripheral and brainstem auditory function in paroxysmal [px] white leghorn chicks. *Brain Research, 406,* 93-98.

Beck, M. M., & Jones, T. A. (1984). Auditory brainstem responses (ABR's) in normal and paroxysmal white leghorn chicks. [Abstract]. *Society for Neuroscience, 10,* 1141.

Blum, P. S., Day, M. J., Carpenter, M. B., & Gilman, S. (1979). Thalamic components of the ascending vestibular system. *Experimental Neurology, 64,* 587-603.

Bohmer, A., Hoffman, L. F., & Honrubia, V. (1995). Characterization of vestibular potentials evoked by linear acceleration pulses in the chinchilla. *American Journal of Otology, 16,* 498-504.

Braunstein, E. M., Crenshaw, III, E. B., Morrow, B. E., & Adams, J. C. (2008). Cooperative function of Tbx1 and Brn4 in the periotic mesenchyme is necessary for cochlea formation. *Journal of The Association for Research in Otolaryngology, 9,* 33-43.

Brown-Borg, H. M., Beck, M. M., & Jones, T. A. (1987). Origins of peripheral and brainstem auditory responses in the white leghorn chick. *Comparative Biochemistry and Physiology, 88A,* 391-396.

Buchwald, J. S., & Huang, C. M. (1975). Far-field acoustic response: Origins in the cat. *Science, 189,* 382-384.

Burkard, R. F., Don, M., & Eggermont, J. J. (2007). *Auditory evoked potentials basic principles and clinical application.* Baltimore, MD: Lippincott Williams & Wilkins.

Burke, R. E., & Edgerton, V. R. (1975). Motor unit properties and selective involvement in movement. *Exercise and Sport Sciences Reviews, 3,* 31-81.

Campbell, W. B., & Halushka, P. V. (1996). Lipid-derived autocoids, eicosanoids and platelet-activating factor. In J. G. Hardman, L. E. Limbird, P. B. Molinoff, R. W. Ruddon, & A. G. Gilman (Eds.), *Goodman and Gilman's the pharmacological basis of therapeutics* (9th ed., pp. 601-657). New York, NY: McGraw-Hill.

Carpenter, M. B. (1976). *Human neuroanatomy.* (7 ed.) Baltimore: Waverly Press, Inc.

Colebatch, J. G. (2001). Vestibular evoked potentials. *Current Opinion in Neurology, 14,* 21-26.

De Vries, H. (1950). The mechanics of the labyrinth otoliths. *Acta Oto-Laryngologica, 38,* 262-273.

Di Palma, F., Holme, R. H., Bryda, E. C., Belyantseva, I. A., Pelligrino, R., Kachar, B., Noben-Trauth, K., & Steel, K. P. (2001). Mutations in Cdh23, encoding a new type of cadherin cause stereocilia disorganization in waltzer, the mouse model for Usher syndrome type 1D. *Nature Genetics, 27,* 103-107.

Domer, F. (1990). Characterization of the analgesic activity of ketorolac in mice. *European Journal of Pharmacology, 177,* 127-135.

Dunlap, M. D., Spoon, C. E., & Grant, J. W. (2012). Experimental measurement of utircle dynamic response. *Journal of Vestibular Research, 22,* 57-68.

Durrant, J. D., & Boston, J. R. (2007). Stimuli for Auditory Evoked Potential Assessment. In *Auditory evoked potentials* (pp. 42-72). Baltimore, MD: Lippincott Williams & Wilkins.

Eggermont, J. J. (2007). Electric and magnetic fields of synchronous neural activity. In R. F. Burkard, M. Don, & J. J. Eggermont (Eds.), *Auditory evoked potentials basic principles and clinical application* (pp. 2-21). Baltimore, MD: Lippincott Williams & Wilkins.

Elidan, J., Langhofer, L., & Honrubia, V. (1987a). Recording of short-latency vestibular evoked potentials induced by acceleration impulses in experimental animals: Current status of the method and its applications. *Electroencephalography and Clinical Neurophysiology, 68,* 58-69.

Elidan, J., Langhofer, L., & Honrubia, V. (1987b). The neural generators of the vestibular evoked response. *Brain Research, 423,* 385-390.

Elidan, J., Li, G., & Sohmer, H. (1995). The contribution of cranial-nerve nuclei to the short latency vestibular evoked potentials in cat. *Acta Oto-Laryngologica, 115,* 141-144.

Elidan, J., Lin, J., & Honrubia, V. (1986). The effect of loop diuretics on the vestibular system. Assessment by recording the vestibular evoked response. *Archives of Otolaryngology Head and Neck Surgery, 112,* 836-839.

Evans, D. G., Sainio, M., & Baser, M. E. (2000). Neurofibromatosis type 2. *Journal of Medical Genetics, 37,* 897-904.

Fernandez, C., & Goldberg, J. M. (1976). Physiology of peripheral neurons innervating otolith organs of the squirrel monkey. I. Response to static tilts and to long-duration centrifugal force. *Journal of Neurophysiology, 39,* 970-984.

Franklin, K., & Paxinos, G. (2007). *The mouse brain in stereotaxic coordinates.* (3 ed.) New York, NY: Academic Press.

Gacek, R. R. (1969). The course and central termination of first order neurons supplying vestibular endorgans in the cat. *Acta Oto-Laryngologica Supplement, 254,* 4-66.

Gerrits, N. M., Epema, A. H., van Linge, A., & Dalm, E. (1989). The primary vestibulocerebellar projection in the rabbit: absence of primary afferents in the flocculus. *Neuroscience Letters, 105,* 27-33.

Goldberg, J. M., Wilson, V. J., Cullen, K. E., Angelaki, D. E., Broussard, D. M., Buttner-Ennever, J. A., Fukushima, K., & Minor, L. B. (2012). *The vestibular system: A sixth sense.* New York, NY: Oxford University Press.

Goldenberg, R. A., & Derbyshire, A. J. (1975). Averaged evoked potentials in cats with lesions of auditory pathway. *Journal of Speech and Hearing Research, 18,* 420-429.

Grinnell, A. D. (1963). The neurophysiology of audition in bats: intensity and frequency parameters. *Journal of Physiology, 167,* 38-66.

Hain, T. C., & Rudisill, H. (2008). Practical anatomy and physiology of the ocular motor system. In *Balance function assessment and management* (pp. 13-26). Abingdon, Oxfordshire, UK: Plural Publishing.

Hall, J. W. (2007). *New handbook of auditory evoked potentials.* Upper Saddle River, NJ: Pearson Education.

Hampton, L. L., Wright, C. G., Alagramam, K. N., Battey, J. F., & Noben-Trauth, K. (2003). A new spontaneous mutation in the mouse Ames waltzer gene. *Hearing Research, 180,* 67-75.

Henry, K. R. (1979a). Auditory brainstem volume-conducted responses: Origins in the laboratory mouse. *Journal of the American Auditory Society, 4,* 1-7.

Henry, K. R. (1979b). Differential changes of auditory nerve and brain stem short latency evoked potentials in the laboratory mouse. *Electroencephalography and Clinical Neurophysiology, 46,* 452-459.

Hillier, K. (1981). BPPC. *Drugs of the future, 6,* 669-670.

Honrubia, V., Kuruvilla, A., Mamikunian, D., & Wichel, J. E. (1987). Morphological aspects of the vestibular nerve of the squirrel monkey. *Laryngoscope, 97,* 228-238.

Huang, C. M., & Buchwald, J. S. (1977). Interpretation of the vertex short-latency acoustic response: A study of single neurons in the brain stem. *Brain Research, 137,* 291-303.

Jacobson, G. P., & McCaslin, D. L. (2007). The vestibular evoked myogenic potential and other sonomotor evoked potentials. In R. Burkard, M. Don, & J. J. Eggermont (Eds.), *Auditory evoked potentials basic principles and clinical application* (pp. 572-598). Baltimore, MD: Lippincott Williams & Wilkins.

Jacobson, G. P., & Shepard, N. T. (2008). *Balance function assessment and management.* Abingdon, Oxfordshire, UK: Plural Publishing.

Jett, M. F., Ramesha, C. S., Brown, C. D., Chiu, S., Emmett, C., Voronin, T., Sun, T., O'Yang, C., Hunter, J. C., Eglen, R. M., & Johnson, R. M. (1999). Characterization of the analgesic and anti-inflammatory activities of ketorolac and its enantiomers in the rat. *The Journal of Pharmacology and Therapeutics, 288,* 1288-1297.

Jewett, D. L. (1970). Volume-conducted potentials in response to auditory stimuli as detected by averaging in the cat. *Electroencephalography and Clinical Neurophysiology 28*, 609-618.

Jewett, D. L., & Romano, M. N. (1972). Neonatal development of auditory system potentials averaged from the scalp of rat and cat. *Brain Research, 36,* 101-115.

Jewett, D. L., & Williston, J. S. (1971). Auditory-evoked far fields averaged from the scalp of humans. *Brain, 94,* 681-696.

Jones, S. M. (2008). Vestibular sensory evoked potentials. In G. P. Jacobson & N. T. Shepard (Eds.), *Balance function assessment and management* (pp. 379-404). San Diego, CA: Plural Publishing.

Jones, S. M., Erway, L. C., Bergstrom, R. A., Schimenti, J. C., & Jones, T. A. (1999). Vestibular responses to linear acceleration are absent in otoconia-deficient C57BL/6JEi-*het* mice. *Hearing Research, 135,* 56-60.

Jones, S. M., Erway, L. C., Yu, H., Johnson, K. R., & Jones, T. A. (2004). Gravity receptor function in mice with graded otoconial deficiencies. *Hearing Research, 191,* 34-40.

Jones, S. M., & Jones, T. A. (1996). Short latency vestibular evoked potentials in the chicken embryo. *Journal of Vestibular Research, 6,* 71-83.

Jones, S. M., & Jones, T. A. (2000). Ontogeny of vestibular compound action potentials in the domestic chicken. *Journal of The Association for Research in Otolaryngology, 1,* 232-242.

Jones, S. M., Jones, T. A., Bell, P. L., & Taylor, M. J. (2001). Compound gravity receptor polarization vectors evidenced by linear vestibular evoked potentials. *Hearing Research, 154,* 54-61.

Jones, S. M., Jones, T. A., & Shukla, R. (1997). Short latency vestibular evoked potentials in the japanese quail (*Coturnix coturnix japonica*). *Journal of Comparative Physiology A, 180,* 631-638.

Jones, S. M., Subramanian, G., Avniel, W., Guo, Y., Burkard, R. F., & Jones, T. A. (2002). Stimulus and recording variables and their effects on mammalian vestibular evoked potentials. *Journal of Neuroscience Methods, 118,* 23-31.

Jones, T. A. (1992). Vestibular short latency responses to pulsed linear acceleration in unanesthetized animals. *Electroencephalography and Clinical Neurophysiology, 82,* 377-386.

Jones, T. A., Beck, M. M., Brown-Borg, H. M., & Burger, R. E. (1987). Far-field recordings of short latency auditory responses in the white leghorn chick. *Hearing Research, 27,* 67-74.

Jones, T. A., & Jones, S. M. (1999). Short latency compound action potentials from mammalian gravity receptor organs. *Hearing Research, 136,* 75-85.

Jones, T. A., & Jones, S. M. (2007). Vestibular Evoked Potentials. In R.F.Burkard, J. J. Eggermont, & M. Don (Eds.), *Auditory evoked potentials: basic principles and clinical application* (pp. 622-650). Baltimore, MD: Lippincott Williams & Wilkins.

Jones, T. A., Jones, S. M., & Colbert, S. (1998). The adequate stimulus for avian short latency vestibular responses to linear translation. *Journal of Vestibular Research, 8,* 253-272.

Jones, T. A., Jones, S. M., & Hoffman, L. F. (2008). Resting discharge patterns of macular primary afferents in otoconia-deficient mice. *Journal of The Association for Research in Otolaryngology, 9,* 490-505.

Jones, T. A., Jones, S. M., Vijayakumar, S., Brugeaud, A., Bothwell, M., & Chabbert, C. (2011). The adequate stimulus for mammalian linear vestibular evoked potentials (VsEPs). *Hearing Research, 280*, 133-140.

Jones, T. A., & Pedersen, T. L. (1989). Short latency vestibular responses to pulsed linear acceleration. *American Journal of Otolaryngology, 10,* 327-335.

Jones, T. A., Stockard, J. J., Rossier, V. S., & Bickford, R. G. (1976). Application of cryogenic techniques in the evaluation of afferent pathways and coma mechanisms. *Proceedings of the San Diego Biomedical Symposium, 15,* 249-255.

Jones, T. A., Stockard, J. J., & Weidner, W. J. (1980). The effects of temperature and acute alcohol intoxication on brain stem auditory evoked potentials in the cat. *Electroencephalography and Clinical Neurophysiology, 49,* 23-30.

Jones, T. A., & Weidner, W. J. (1986). Effects of temperature and elevated intracranial pressure on peripheral and brain stem auditory responses in dogs. *Experimental Neurology, 92,* 1-12.

Keats, B. J. B., & Corey, D. P. (1999). The usher syndromes. *American Journal of Medical Genetics, 89,* 158-166.

Kushiro, K., Zakir, M., Ogawa, Y., Sato, H., & Uchino, Y. (1999). Saccular and utricular inputs to sternocleidomastoid motoneurons of decerebrate cats. *Experimental Brain Research, 126,* 410-416.

Lange, M. E. (1988). *Mammalian far-field responses to pulsed linear acceleration.* (Unpublished doctoral dissertation). University of Nebraska, Lincoln, NE.

Lange, M. E., & Jones, T. A. (1989). Mammalian short latency electrophysiological responses to pulsed linear acceleration. [Abstract]. *ASGSB Bulletin, 3*, 31.

Lange, M. E., & Jones, T. A. (1990). Short latency electrophysiological responses to pulsed linear acceleration in the mammal. *Association for Research in Otolaryngology*, 343.

Latash, M. L. (2008). Motor units and electromyography. In *Neurophysiological basis of movement* (2 ed., pp. 49-57). Champaign, IL: Human Kinetics.

Lee, W. S., Suarez, C., Newman, A., & Honrubia, V. (1990). Central projections of the individual vestibular sensory end-organs of the chinchilla. In T. Sacristan, J. J. Alvarez-Vicent, J. Bartual, & F. Antoli-Candela (Eds.), *Otorhinolaryngology, head and neck surgery* (pp. 121-124). Amsterdam: Kugler And Ghedini Publications.

Leigh, R. J., & Zee, D. S. (2006). *The neurology of eye movements.* (4 ed.) (Vol. 70) New York, NY: Oxford University Press.

Lev, A., & Sohmer, H. (1972). Sources of averaged neural responses recorded in animal and human subject during cochlear audiometry [electro-cochleogram]. *Archiv fur Klinische und Experimentelle Ohren-, Nasen- und Kehlkopfheilkunde, 201,* 79-90.

Li, G., Elidan, J., Meyler, Y., & Sohmer, H. (1997). Contribution of the eighth nerve and cranial nerve nuclei to the short-latency vestibular evoked potentials in cats. *Otolaryngology-Head & Neck Surgery, 116,* 181-188.

Li, G., Elidan, J., & Sohmer, H. (1993). The contribution of the lateral semicircular canal to the short latency vestibular evoked potentials in cat. *Electroencephalography and Clinical Neurophysiology, 88,* 225-228.

Li, G., Elidan, J., & Sohmer, H. (1995). Peripheral generators of the vestibular evoked potentials in the cat. *Archives of Otolaryngology Head and Neck Surgery, 121,* 34-38.

Ludbrook, J. (1998). Multiple comparison procedures updated. *Clinical and Experimental Pharmacology and Physiology, 25,* 1032-1037.

Lutkenhoner, B., & Mosher, J. C. (2007). Source analysis of auditory evoked potentials and fields. In *Auditory evoked potentials: Basic principles and clinical application* (pp. 546-569). Baltimore, MD: Lippincott Williams and Wilkins.

Marsh, R. R., Yamane, H., & Potsic, W. P. (1984). Auditory brain-stem response and temperature: relationship in the guinea pig. *Electroencephalography and Clinical Neurophysiology, 57,* 289-293.

Mock, B. E., Jones, T. A., & Jones, S. M. (2011). Gravity receptor aging in the CBA/CaJ Strain: A comparison to auditory aging. *Journal of The Association for Research in Otolaryngology, 12,* 173-183.

Møller, A. R. (2006). *Hearing: Anatomy, physiology, and disorders of the auditory system.* (2 ed.) Burlington, MA: Elsevier.

Møller, A. R., & Jannetta, P. J. (1983). Monitoring auditory functions during cranial nerve microvascular decompression operations by direct recording from the eighth nerve. *Journal of Neurosurgery, 59,* 493-499.

Mroszczak, E. J., Lee, F. W., Combs, D., Sarnquist, F. H., Huang, B.-L., Wu, A. T., Tokes, L. G., Maddox, M. L., & Cho, D. K. (1987). Ketorolac tromethamine absorbtion, distribution, metabolism, excretion, and pharmacokinetics in animals and humans. *Drug Metabolism and Disposition, 15,* 618-626.

Murofushi, T., & Kaga, K. (2009). *Vestibular evoked myogenic potentials: Its basics and clinical applications.* Tokyo, Japan: Springer.

Musiek, F. E., & Baran, J. A. (2006). *The auditory system: anatomy, physiology and clinical correlates.* (1 ed.) Boston, MA: Allyn & Bacon, Incorporated.

Musiek, F. E., & Geurkink, N. A. (1982). Auditory brain stem response and central auditory test findings for patients with brain stem lesions: A preliminary report. *Laryngoscope, 92,* 891-900.

Nazareth, A. M., & Jones, T. A. (1991a). Central and peripheral generators of short latency vestibular responses. *Neuroscience Abstracts, 17*, 29.

Nazareth, A. M., & Jones, T. A. (1991b). Vestibular nerve components of responses to pulsed linear acceleration. *ASGSB Bulletin, 5,* 40.

Nazareth, A. M., & Jones, T. A. (1998). Central and peripheral components of short latency vestibular responses in the chicken. *Journal of Vestibular Research, 8,* 233-252.

Newlands, S. D., & Perachio, A. A. (2003). Central projections of the vestibular nerve: a review and single fiber study in the Monogolian gerbil. *Brain Research Bulletin, 60,* 475-495.

Otti, T., Weindel, M., & Bastani, B. (1997). Ketorolac induced acute reversible hearing loss in a patient maintained on CAPD. *Clinical Nephrology, 47,* 208-209.

Parent, A. (1996). *Carpenter's human neuroanatomy.* (9 ed.) Media, PA: Williams and Wilkins.

Pasloske, K., Renaud, R., Burger, J., & Conlon, P. (1999). Pharmacokinetics of ketorolac after intravenous and oral single dose administration in dogs. *Journal of Veterinary Pharmacology and Therapeutics, 22,* 314-319.

Picton, T. W., Hillyard, S. A., Krausz, H. I., & Galambos, R. (1974). Human auditory evoked potentials I: Evaluation of components. *Electroencephalography and Clinical Neurophysiology, 36,* 179-190.

Plotnik, M., Elidan, J., Mager, M., & Sohmer, H. (1997). Short latency vestibular evoked potentials (VsEPs) to linear acceleration impulses in rats. *Electroencephalography and Clinical Neurophysiology, 104,* 522-530.

Plotnik, M., Sichel, J.-Y., Elidan, J., Honrubia, V., & Sohmer, H. (1999). Origins of the short latency vestibular evoked potentials (VsEPs) to linear acceleration impulses. *American Journal of Otology, 20,* 238-243.

Plumb, D. C. (2008). *Plumb's veterinary drug handbook.* (6 ed.) Ames, IA: Blackwell Publishing.

Pompeiano, M., & Brodal, A. (1957). The origin of vestibulospinal fibers in the cat. An experimental study, with comments on descending medial longitudinal fasciculus. *The Italian Archives of Biology, 95,* 166-195.

Rabionet, R., Gasparini, P., & Estivill, X. (2000). Molecular genetics of hearing impairment due to mutations in gap junction genes encoding beta connexins. *Human Mutation, 16,* 190-202.

Reinhart, D. J. (2000). Minimizing the adverse effects of ketorolac. *Drug Safety, 22,* 487-497.

Rooks, W. H., Maloney, P. J., Shott, L. D., Schuler, M. E., Sevelius, H., Strosberg, A. M., Tanenbaum, L., Tomolonis, A. J., Wallach, M. B., Waterbury, D., & Yee, J. P. (1985). The analgesic and anti-inflamatory profile of ketorolac and its tromethane salt. *Drugs under Experimental and Clinical Research, 11,* 479-492.

Rooks, W. H., Tomolonis, A. J., Maloney, P. J., Wallach, M. B., & Schuler, M. E. (1982). The analgesic and anti-inflammatory profile of (+/-)-5-benzoyl-1,2-dihydro-3H-pyrrolo[1,2a]pyrrle-1-carboxylic acid (RS-37619). *Agents and Actions, 12,* 684-690.

Schaab, K. C., Dickinson, E. T., & Setzen, G. (1995). Acute sensorineural hearing loss following intravenous ketorolac administration. *The Journal of Emergency Medicine, 13,* 509-513.

Shiroyama, T., Kayahara, T., Yasui, Y., Nomura, J., & Nakano, K. (1999). Projections of the vestibular nuclei to the thalamus in the rat: A *Phseolus vulgaris* leucoagglutinin study. *The Journal of Comparative Neurology, 407,* 318-332.

Shrout, P. E., & Fleiss, J. L. (1979). Interclass Correlations: Uses in assessing rater reliability. *Psychological Bulletin, 86,* 420-428.

Sininger, Y. S., & Don, M. (1989). Effects of click rate and electrode orientation on threshold of the auditory brainstem response. *Journal of Speech and Hearing Research, 32,* 880-886.

Sohmer, H., Feinmesser, M., & Szabo, G. (1974). Sources of electrocochleographic responses as studied in patients with brain damage. *Electroencephalography and Clinical Neurophysiology, 37,* 663-669.

Starr, A., & Hamilton, A. E. (1976). Correlation between confirmed sites of neurological lesions and abnormalities of far-field auditory brainstem responses. *Electroencephalography and Clinical Neurophysiology, 41,* 595-608.

Trimble, M. V., & Jones, S. M. (2001). Vestibular evoked potentials to rotary stimulation in the head tilt (*het*) mouse. [Abstract]. *Association for Research in Otolaryngology 24*, 19.

Vaughan, H. G., & Ritter, W. (1970). The sources of auditory evoked responses recorded from the human scalp. *Electroencephalography and Clinical Neurophysiology, 28,* 360-367.

Wada, S. I., & Starr, A. (1983a). Generation of auditory brain stem responses [ABR's]. I. Effects of infection of a local anesthetic [procaine HCL] into the trapezoid body of guinea pigs and cat. *Electroencephalography and Clinical Neurophysiology, 56,* 326-339.

Wada, S. I., & Starr, A. (1983b). Generation of auditory brain stem responses [ABR's]. II. Effects of surgical section of the trapezoid body on the ABR in guinea pigs and cat. *Electroencephalography and Clinical Neurophysiology, 56,* 340-351.

Wada, S. I., & Starr, A. (1983c). Generation of auditory brain stem responses [ABR's]. III. Effects of lesions of the superior olive, lateral lemniscus and inferior colliculus on the ABR in guinea pig. *Electroencephalography and Clinical Neurophysiology, 56,* 352-366.

Webster, D. B., & Fay, R. R. (1992). *Mammalian auditory pathway: Neuroanatomy.* New York, NY: Springer.

Weisleder, P., Jones, T. A., & Rubel, E. W. (1990). Peripheral generators of the vestibular evoked potentials [VsEP] in the chick. *Electroencephalography and Clinical Neurophysiology, 76,* 362-369.

Wilson, V. J., & Yoshida, M. (1969). Monosynaptic inhibition of neck motoneurons by the medial vestibular nucleus. *Experimental Brain Research, 9,* 365-380.

Yates, B. J., & Miller, A. D. (1998). Physiological evidence that the vestibular system participates in autonomic and respiratory control. *Journal of Vestibular Research, 8,* 17-25.

Zhou, G., & Cox, L. C. (2004). Vestibular evoked myogenic potentials: history and overview. *American Journal of Audiology, 13,* 135-143.

APPENDIX A: Animal Care and Use Approval

East Carolina University

Animal Care and Use Commitee
212 Ed Warren Life Sciences Building
East Carolina University
Greenville, NC 27834

252-744-2436 office
252-744-2355 fax

August 11, 2010

Tim Jones, Ph.D.
Department of CSDI
3310 Health Sciences Building
East Carolina University

Dear Dr. Jones:

The Amendment to your Animal Use Protocol entitled, "Generators of Vestibular Evoked Myogenic Potentials (VEMPs) and Vestibular Evoked Potentials (VsEPs)", (AUP #P057) was reviewed by this institution's Animal Care and Use Committee on 8/11/10. The following action was taken by the Committee:

"Approved as amended"

****Please contact Dale Aycock prior to any biohazard use**

A copy of the Amendment is enclosed for your laboratory files. Please be reminded that all animal procedures must be conducted as described in the approved Animal Use Protocol. Modifications of these procedures cannot be performed without prior approval of the ACUC. The Animal Welfare Act and Public Health Service Guidelines require the ACUC to suspend activities not in accordance with approved procedures and report such activities to the responsible University Official (Vice Chancellor for Health Sciences or Vice Chancellor for Academic Affairs) and appropriate federal Agencies.

Sincerely yours,

Robert G. Carroll, Ph.D.
Chairman, Animal Care and Use Committee

RGC/jd

enclosure